UNIVERSITÀ
DEGLI STUDI
DI PADOVA

UNIVERSITA' DEGLI STUDI DI PADOVA

Dipartimento Della Salute della Donna e del Bambino

SCUOLA DI DOTTORATO DI RICERCA IN MEDICINA DELLO SVILUPPO E SCIENZE DELLA PROGRAMMAZIONE
Indirizzo: Ematooncologia,Genetica, Malattie Rare e Medicina Predittiva
CICLO: XXVII

ROLE OF FOXM1 AND FOXO3a IN B-LYMPHOBLASTIC LEUKAEMIA PROGRESSION AND GLUCOCORTICOID RESPONSIVENESS

Direttore della Scuola : Ch.mo Prof. GIUSEPPE BASSO

Supervisore : Dott. GIAMPIETRO VIOLA

Dottoranda: Consolaro Francesca

Anno Accademico 2013/2014

ABBREVIATIONS

FOX	Forkhead Box
PBMC	Peripheral Blood Mononuclear Cells
B-ALL	B-Acute Lymphoblastic Leukaemia
NRD	N-Terminal Repressor Domain
FKH	Forkhead Domain
TAD	Transactivation Domain
DBD	DNA Binding Domain
MMPs	Metalloproteinases
EMT	Epithelial Mesenchymal Transition
CI	Combination Index
IGF-1	Insuline-like Grow Factor 1
CK	Casein Kinase
LIC	Leukaemia Initiating Cells
MDR	Multidrug Resistance
CDK	Cyclin-Dependent Kinase
$p27^{Kip1}$	Cyclin-dependent kinase inhibitor 1B($p27^{Kip1}$
p21	CDK-interacting protein 1
APAF-1	Apoptotic Protease Activating Factor-1
Bcl-2	B-cell lymphoma 2
Bcl-XL	B-cell lymphoma-extra large
Mcl-1	Induced Myeloid Leukemia Cell Differentiation protein
VDA	Vascular Disrupting Agents
CA-4	Combretastatin A-4
ROS	Reacting Oxygen Species
FOXO	Forkhead box protein

SOD	Super Oxide Dismutase
TRX	Thioredoxin
GSH	Glutathione
GSSG	Glutathione disulfide
NADPH	Nicotinamide Adenine dinucleotide phosphate
HE	Hydroxyethidine
IC_{50}	Half maximal inhibitory concentration
PI	Propidium Iodide;
PARP	PolyADP-ribose Polymerase
PBL	Peripheral Blood Lymphocytes
PHA	Phytohemaglutinin
BSA	Bovine Serum Albumin
PBS	Phosphate-buffered saline
SDS-PAGE	Sodium dodecyl sulfate polyacrylamide gel electrophoresis
HUVEC	Human umbilical vein endothelial cell
LSGS	Low serum growth supplement
H_2DCFDA	2',7'-dichlorodihydrofluorescein diacetate
FITC	Fluorescein isothiocyanate

To my lovely parents

ACKNOWLEDGEMENTS

First, I'm extremely grateful to Professor Giuseppe Basso, who gave me the opportunity to do the PhD in his Laboratory, composed by very competent lab members and with an extremely excellent scientific environment reached in facilities and competences.

I'd love to thank my supervisor Giampietro Viola who constantly supported me during my PhD. I cannot forget Roberta and Elena, my lab members that during this experience helped me to go through the project with an incisive point of view.

A special thank you to Eric Lam, who kindly gave me the opportunity to be part of his Lab for more than one year. Professor Eric W-F Lam has been a very great supervisor throughout this period providing me guidance, support, help and friendship. I'll never forget this period! I would also like to thank you my mentor Professor Sadaf Ghaem-Maghami, who very kingly gave me the possibility to work with her group sharing space and biologics concepts. I must say a big thank you to my lovely 'UK family': Stefania, Laura, Ana, Gabi, Patty, Matty, Sassi, Gift, Upenka, Kazu, Jimmy. I'll miss all of you a lot! A big hug to Maria for all the laughs, the company and supports that she gave to me.

An important thank you to my family. I must particularly thank my mother Grazia and my father Daniele. I've never met such supportive parents. They are responsible for my determination and success. They helped and supported me in each step of my life. A big thank you to my brothers Alberto, Federico, Gianpietro and to my sister Anna.

Finally to my husband, Paolo, a big thank you for being there for me and having patience to support me during this crazy PhD period.

RIASSUNTO

La leucemia linfoblastica acuta di tipo B (B-ALL) è un tumore caratterizzato dall'accumulo nel midollo osseo di linfociti immaturi, blasti, di tipo B che successivamente invadono il sangue, raggiungendo anche i linfonodi, la milza, il fegato e il sistema nervoso centrale. I pazienti B-ALL che alla diagnosi non rispondono al trattamento con glucocorticoidi, sono spesso soggetti a prognosi infausta e a ricaduta della malattia. Comprendere quindi quali siano i meccanismi molecolari sottostanti a questa resistenza ai glucocorticoidi permetterebbe di evitare fenomeni di ricaduta e potenzialmente di trovare nuove efficaci terapie antitumorali. FOXO3a e FOXM1 appartengono alla stessa famiglia di fattori di trascrizione denominati *forkhead*. Sebbene non sia ancora stato chiarificato quale sia il ruolo svolto da questi due fattori di trascrizione nelle B-ALL, i lavori riportati in letteratura dimostrano che FOXO3a e FOXM1 generalmente svolgono ruoli opposti all'interno della cellula. FOXM1 infatti è un importante oncogene che regola principalmente la proliferazione cellulare promuovendo la progressione tumorale. Per questo motivo, FOXM1 è spesso sovraespresso in diversi tipi di tumori, contribuendo quindi alla resistenza terapeutica e alla progressione tumorale. FOXO3a al contrario è un noto soppressore tumorale la cui attivazione è fondamentale per favorire la citotossicità di molti composti chemioterapici. Tuttavia la sua localizzazione intracellulare ed attività trascrizionale sono regolate da una complicata rete di modificazioni post-traslazionali, quali la fosforilazione, l'acetilazione, la metilazione e l' ubiquitinazione.

Nella prima parte di questo studio abbiamo quindi esaminato se questi due fattori di trascrizione, FOXO3a e FOXM1, svolgono un ruolo nelle B-ALL. In particolare abbiamo analizzato se FOXM1 è coinvolto nella proliferazione cellulare e nella risposta al trattamento chemioterapico. Inoltre abbiamo svolto una serie di esperimenti per comprendere se FOXO3a è coinvolto nella risposta al trattamento coi glucocorticoidi (desametasone) e se la sua attività trascrizionale viene modulata da modificazioni post transazionali quali la fosforilazione e l'acetilazione. I dati ottenuti hanno dimostrato che entrambi i fattori di trascrizione, FOXM1 e FOXO3a svolgono un ruolo chiave nelle leucemie B-ALL. FOXM1 è un importante regolatore della proliferazione tumorale, infatti la sua downregolazione provoca una significativa diminuzione della proliferazione cellulare associata all'arresto del ciclo cellulare in G2/M. FOXM1 inoltre risulta essere un importante target terapeutico per le B-ALL in quanto la sua inibizione può significativamente incrementare l'effetto citotossico dei chemioterapici che sono

normalmente utilizzati per trattare i pazienti affetti da B-ALL. Il fattore di trascrizione FOXO3a gioca un ruolo centrale nel mediare la risposta al trattamento con desametasone. Infatti, in seguito al trattamento, FOXO3a diventa trascrizionalmente attivo solo nelle cellule che sono sensibili (RS4;11 e SUP-B15). FOXO3a trasloca nel nucleo dove regola l'espressione di geni proapoptotici. Diversamente nelle cellule resistenti al desametasone, REH, FOXO3a rimane inattivo e localizzato nel citoplasma. Inoltre, FOXO3a diventa maggiormente fosforilato e acetilato, nei siti Ser7 e Lys242/245 rispettivamente, solo nelle cellule sensibili, suggerendo che probabilmente queste due modificazioni post-translazionali contribuiscono nel promuovere la sua attivazione trascrizionale.

Nella seconda parte dello studio ho analizzato il meccanismo molecolare di due classi di composti antitumorali, gli arilamino triazoli e le fenilcinammidi, entrambi sintetizzati per inibire, in maniera selettiva, la proliferazione ed indurre morte cellulare nelle cellule tumorali. In particolare, è stato studiato l'effetto di tali molecole sulla polimerizzazione della tubulina, sul ciclo cellulare e sull'attivazione dell'apoptosi per la delucidazione di un possibile meccanismo d'azione. I composti testati hanno mostrato attività antiproliferativa comparabile o superiore rispetto ai composti di riferimento. Per quanto riguarda il meccanismo d'azione, in generale, entrambi questi composti inducono un blocco del ciclo cellulare in fase G2/M il quale porta all'attivazione del processo apoptotico caspasi-dipendente. Tuttavia gli arilamino triazoli agiscono principalmente come inibitori della polimerizzazione della tubulina, mentre le fenilcinammidi agiscono riducendo significativamente i livelli di antiossidante intracellulare glutatione, provocando quindi un aumento dello stress ossidativo intracellulare che in ultima analisi porta ad apoptosi.

CHAPTER 1

FOXM1 AND FOXO3a ROLE IN B-ALL

SUMMARY

B-cell acute lymphoblastic leukaemia (B-ALL) is one of the most common paediatric disorders characterized by an accumulation of B-cell blasts reminiscent of normal stages of differentiation and by infiltration of various extramedullary sites.

B-ALL patients that respond poorly to glucocorticoid therapy when diagnosed are usually predicted to undergo relapse. Therefore understanding the biological mechanisms underlying this poor responsiveness is crucial for the development of more effective therapies. FOXM1 belongs to the Forkhead Box (FOX) superfamily of transcriptional factors and is a major regulator of cell proliferation and cell cycle progression. Its expression increases at the entry of cell cycle S-phase, remains stable during G2/M phase, and finally, is degraded at the mitotic exit. FOXM1 is a bona fide proto-oncogene and its up-regulation is often associated with a high proliferation rate, resistance to drugs and poor prognosis of many tumours, as well as with the development and progression of many malignancies. Therefore, downregulation of FOXM1 expression and activity might be a key strategy to inhibit tumour progression. In the first study we investigated the potential role of FOXM1 in B-ALL cell proliferation, aiming to understand if FOXM1 can be targeted to either increase the efficiency of chemotherapeutic treatment, or to overcome drug resistance in this haematological malignancy. We observed that FOXM1 protein and mRNA levels are higher in B-ALL patients and cell lines when compared to lymphocytes of healthy donors (peripheral blood mononuclear cells, PBMCs). We then downregulated FOXM1 in REH and NALM-6 cell lines using a specific FOXM1 siRNA or thiostrepton treatment: there was a significant reduction in cell proliferation, cell cycle arrest in G2/M and an increase in sub-G1 cells. Importantly, we observed that thiostrepton acts in synergy with conventional chemotherapeutic agents, increasing their efficiency and partially reversing the glucocorticoid resistance in REH cells. Altogether, our results suggest that FOXM1 inhibition could be a useful strategy to increase the efficacy of existing therapeutics for B-ALL and to overcome drug resistance.

In the second study we focused our attention on another FOX family member: the transcription factor FOXO3a. Although FOXO3a is mainly described as a bona fide

tumour suppressor, literature reveals that it might also play a role as a proto-oncogene, by inducing cancer development and drug resistance according to the cellular context.

FOXO3a transcriptional activity is regulated by a complex array of post-translational modifications. Amongst there, phosphorylation and acetylation are the major regulators of FOXO3a subcellular localization and transcriptional function. In this work, we investigated whether FOXO3a is involved in dexamethasone responsiveness of B-lymphoblastic leukaemia (B-ALL). Western blot and immunostaining data showed that FOXO3a becomes active only in sensitive cells following dexamethasone treatment. In dexamethasone sensitive cells (RS4;11 and SUP-B15), FOXO3a translocates from the cytoplasm to the nucleus, where it induces the expression of BIM, p27 and the activation of apoptosis signature through caspase-3 cleavage. Moreover knockdown experiments clearly reveal that FOXO3a expression and function is fundamental for dexamethasone mediated cytotoxicity. We then performed a series of experiments to clarify if its activity is regulated by phosphorylation and/or acetylation. More importantly, two post-translational modifications, phosphorylation on Ser7 and acetylation on Lys242 and Lys245, appeared to be crucial for dexamethasone-mediated FOXO3a activation in sensitive cells. Clarifying which are the biological processes that prevent these post-translational modifications from occurring in dexamethasone-resistant REH cells, might pave the way to overcoming glucocorticoid resistance in B-ALL.

1 GENERAL INTRODUCTION

Forkhead box (FOX) proteins are evolutionarily conserved transcriptional regulators which control a wide spectrum of biological processes such as cell cycle progression, proliferation, differentiation, metabolism, senescence, survival and apoptosis[1]. Therefore, a loss or gain of FOX function might alter the cell's fate and promote tumorigenesis as well as cancer progression.

FOXO3a and FOXM1, two of the most important members of FOX's family of transcription factors, are key players in cancer initiation, progression, drug response and chemotherapy resistance[2]. Accordingly, FOXO3a and FOXM1 proteins are indirect targets of several widely used cancer drugs. Some chemotherapeutic drugs, such as doxorubicin, epirubicin and cisplatin, mediate their cytotoxic effects partly by targeting and perturbing the FOXO3a and FOXM1 function[3]. However, the role exerted by FOXM1 and FOXO3a in B-ALL cells proliferation and drug response has not been clarified yet.

1.1 B-ACUTE LYMPHOBLASTIC LEUKAEMIA (B-ALL)

B-lymphoblastic leukaemia (B-ALL) is the most common childhood tumor and dominates within the lymphoid leukaemia groups in children (where >80% ALLs are B-ALLs)[4].

B-ALL malignant disorder derives from clonal proliferation of B-lymphoid precursors with arrested maturation[5]. B-ALL symptoms are caused by the decrease in production of normal marrow elements and by the direct B-leukaemic cell infiltration in the marrow or other organs. Symptoms can include fever, increased risk of infection, increased tendency to bleed (due to thrombocytopenia) and signs indicative of anaemia including pallor, tachycardia, fatigue and headache[6].

Standard treatment options for newly diagnosed childhood B-ALL patients include chemotherapy treatment and, more commonly, a four-drug induction regimen, composed of vincristine, corticosteroid (dexamethasone or prednisone), L-asparaginase, Ara-c (Cytarabine) and either doxorubicin or daunorubicin. Over the years, the association of primary glucocorticoid resistance with poor prognosis in childhood B-ALL has been described frequently. Poor response to glucocorticoid has been correlated with increased risk of relapse and therapeutic failure[7–9]. Understanding the mechanisms that regulate

dexamethasone responsiveness is therefore an important goal to evade bad prognosis in paediatric B-ALL.

1.2 FORKHEAD BOX TRANSCRIPTION FACTORS

Forkhead box (FOX) superfamily of transcription factors play a major role in cell fate decisions. They regulate crucial biological processes such as cell proliferation, differentiation, metabolism, tissue homeostasis, senescence, survival, apoptosis, and DNA damage repair[3]. All members of this family are characterized by a highly conserved "winged-helix" DNA- binding domain (DBD) which is composed of about 110 amino acids. In the human genome, fifty forkhead proteins have been identified and categorized into 19 subgroups on the basis of sequence homology and forkhead domain structure[10].
Several FOX factors activate target genes by binding to forkhead response elements (FHREs) in the gene's promoter region. This is followed by the recruitment of the co-activator histone acetyltransferase CBP/p300, which creates a relaxed open chromatin structure that permits binding of the transcriptional machinery[11,12]. Literature shows that FOX proteins might exert opposite roles in cell fate decisions by regulating a wide range of gene networks that are involved in cell cycle progression, proliferation, differentiation, as well as in cellular metabolism, senescence, survival and apoptosis[1].
It has been demonstrated that two of the mostly studied FOX's transcription factors, FOXM1 and FOXO3a, bind to the same DNA motif in target promoters. However, they produce opposing transcriptional effects[2,13]: FOXO3a mainly plays as a tumor suppressor, whereas FOXM1 acts primarily as proto-oncogene. Inactivation of FOXO3a or overexpression of FOXM1 is therefore often associated with tumorigenesis and cancer progression. However, FOXO3a can also contribute to cancer's drug resistance by driving the expression of genes important for drug efflux, DNA repair and cell survival pathways in drug resistant cancers[14,15]. Given their pivotal roles in drug sensitivity and resistance, both FOXO3a and FOXM1 could be important targets for the treatment of cancer and for overcoming drug resistance[16].

1.2.1 FOXM1

Forkhead Box M1 (FOXM1), also previously known as Trident (in mouse), HFH-11 (in human), WIN or INS-1 (in rat), MPP-2 (partial human cDNA) and FKHL-16 is a member of the Forkhead superfamily of transcription factors[3]. There are three FOXM1 isoforms, A, B and C. Isoform FOXM1A has been shown to be transcriptionally inactive, whereas FOXM1B e C are transcriptionally active.

Structurally, FOXM1 full-length protein can be divided into three distinct functional regions: an N-terminal Repressor Domain (NRD), a Forkhead/Winged-helix domain (FKH) and a Transactivation Domain (TAD). It is believed that the NRD folds back to suppress the transactivational activity of the TAD[17].

Figure 1: FOXM1 protein domains: NRD, FKH and TAD. (Adapted from Ref [3]).

FOXM1 plays a major role in regulating cell proliferation and cell cycle progression[18–20]. As such, it is ubiquitously expressed in all embryonic tissues, and proliferating cells of both epithelial and mesenchymal origin[21]. However, FOXM1 can also be a potent oncogene of which deregulation leads to cancer initiation, progression and to development of cancer drug resistance: FOXM1 has been found to be upregulated in many human solid tumours such as liver, prostate, brain, breast, lung, colon, pancreas, skin, cervix, ovary, mouth, blood and nervous system[22].

1.2.1.1 FOXM1 IN TUMORIGENESIS

FOXM1 exerts its oncogenic function regulating a wide spectrum of biological processes, including cell proliferation, cell cycle progression, cell differentiation, DNA damage repair, angiogenesis, metastasis, apoptosis and drug resistance[3].

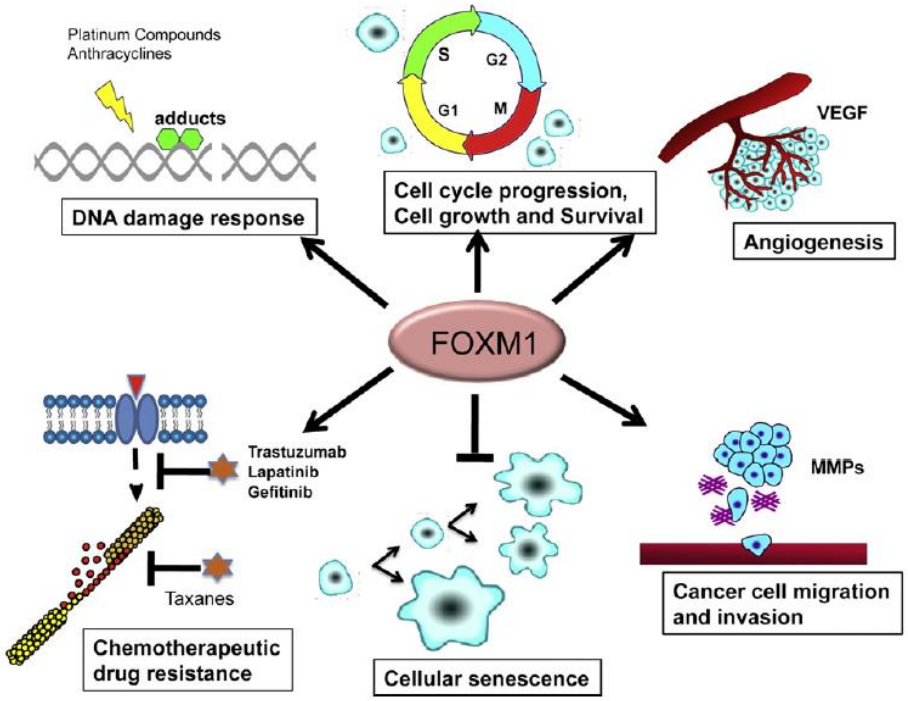

Figure 2: FOXM1 regulates several biological processes. (Adapted from Ref[20]).

❖ Cell cycle progression and cell proliferation

FOXM1 is a master regulator of genes fundamental for cell cycle progression: its overexpression is necessary for the hyper-proliferative pattern of tumor cells. FOXM1 synthesis starts in the early G_1-phase and is stimulated by growth factors. FOXM1 activity increases at the entry of cell cycle S-phase, remaining stable during G2/M phase, and is finally degraded at the mitotic exit. To exert its activity, FOXM1 associates itself with cyclin E-cdk2 complexes in the G1 and S phases of the cell cycle, whereas it preferentially binds the cyclin B-cdk1 complex in the G2 phase[23]. Through the G1-S phases, FOXM1 regulates the transcriptional activity of a number of genes, including genes encoding Plk1, Aurora B, Cyclin B1, CDC25B, CENP-A, and Survivin. This will promote several events of early mitosis, such as chromosome condensation, nuclear envelope disruption and the attachment of the mitotic spindle to the centromere. FOXM1 also regulates a series of genes essential for mitotic spindle integrity, such as CENPA, CENPF, NEK2 and KIF20[20,24]. Furthermore, FOXM1

activity induces $p27^{Kip1}$ and $p21^{Cip1}$ degradation through upregulation of S-phase kinase-associated protein 2 (skp2) and CDK subunit 1. Thus, FOXM1 depletion results in cell cycle arrest in G2/M phase, mitotic spindle defects, chromosome disaggregation and mitotic catastrophe[25].

- **Senescence and Stem cells**: FOXM1 protects cells from genotoxic agent-induced senescence by enhancing DNA repair[26,27]. Furthermore, FOXM1 promotes stem cell-like properties, such as cell renewal, immortalisation, sustained proliferative ability and pluripotency, by enhancing the OCT4 gene expression and so suppressing cellular differentiation. In this way FOXM1 can also enhance the WNT signalling pathway, which is crucial for the stem cell renewal[28,29].

- **Angiogenesis**: FOXM1 directly regulates VEGF expression, thus promoting the formation of the new blood vessels around the growing tumour, essential for the tumour's growth[30,31]. In pancreatic cells FOXM1 induces the expression of caveolin, a structural component of caveolar membrane thus promoting tumor invasion[31].

- **Metastasis:** FOXM1 induces the epithelial-mesenchymal transition (EMT) phenotype in pancreatic cancer cells by activating mesenchymal cell markers, rendering tumor cells more invasive and aggressive[32]. Moreover, it has been documented in different malignancies, such as glioblastoma, colorectal carcinoma, and breast carcinoma, that FOXM1 enhances metalloproteinases (MMPs) expression[33–35].

- **Drug resistance:** Recent research findings also place FOXM1 at the centre of drug resistance[20]. FOXM1 confers resistance to genotoxic drugs and radiation therapy by regulating DNA damage repair genes, particularly those involved in homologous recombination, including XRCC1, BRCA2, CHEK1 (also known as CHK1), RAD51 and BRIP1[3]. Congruously, FOXM1 silencing re-sensitizes drug-resistant cells to chemotherapy[27].

1.2.1.2 FOXM1 REGULATION

Through-out cell cycle progression, FOXM1 transcriptional activity depends upon its phosphorylation by cyclin, cyclin-dependent kinases (cdk) and Plk1 kinase. FOXM1 is firstly phosphorylated in the C-terminal activation domain by cyclin/cdks. Only then Plk1-dependent phosphorylation can occur. The phosphorylated and transcriptionally active FOXM1 accumulates as the cells progress through the cell-cycle. At the end of the M-phase, FOXM1 becomes dephosphorylated, and, in the early G_1-phase of the next cycle, it is polyubiquitinated by APC/C-Cdh1 for degradation by the proteasome. FOXM1 degradation in the early G_1-phase is important for regulated entry into S-phase. Thus, in proliferating cells, FOXM1 is synthesized and degraded in every cycle of cell division. FOXM1 can also regulate its own expression: Halasi et al. showed that FOXM1 is involved in a positive auto-regulatory loop since it binds and activates its own proximal promoter[36]. Therefore, FOXM1 inhibition mediated by the thiazole antibiotic thiostrepton, not only downregulates FOXM1 transcriptional activity, but it also reduces its mRNA and protein levels[37]. It is believed that FOXM1 NRD domain might fold back to suppress the transactivational activity of the TAD domain.

1.2.1.3 FOXM1 AND LEUKAEMIA

FOXM1 also plays a major role in the promotion of cell proliferation and tumor progression in haematological malignancies. Previous studies conducted by Nakamura et al. in myeloid leukaemia, showed that FOXM1 has a capacity to regulate the cell cycle progression[38]. Interestingly Tüfekçi et al. found that the FOXM1 gene is overexpressed in the T-ALL cell line, and that dexamethasone and siomycin A caused a reduction in the gene expression levels of FOXM1[39]. Other studies have also revealed that FOXM1 downregulation induces the inhibition of cell growth in B-lymphoma. However, FOXM1's involvement in B-lymphoblastic leukaemia progression and therapy has not been investigated yet. Bhatla et al. have identified in a cohort of relapsed B-ALL paediatric patients, a series of genes which are up-regulated included FOXM1. Recently Zhao et al. highlighted the hypothesis that FOXM1 could be an important target in B cell malignancy. FOXM1 acts as a coactivator of the nuclear factor kB (NFkB) in lymphoblastoid B cell

lines (LCLs), promoting cell proliferation and cancer transformation[40]. Taken together, this data suggests that FOXM1 might be a key biological target to block cancer cell proliferation and tumor development in B-ALL.

1.2.2 FOXO3a TRANSCRIPTION FACTORS

The FOXO proteins represent a subfamily within the larger group of FOX transcription factors. In mammals it consists of three members: FOXO1 (also called FKHR), FOXO3a (also called FKHRL1), and FOXO4 (also called AFX)[41].

FOXO3a regulates a multitude of important cellular processes, including proliferation, apoptosis, differentiation, and metabolism[42,43]. This transcription factor is structurally characterized by the presence of four domains: the highly conserved DNA binding domain (DBD or FHD) that defines all forkhead proteins, a nuclear localisation signal (NLS) located just downstream of DBD, a nuclear export sequence (NES) and a C-terminal transactivation domain (TAD).

Figure 3: FOXO3a protein domains: FHD, NLS, NES and TAD. (Adapted from Ref [3]).

FOXO3a exerts its transcriptional function only when it is localized in the nucleus. However, its intracellular localization and activity is often strongly influenced by an intricate network of signal transduction cascades that might induce its translocation from the nucleus to the cytoplasm and subsequent proteasomal degradation.

1.2.2.1 POST-TRANSLATIONAL MODIFICATIONS (PTMS) OF FOXO3a

FOXO3a is regulated by a broad variety of external stimuli, including insulin, insulin-like growth factor (IGF-1), nutrients, cytokines and oxidative stress. These environmental stimuli control FOXO3a activity by altering the complicated combination of post-translational modifications that regulate FOXO3a protein expression, subcellular localization or DNA binding. The post-translational modifications that primarily regulate FOXO3a subcellular localization and function are phosphorylation, acetylation, ubiquitination and methylation.

- **Phosphorylation**

The most important control mechanism characterized for FOXO3a is its regulation by the PI3K/Akt pathway[42]. Upon PI3K activation by growth or survival factors, Akt phosphorylates FOXO3a at the conserved residues Thr32, Ser253 and Ser315. This leads to 14-3-3 proteins binding, nuclear exportation and subsequent FOXO3a degradation via the ubiquitination-mediated proteasome pathway[44,39]. Another factor that can promote the nuclear export of FOXO3a is the Casein kinase (CK) 1 dependent FOXO3a phosphorylation at Ser318 [45,46].

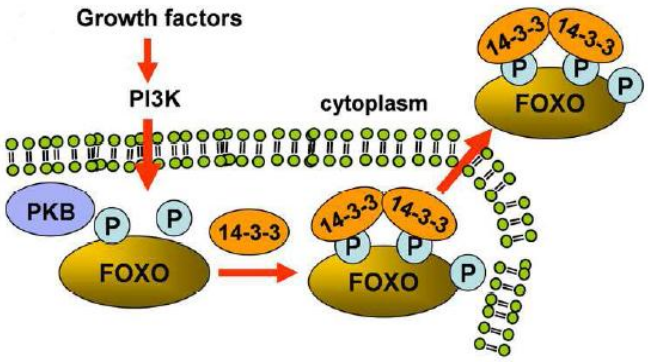

Figure 4: FOXO3a translocates from nucleus to the cytoplasm following PI3K/Akt dependent phosphorylation.

Similarly, ERK-mediated phosphorylation of FOXO3a on S294, S344 and S425 residues provokes FOXO3a cytoplasm retention and its degradation through ubiquitin E3 ligases,

MDM2[47]. Conversely, under stress conditions, FOXO3a can be phosphorylated by two of the three canonical MAPKs (*i.e.* ERK, p38, and JNK), p38 and JNK/SAPK kinases, leading to its nuclear relocalization and transcriptional activation. JNK activates FOXO3a by phosphorylation, as it acts on the related FOXO4 at Thr447 and Thr451, whereas p38 phosphorylates FOXO3a on Ser7[48,42].

- **Ubiquitination**

When FOXO3a is phosphorylated at specific residues, the ubiquitination process promotes its proteasomal recognition and degradation. The ubiquitin E3 ligases (MDM2) binds to FOXO3 as a consequence of ERK mediated FOXO3a phosphorylation whereas Skp2, another E3 ligase, can recognize the Ser253 phosphorylated FOXO3a and degrade it by polyubiquitination[49,50].

- **Acetylation**

Similarly to phosphorylation, acetylation might both promote or decrease FOXO3a transcriptional activity. The effect of acetylation on FOXO3a is controlled by histone acetyltransferase and by histone deacetylases. Immuno-precipitation analysis revealed that the acetyltransferase CBP/p300 binds to the first 52 amino acids of the N-terminal region of FOXO3a[51]. p300 might also directly acetylate FOXO transcription factors at Lys-242, Lys-245 and Lys-262 residues[52]. However, p300-dependent acetylation was shown to have a dual function in FOXO-mediated transcription: it can either attenuate its transcriptional activity or it can promote the recruitment and assembly of the transcriptional machinery, thus increasing FOXOs DNA-binding ability and transcriptional activity[53,54]. FOXO3a acetylation status can be further modulated by class III histone deacetylases (sirtuins), such as SIRT1, SIRT2, SIRT3 and SIRT6. Motta et al. showed that the nicotinamide adenine dinucleotide (NAD)-dependent histone deacetylase, SIRT1 contracts the p300-mediated transactivation of FOXO3a[55]. Furthermore, SIRT6 overexpression correlates to FOXO3a inactivation and SIRT6 depletion sensitizes MCF7 cells to both paclitaxel and epirubicin treatment[56]. Altogether, these evidences suggest that FOXO3a acetylation might be fundamental for its activation.

- **Methylation**

It has been found that FOXO3 methylation at lysine 270 inhibits FOXO3a-mediated oxidative stress and apoptosis[57]. Accordingly, Calnan et al. showed that methylation of FOXO3a at lysine 271 by methyltransferase Set9 decreases its protein stability, while moderately increasing FOXO3a transcriptional activity[58].

All these post-translational modifications might strongly influence FOXO3a activity. Although FOXO3a is mainly described as a bona fide tumour suppressor, literature reveals that this transcription factor might also act as a proto-oncogene contributing to cancer development and drug resistance. However, the mechanisms that allow FOXO3a to play a controversial role in cancer cells have not been well clarified. Studies suggest that FOXO3a transcriptional output might be related to its pattern of post-translational modifications resulting from different external stimuli[59,45].

1.2.2.2 FOXO3a IN LEUKAEMIA

FOXO3a has crucial role in controlling cell cycle arrest, apoptosis and self-renewal in haematopoietic progenitor cells. However, FOXO3a might play an antagonistic role at the axis of cancer drug sensitivity and resistance: FOXO3a has been described both as a tumor suppressor and as proto-oncogene. Consistently with its putative role as tumor suppressor, a report by Kornblau, et al. showed that high levels of FOXO3a phosphorylation are correlated to an adverse prognosis in AML[60]. Recently, Ausserlechner et al. showed that activating the transcription factor FOXO3a induces apoptotic cell death in therapy-resistant T-ALL cells[61]. Furthermore, deletion of FOXO family members in mice leads to the development of T-cell lymphoma[62]. Beside its function as a tumor suppressor, FOXO3a might also facilitate cancer cell survival under certain circumstances. Naka et al. found that chronic myeloid leukaemic cells with nuclear localization of FOXO3a and decreased Akt phosphorylation are enriched in the LIC population (leukaemia initiating cells)[63]. Moreover, FOXO3a induces the expression of multidrug resistance (MDR) pumps following doxorubicin treatment[14].

The involvement of FOXO3a in B-ALL progression and therapy has not been investigated so far. A previous study of Bachmann et al. reported a correlation between dexamethasone resistance and BIM expression in childhood T and B- ALL[64]. More specifically, the glucocorticoid resistance seemed to correlate with defective induction of the pro-apoptotic protein BIM, a FOXO3a target gene. Furthermore, Dewar et al. depicted that FOXO3a tumor suppressor activity is attenuated in BCR-ABL-mediated diseases and, more importantly, the therapeutic mediated reactivation of FOXO3a induces remission[65].

1.2.2.3 FOXO3a-FOXM1 INTERPLAY

FOXO3a has been described as a functional antagonist of FOXM1. It has been found that FOXM1 is a direct transcriptional target repressed by FOXO3a proteins and a vital downstream effector of the PI3K-Akt-FOXO axis[66]. FOXO3a can act by either displacing FOXM1 from the response elements (FHRE) of promoters of its target genes, or by inducing the chromatin condensation, reducing then the FOXM1 accessibility to the gene promoter, or by directly repressing FOXM1 gene expression[20].

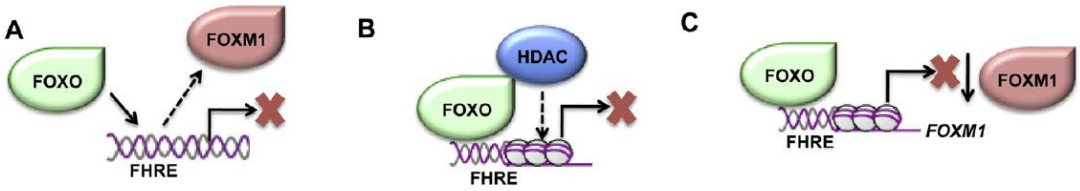

Figure 5: FOXO3a and FOXM1 antagonize each other's activity. (Adapted from Ref[20]).

Although FOXO3a and FOXM1 compete for binding to the same response elements in target genes, they are capable of regulating distinct functional gene networks.

For instance, FOXM1 activates while FOXO3a represses VEGF expression to control breast cancer cell angiogenesis and migration[66]. Importantly, FOXO3a downregulation drives the expression of genes essential for cell proliferation, survival and DNA damage repair, as well as cancer cell maintenance and progression[13]. Consistently, FOXM1 is often overexpressed and activated, whereas FOXO3a activity is frequently repressed, in drug-resistant cancer cells[13,67]. Therefore, targeting the FOXO3a–FOXM1 axis is an attractive strategy for overcoming drug resistance.

1.3 AIM OF THE PROJECT

FOXO3a and FOXM1 forkhead transcription factors are key players in cancer initiation, progression and drug resistance. However the role exerted by these transcription factors in B-ALL is still unknown.

FOXM1 is a well-known oncogene that promotes tumor progression by improving cell cycle progression and cell proliferation. However, although its proto-oncogene function has been described in myeloid leukaemia and B-lymphoma, FOXM1 involvement in B-lymphoblastic leukaemia has not been investigated yet.

We performed a series of experiments to investigate whether FOXM1 plays a role in B-lymphoblastic leukaemia progression. We further analysed whether FOXM1 inhibition by either knockdown or thiostrepton treatment might suffice to increase chemotherapy efficiency and overcome drug resistance.

Furthermore, since the role exerted by FOXO3a in B-ALL is also still not clear, we performed a series of experiments to investigate if this transcription factor might regulate dexamethasone responsiveness in B-ALL. In addition, we analysed if phosphorylation and acetylation might modulate FOXO3a activity and thus sensitise cells to glucocorticoid therapy.

1.4. RESULTS

FOXM1 is overexpressed in B-Acute Lymphoblastic Leukaemia (B-ALL) and its inhibition sensitizes B-all cells to chemotherapeutic drugs

Francesca Consolaro[a,b], Giuseppe Basso[a], Sadaf Ghaem-Magami[b], Eric W-F Lam[b*], Giampietro Viola[a*]

[a]*Dipartimento di Salute della Donna e del Bambino, Laboratorio di Oncoematologia, Università di Padova, 35131 Padova, Italy*

[b]*Department of Surgery and Cancer, Imperial College London, Imperial Centre for Translational and Experimental Medicine (ICTEM), London, UKW12 0NN*

* Co-corresponding authors

1.4.1 ABSTRACT

Background: The Forkhead box protein M1 (FOXM1) is a transcriptional factor that play a central role in the regulation of cell cycle, proliferation, DNA repair, and apoptosis. Since FOXM1 is overexpressed in many tumor types and its up-regulation has been linked to high proliferation rates and poor prognosis, we studied the role of FOXM1 in B-lymphoblastic leukaemia (B-ALL) in order to understand if FOXM1 could be a key target for leukaemia therapy.

Methods: RT-PCR and western blot analysis was carried out in a small cohort of pediatric B-ALL patients to evaluate FOXM1 levels. To assess the biological relevance of FOXM1, in B-lymphoblastic leukemic (B-ALL), its expression was downmodulated by transient RNA interference in B-ALL cell lines (REH and NALM-6).

Results: Our results showed that FOXM1 expression is higher in both B-ALL patients and cell lines compared to PBMC or $CD19^+$ cells from healthy donors. Furthermore, blocking FOXM1 activity in two B-ALL cell lines, by either knockdown or treatment with the FOXM1 inhibitor thiostrepton, causes significant decreases in the cell proliferation in both cell lines. The decrease in cell proliferation was accompanied by an induction of G2/M arrest of the cell cycle along with a reduction in the S phase. Moreover, thiostrepton synergises with chemotherapeutic agents commonly used in B-ALL therapy increasing their efficiency. **Conclusion:** Our results suggest that FOXM1 is highly express in both patients and B-ALL cells both and that targeting FOXM1 could be an attractive strategy for leukaemia therapy and for overcoming drug resistance.

Keywords. FOXM1; B-acute lymphoblastic leukemia; chemotherapy; drug resistance; thiostrepton

1.4.2 INTRODUCTION

FOXM1 is a member of the Forkhead family of transcription factors, also known previously as Trident (in mouse), HFH-11 (in human), WIN or INS-1 (in rat), MPP-2 (partial human cDNA) and FKHL-16.(Lam *et al*, 2013) FOXM1 is a potent oncogene whose expression is frequently up-regulated during cancer initiation. FOXM1 expression increases at the entry of the S-phase of the cell cycle, remains stable during G2/M phase, before it is degraded at mitotic exit.(Laoukili *et al*, 2005, 2008) FOXM1 also controls mitosis through regulating the transcription of the mitotic regulatory genes, including PLK, cyclin B1, Aurora A and B kinases (Wang *et al*, 2005) and in addition, it play a major role in maintaining chromosome stability.(Laoukili *et al*, 2005) FOXM1 has an important role in cell cycle progression and cell proliferation. As such, its expression levels correlate with the proliferative state of a cell. In fact, FOXM1 is highly expressed in all embryonic tissues, and in particular in proliferating cells of epithelial and mesenchymal origin.(Gemenetzidis *et al*, 2010) Its expression is also detected at increased levels in numerous human cancer cell lines and is associated with the development and progression of many malignancies(Huynh *et al*, 2011; Wang *et al*, 2011), high proliferation rates, drug(Khongkow *et al*, 2013; Li *et al*, 2013; Monteiro *et al*, 2013) and poor prognosis in many cancer types.(Liu *et al*, 2006; Bektas *et al*, 2008; Martin *et al*, 2008; Chu *et al*, 2012; Xia *et al*, 2012).

B-lymphoblastic leukaemia (B-ALL) is a malignant disorder which derives from clonal proliferation of lymphoid precursors with arrested maturation. The involvement of FOXM1 in B-ALL progression and therapy has not been investigated so far. A previous study by Nakamura *et al*. has investigated the cell proliferation role of FOXM1 in myeloid leukaemia, showing its capability to promote cell cycle progression.(Nakamura *et al*, 2010) Another report by Uddin *et al.* has also described the involvement of FOXM1 in B-cell lymphoma migration and invasion.(Uddin *et al*, 2012) Other studies have also demonstrated that FOXM1 downregulation provokes the inhibition of cell proliferation in B-lymphoma(Wang *et al*, 2013) and very recently it has pointed out that FOXM1 pathway could be a potential therapeutic target in B cell malignancy.(Zhao *et al*, 2014) The fact that FOXM1 is an oncogene that promote tumor progression and that it is up-regulated in relapsed B-ALL patients(Bhatla *et al*, 2012) prompted us to investigate a potential role of

FOXM1 in B-ALL cell proliferation with the aim of understanding if it can be targeted to increase the efficiency of chemotherapeutic treatment, and to overcome drug resistance in this haematological malignancy.

1.4.3 MATERIALS AND METHODS

Primary leukaemia cell cultures

The mRNA and protein samples of PBMC from healthy donors were obtained from cells separated by Ficoll-Paque centrifugation. Diagnostic RNA samples of bone marrow (BM) aspirates of B-leukaemic patient's with a blast count of 80–95 % were kindly allowed from the cell bank of the Dipartimento di Salute della Donna e del Bambino, University of Padova, Italy. B-ALL patient samples were obtained after informed consent following the tenets of the Declaration of Helsinki. The study was approved by the Italian Association of Pediatric Onco-Hematology (AIEOP). All analyzed BCP-ALL samples were obtained at the time of diagnosis before treatment, after Ficoll-Hypaque (Pharmacia, Uppsala, Sweden) separation of mononuclear cells as described previously.(Accordi *et al*, 2013) The percentage of $CD19^+$ cells ranged from 80% to 95%. Human B-leukaemia cell lines, REH, SEM, MHH-CALL2, RS4;11 and NALM-6, were grown in RPMI-1640 medium (Gibco, Milano, Italy) all supplemented with 115 units/mL penicillin G (Gibco, Milano, Italy), 115 μg/mL streptomycin (Invitrogen, Milano, Italy), 10 % fetal bovine serum (Invitrogen, Milano, Italy), and maintained at 37 °C in a humidified atmosphere with 5 % CO_2.

Quantitative Real time PCR

Total RNA was isolated from frozen cell pellets using the RNeasy Mini kit (Qiagen, UK) according to manufactures' instructions and RNA purity and concentration were determined by measuring the spectrophotometric absorption at 260 nm and 280 nm on NanoDrop ND-1000. 1 μg of total RNA was reversed transcribed into first starnd cDNA using Superscript III first stand cDNA synthesis (Life technologies, UK) Briefly, 1 μl of 50 μM oligo(dT)20 and 1 μl of 10 mM dNTPs mix were added to the RNA before the volume was adjusted to 11 μl using Rnase–free water. Samples were denaturated at 65 ºC for 5 min and then quickly chilled on ice for 1 min. Subsequently, 1 μl of the reverse transcriptase Superscript III (200U/ μl) was added, along with 1 μl 0.1 M DTT, 1 μl Rnase OUT

Recombinase Inhibitor and 1 x First Stand Buffer. The solution was incubated at 25 ºC for 5 min then heated at 50 ºC for 50 min. The reaction was inactivated by heating at 70 ºC for 15 min. For real-time quantitative PCR, 1 µl of cDNA was used as template in a 24 µl reaction carried out with Power SYBR Green kit (Applied Biosystems, UK) with ABI 7800 system (Applied Biosystems, UK). The mRNA levels of target genes were calculated relative to the expression of L19 mRNA levels using the ΔCt method.

Primers used: FOXM1-fwd 5'TGCAGCTAGGGATGTGAATCTTC3'; FOXM1-rv 5' GGAGCCCAGTCCATCAGAACT3'; MKI67-F, 5'- CGACGGTCCCCACTTTCC-3'; MKI67-R,5' GCTGGATACGGATGTCACATTC-3'; CCNB1-F, 5'-CAGTTATGCAGCACCTGGCTAAG-3'; CCNB1-R, 5'-TGTGGTAGAGTGCTGATCTTAGCAT-3' ;AURKB-F, 5'-CAGTGGGACACCCGACATC-3' ; AURKB-R, 5'-GCCCAATCTCAAAGTCATCAATT-3' ; L19-F ; 5'- GCGGAAGGGTACAGCCAAT-3' ; L19-R, 5'- GCAGCCGGCGCAAA-3'.

Western Blot Analysis

REH, SEM, MHH-CALL2, RS4;11 and NALM-6, after experimental conditions, were collected, centrifuged, and washed two times with ice cold phosphate buffered saline (PBS). For western blot analysis cells were lysed as described previously.(Hui *et al*, 2008) Proteins were resolved by sodium dodecyl sulphate-polyacrylamide gel electrophoresis (SDS−PAGE) (using 7 or 10 % acrylamide gels), transferred to PVDF Hybond-P membrane (GE Healthcare) and immunoblotted with primary antibodies against, FOXM1 (Santa cruz, C-20), β-Tubulin (Santa cruz), Aurora B (Cell Signalling), Cyclin B1 (Santa cruz). The membranes were washed four times with Tris-Buffered Saline and Tween 20 (TBS-T) for 15 min prior to incubation with the respective peroxidise (HRP)-conjugated secondary antibody (Dako, Ely, UK), at 1:2000 dilution for 30 min at room temperature and again washed four times with TBST-T for 20 min. Protein were visualised using enhanced chemiluminescence (ECL) detection system (PerkinElmer, Seer Green, UK) with Amsterdam Hyperfilm ECL (GE Helthcare, Little Chalfont, UK) and signal was detected using the SRX-101A X-ray developer (Konica Minolta, Tokio, Japan).

RNA interference with small interfering RNAs (siRNAs)

For FOXM1 silencing, REH or NALM-6 cells were transiently transfected with siRNA SMARTpool reagents purchased from Thermo Scientific Dharmacon (Lafayette, CO, USA) using the transfection reagent Oligofectamine (Life Technologies, UK) according to the manufactures instructions. SMARTpool siRNAs used were: siRNA FOXM1 (l-009762-00) and the non-specific (NS) control siRNA, ON-TARGET*plus* Non-Targeting pool (D-001810-10) confirmed to have minimal targeting of known genes. All siRNA pools were resuspended to 20 µM in 1x siRNA buffer.

Annexin-V assay.

Surface exposure of phosphatidylserine on apoptotic cells was measured by flow cytometry with a Coulter Cytomics FC500 (Beckman Coulter) by adding annexin-V conjugated to fluorescein isothiocyanate (FITC) to cells according to the manufacturer's instructions (Annexin-V Fluos, Roche Diagnostic). Simultaneously, the cells were stained with PI. Excitation was set at 488 nm, and the emission filters were at 525 and 585 nm, respectively, for FITC and PI.

Flow cytometric analysis of cell cycle distribution.

For flow cytometric analysis of DNA content, 5×10^5 of REH, and NALM-6 cells were either treated with 0.5 µM and 1µM of thiostrepton or knocked-down for FOXM1 and after 24, 48 and 72 h of treatment or knockdown, cell cycle analysis was performed as previously described.(Bortolozzi *et al*, 2014)

Drugs Combination studies

Cell proliferation was assessed by MTT (3-4,5-dimethylthiazol-2-yl-2,5-diphenyl tetrazolium bromide) assay after treatment. Equal concentrations of cells were plated in triplicate in a 96-well plate and incubated with 10 µl of MTT (Sigma-Aldrich, St Louis, MO, USA) for 4 h. Absorbance was measured at 562 nm using Victor^{3TM} 1420 Multilabel Counter (PerkinElmer, Waltham, MA, USA). Cells were treated for 48 h using scalar dilutions of thiostrepton (Sigma-Aldrich), combined with cytarabine (Aractyn, Pfizer), daunorubicin (Pfizer), vincristine, dexamethasone (Sigma-Aldrich). Thiostrepton was also added to drug solutions at fixed combination ratios. The effectiveness of various drug

combinations was analyzed by the Calcusyn Version 2.1 software (Biosoft). The combination index (CI) was calculated according to the Chou-Talalay method.(Chou, 2010) A combination index of 1 indicates an additive effect of the 2 drugs. Combination index values less than 1 indicate synergy, and combination index values more than 1 indicate antagonism.

Statistical Analysis

Results are presented as the mean ± SEM. The differences between different conditions were analyzed using the two-sided Student's t test. P values lower than 0.05 were considered significant. *, $p \leq 0.05$: **, $p \leq 0.01$, ***$p \leq 0.001$.

1.4.4 RESULTS

FOXM1 is overexpressed in B lymphoblastic leukaemic patients

To investigate if FOXM1 transcription factor plays a role in B lymphoblastic leukaemia (B-ALL) proliferation, we analyzed FOXM1 mRNA levels in ten B-ALL pediatric patients and peripheral blood mononuclear cells (PBMC) from healthy donors. For these experiments, the mRNA was extracted from cell pellets of patients recruited at the time of diagnosis. In particular, the first two patients selected were characterized by chromosomal translocations at chromosome 12 and 21 [t(12;21)]; patients 3, 4 and 5 carried the translocation between the chromosome 9 and 22 [t(9;22)], whereas the other five patients were without translocations (**Table S1, supplementary information**). As shown in **Figure 1A**, RT-qPCR data showed that FOXM1 mRNA levels were significantly higher in patients compared to the samples of healthy donors. Interestingly, associated with higher levels of FOXM1 mRNA, there was a significant increment of Cyclin B1 and Aurora B mRNA levels, two genes whose expression is directly regulated by FOXM1 (**Figure S1, supplementary information**). In addition to mRNA levels, protein expression was also examined by western blot analysis. As shown in **Figure 1B**, the expression of FOXM1 as well as its targets Aurora B and Cyclin B1 was generally higher compared to healthy cells, confirming higher FOXM1 activity.

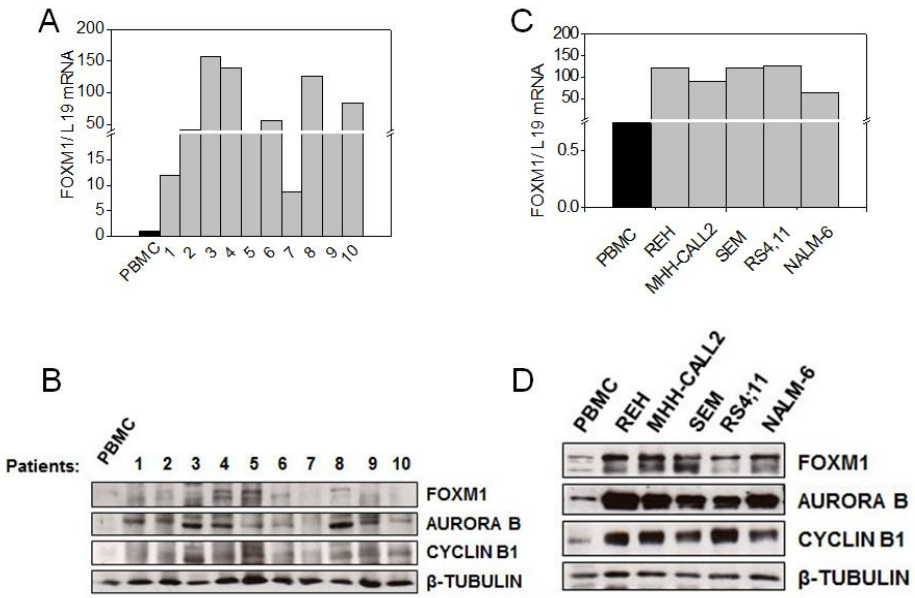

Figure 1. FOXM1 is higher expressed both in B-ALL patients and in B-ALL cell lines compared to healthy donors. A) Basal FOXM1, mRNA levels were analyzed in ten samples of B-ALL patient's and compared to peripheral blood mononuclear cells (PBMC) of healthy donors by RT-qPCR. B) FOXM1 is overexpressed in B-ALL cell lines. Total RNA from five B-ALL cell lines (REH, MHH-CALL2, SEM, RS4;11, NALM-6) was extracted and FOXM1, mRNA levels were analyzed and compared to PBMC of healthy donors by RT-qPCR. The results were normalised with L19 mRNA levels using the DDCt method The median of threshold cycles (Ct) values were normalized to the median of Ct values of the L19 mRNA levels. Results are the average ± SD of three independent experiments in triplicate. C) Cell lysates were obtained from ten B-ALL patients and analyzed for the expression of FOXM1 and its downstream target genes Cyclin B1 and Aurora B in comparison to PBMC. D) REH, MHH-CALL2, SEM, RS4;11, NALM-6 cell lysates were collected at basal conditions for subsequent western blot analysis for the indicated antibodies.

Similar results were obtained when the mRNA or protein expression levels of B-ALL patients were compared to those from CD19 positive cells isolated from healthy donors. In this case due to the scarcity of the protein extract we have performed western blot analysis utilizing the bone marrow of further ten patients, without translocation, obtaining similar results (**figure S2, supplementary information**). Taken together, these data showed that the expression levels and activity of FOXM1 are increased in B-ALL patient samples when compared to healthy lymphocytes, suggesting that FOXM1 plays a key function in supporting the cell proliferation and progression of B-ALL.

FOXM1 is overexpressed in B-ALL cell lines

Next, we investigated the FOXM1 expression levels in five different B-ALL cell lines. More specifically, we analyzed the mRNA levels of FOXM1, at basal conditions, comparing five different B-ALL cell lines (REH, MHH-CALL2, SEM, NALM6, RS4;11) with mRNA samples of PBMC obtained from healthy donors. RT-qPCR analysis showed in **Figure 1C** reveals that FOXM1 mRNA levels were significantly higher in B-ALL cell lines when compared to normal lymphocytes and this pattern was again accompanied by increased transcriptional levels of Cyclin B1 and Aurora B (**Figure S2, supplementary information**). In agreement with the mRNA expression patterns, western blot analysis revealed that FOXM1 expression was generally higher in leukaemic cells compared to normal lymphocytes. This was again associated with Cyclin B1 and Aurora B up-regulation in leukaemic cells (**Figure 1D**). Similar results were obtained when FOXM1 mRNA and protein expression was examined in B-ALLs isolated from patients and healthy $CD19^+$ cells (**figure S2, supplementary information**).

Knockdown of FOXM1 decreases cell proliferation in B-ALL cell lines and induces a G2/M cell cycle arrest

To test if FOXM1 has a role in promoting B-ALL proliferation, we knocked-down its expression in two B-ALL cell lines REH and NALM-6 using a specific FOXM1 siRNA pool and assessed their cell viability after 24, 48, and 72 h post-transfection. FOXM1 silencing was confirmed by western blot and RT-qPCR analysis (**Figure 2A-D**). Aurora B and Cyclin B1 protein levels were clearly downregulated in FOXM1-depleted NALM-6 and REH cells compared to cells transfected with non-specific (NSC) control siRNA pool (**Figure 2A and 2B**). Furthermore, in both REH and NALM-6 cell lines, RT-qPCR analysis revealed a significant decrease in Aurora B mRNA levels, although Cyclin B1 mRNA levels appeared significantly decreased only in REH cells and not in NALM-6 (**Figure 2C and 2D**).

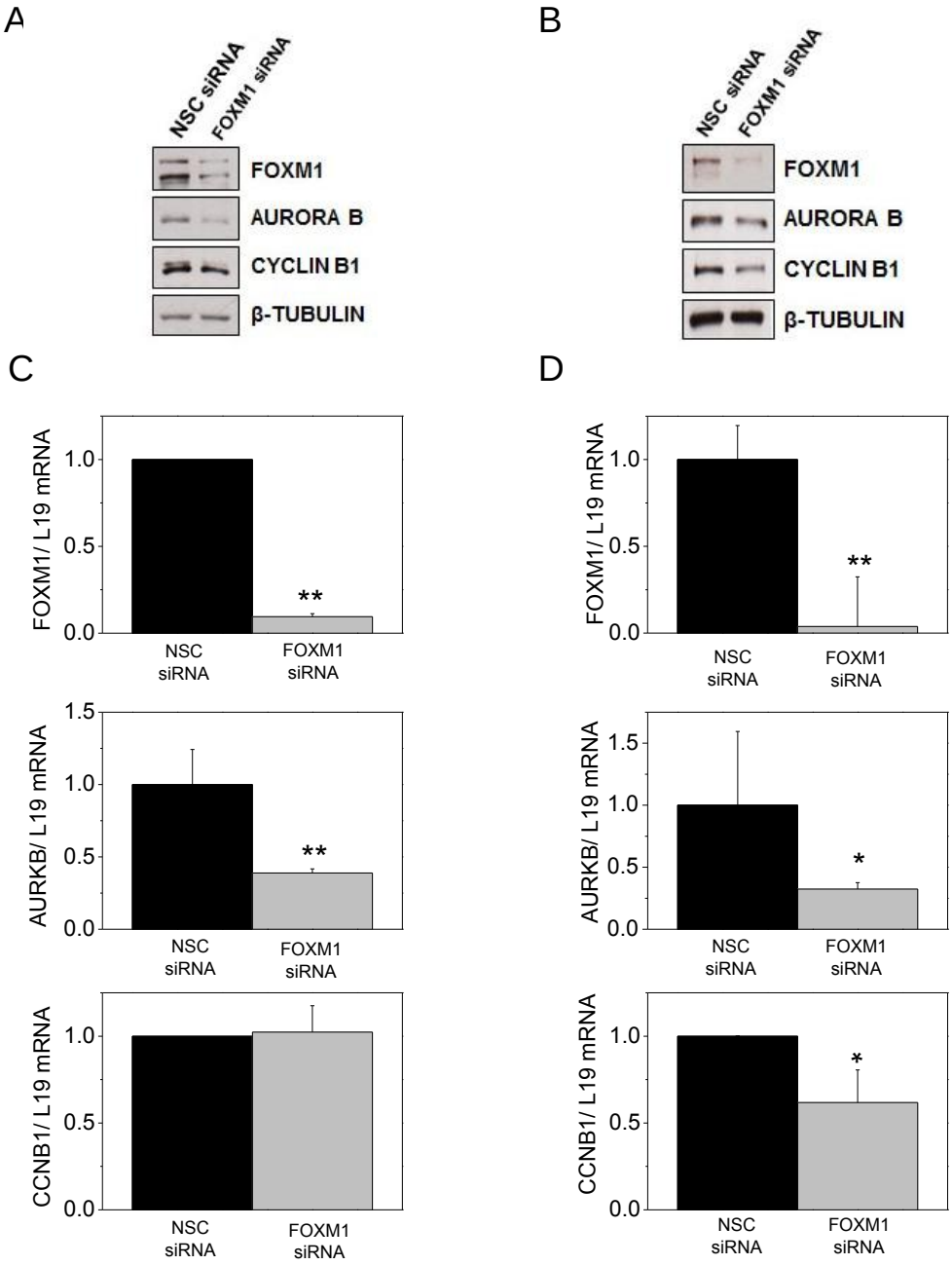
A
NSC siRNA
FOXM1 siRNA
FOXM1
AURORA B
CYCLIN B1
β-TUBULIN
B
NSC siRNA
FOXM1 siRNA
FOXM1
AURORA B
CYCLIN B1
β-TUBULIN
C
FOXM1/ L19 mRNA
1.0
0.5
0.0
**
NSC siRNA
FOXM1 siRNA
AURKB/ L19 mRNA
1.5
1.0
0.5
0.0
**
NSC siRNA
FOXM1 siRNA
CCNB1/ L19 mRNA
1.0
0.5
0.0
NSC siRNA
FOXM1 siRNA
D
FOXM1/ L19 mRNA
1.0
0.5
0.0
**
NSC siRNA
FOXM1 siRNA
AURKB/ L19 mRNA
1.5
1.0
0.5
0.0
*
NSC siRNA
FOXM1 siRNA
CCNB1/ L19 mRNA
1.0
0.5
0.0
*
NSC siRNA
FOXM1 siRNA

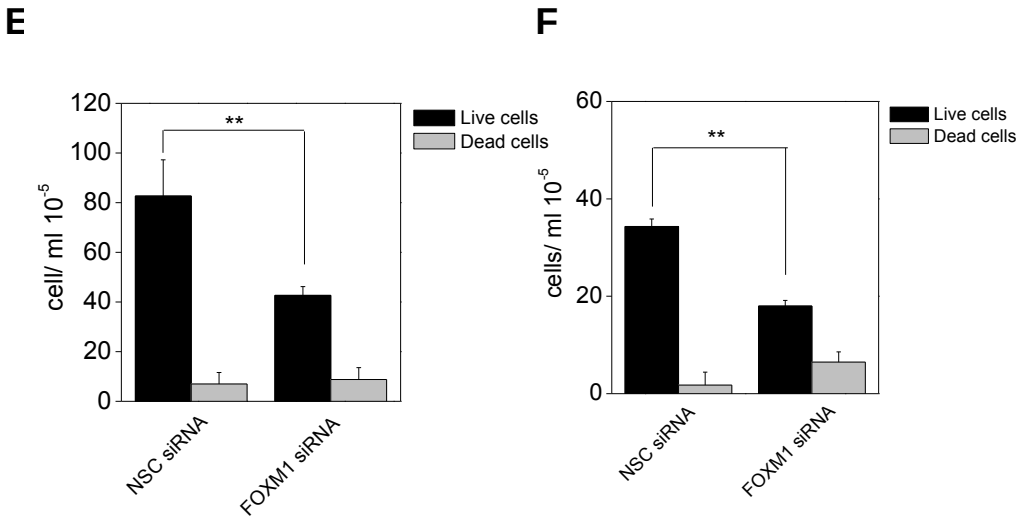

Figure 2. FOXM1 knockdown in REH and NALM6 cells induces a significant decrease in cell proliferation. NALM-6 (A) and REH (B) were transfected with the siRNA FOXM1 and the non-specific (NSC) control siRNA. Western blot analysis and RT-qPCR confirmed the knockdown of endogenous FOXM1 and the reduced expression of Aurora B and Cyclin B1 in NALM-6 cells (C) and REH cells (D). Cell viability analysis, was performed by tripan blue assay, after 72 h of transfection in NALM-6 (E) and after 48 h of transfection in REH (F). Data are presented as mean ± SD of three independent experiments. Statistical analysis was performed using Student's t-tests against the cells transfected with the non-specific (NS) control siRNA. *, $p \leq 0.05$: ** $p \leq 0.01$

Cell proliferation analysis assessed by tripan blue exclusion assay, revealed that upon FOXM1 depletion, there was a significant decrease on cell proliferation after 72 h of transfection in NALM-6 (**Figure 2E**) and after 48 h in REH cells (**Figure 2F**), suggesting that FOXM1 plays an important role in B-ALL cell proliferation. Tripan blue negative population (live cells) was strongly decreased in cells that were knocked-down for FOXM1, and this pattern was associated with no significant changes on dead cell levels (tripan blue positive) in NALM-6, and only with a slight increase in the percentage of dead cells in REH. These results pointed out that FOXM1 play an important role in B-ALL cell proliferation.

To further analyze the role of FOXM1 on cell cycle progression in B-ALL, we analyzed the cell-cycle phase distribution in NALM-6 and REH cells following FOXM1 knockdown. As shown in **Figure 3A and 3B** in both cell lines, there was a significant increase of the percentage of cells in G2/M and a corresponding decrease of cells in S phase compared with non-specific (NSC) control cells.

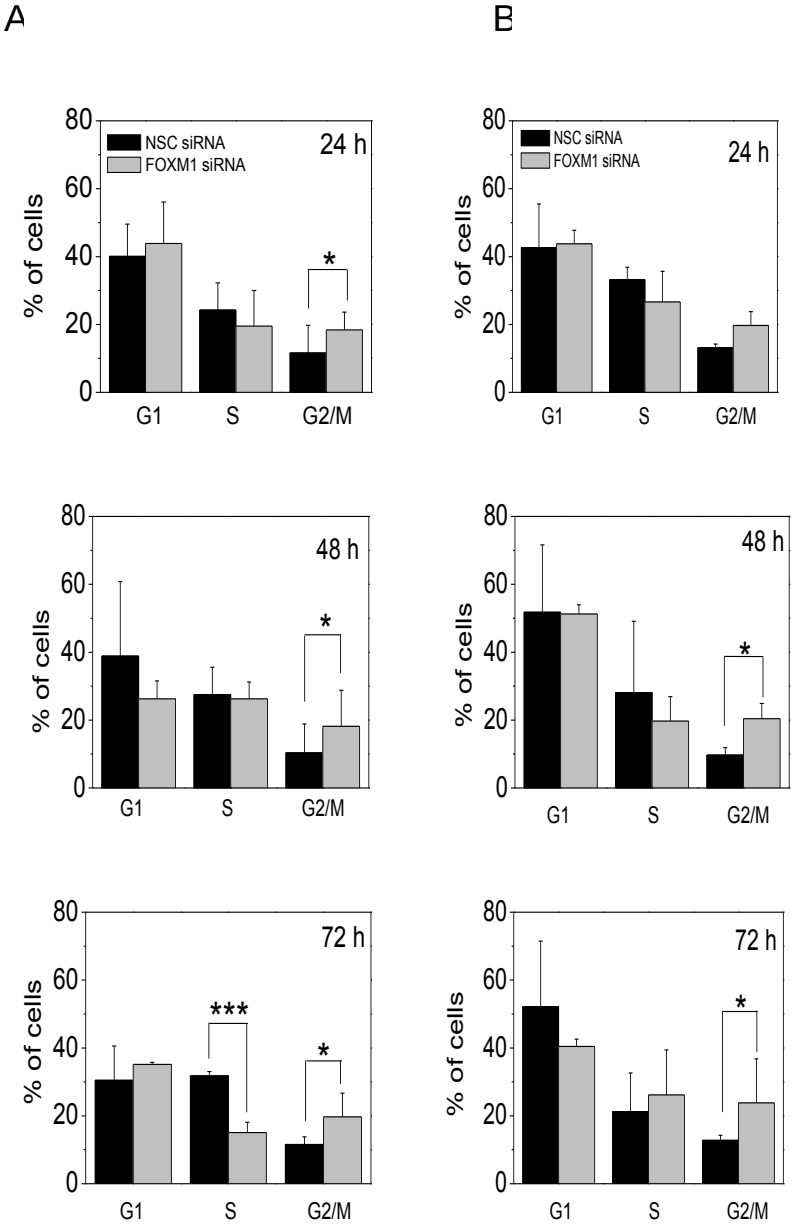

Figure 3. FOXM1 downregulation in REH and NALM6 cells by a specific FOXM1 siRNA pool induce a G2/M cell cycle arrest. In NALM-6 (A) and REH cell (B) lines the endogenous FOXM1 expression was blocked by knockdown performed by using Oligofectamine™ Transfection protocol. After 24, 48 and 72 h of knockdown, cell cycle analysis was performed to investigate the effect of FOXM1 inhibition in cell cycle-phase progression. Results are the average ± SD of three independent experiments in triplicate. Statistical analysis was performed using Student's t-tests against the cells transfected with the non-specific (NSC) siRNA. *, $p \leq 0.05$: **, $p \leq 0.01$, ***$p \leq 0.001$. Effect of FOXM1 knockdown on the expression of proteins involved in cell cycle regulation. In NALM-6 (C) and REH (D) cell lines the endogenous FOXM1 expression was blocked by knockdown and after 48 h, cell were collected, and protein extracts were subjected to western blot analysis for the indicated antibodies.

FOXM1 knockdown reduce the expression of cell cycle regulators

We next evaluated if FOXM1 knockdown induces a modulation of the expression of proteins involved in late phase cell cycle regulation. As depicted in **figure 3,** the silencing of FOXM1 both in NALM-6 (**figure 3C**) and in REH cells (**figure 3D**), caused the downregulation of several cell cycle regulatory proteins such Cyclin B1, Aurora B, Survivin, and Cdc25b that are involved in mitotic progression.

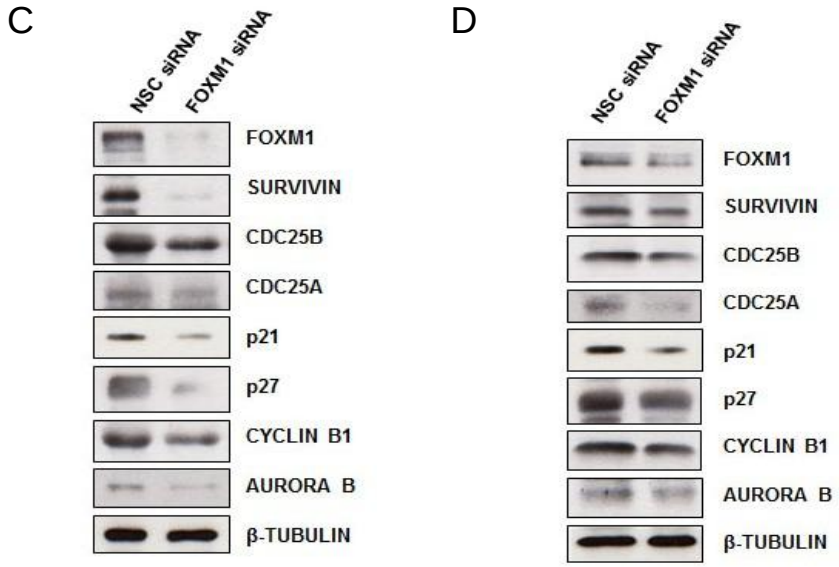

Figure 3 bis. FOXM1 downregulation in REH and NALM6 cells by a specific FOXM1 siRNA pool induce a G2/M cell cycle arrest. Effect of FOXM1 knockdown on the expression of proteins involved in cell cycle regulation. In NALM-6 (C) and REH (D) cell lines the endogenous FOXM1 expression was blocked by knockdown and after 48 h, cell were collected, and protein extracts were subjected to western blot analysis for the indicated antibodies.

The expression of the S-phase promoting Cdc25a phosphatase which plays a major role in G1/ S progression, dephosphorylating Cdk2 and activating CDK2-cyclin E activity (Nilsson & Hoffmann, 2000; Bertoli *et al*, 2013) was strongly reduced. Interestingly, both $p27^{Kip1}$ and $p21^{Cip/Waf1}$, two cyclin-dependent kinase inhibitors (CKI) proteins, which also play a role in the assembly of cyclin-CDK complexes were also downregulated. Altogether these results indicate that FOXM1 is strongly involved in modulating the expression of cell cycle regulatory proteins at both G1/S and at G2/M transitions.

Thiostrepton treatment induces a decrease in cell viability and induce a G2/M arrest

To further confirm the role of FOXM1 on B-ALL cell proliferation, we treated cells with a thiazole ring containing antibiotic, thiostrepton, a well-established specific FOXM1 inhibitor.(Kwok *et al*, 2008; Hegde *et al*, 2011) This drug causes growth inhibition in a small panel of B-ALL cell lines with GI_{50} in the micromolar and submicromolar range (**Figure S5, Supplementary information**). In this context, we treated both NALM-6 and REH cell lines with two different concentrations of thiostrepton, 0.5 µM and 1 µM, respectively for 24, 48, and 72 h. The results showed a significant reduction in cell viability, revealed by the considerable low numbers of trypan bluee negative cells in both NALM-6 and REH cell lines (**Figure4 and 5A**).

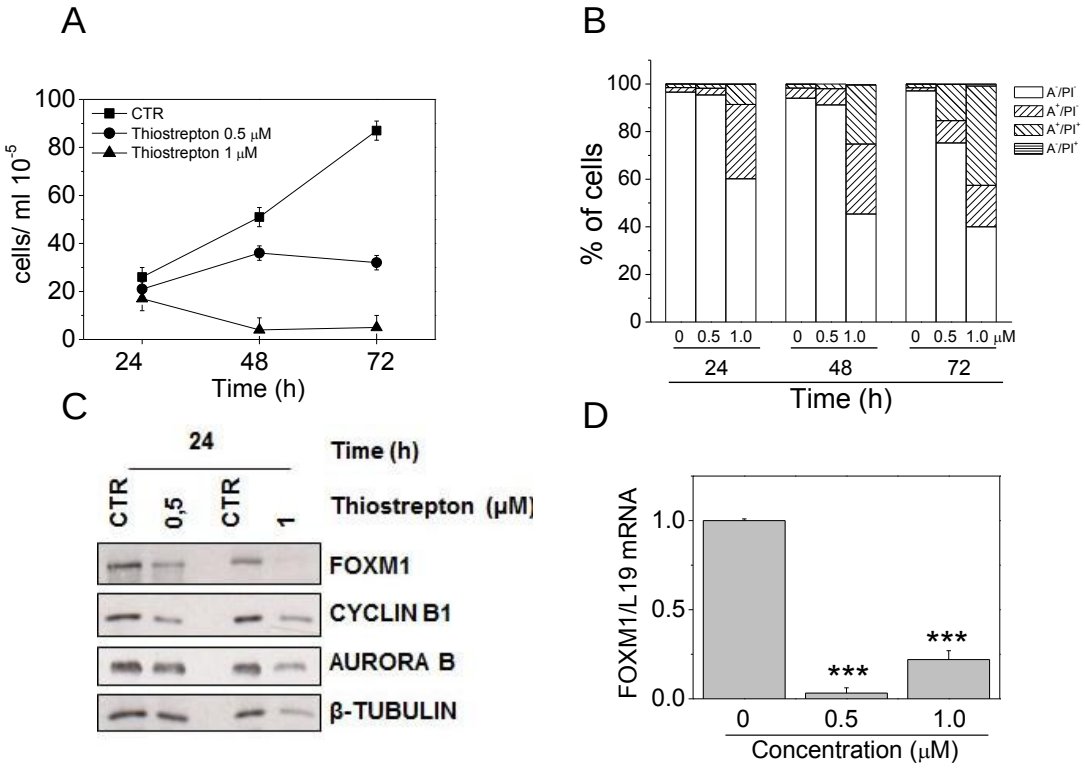

Figure 4. FOXM1 inhibition in NALM-6 cells by thiostrepton treatment induce apoptosis**.** NALM-6 cells were treated with thiostrepton at the concentration of 0.5 µM or 1 µM, for 24, 48 and 72 h. Cell viability analysis was performed by tripan blue assay (A) whereas induction of apoptosis was assessed by flow cytometry after staining of the cells with Annexin-V-FITC and propidium iodide (B). Dual staining permits discrimination between live cells (annexin-V^-/PI^-), early apoptotic cells (annexin-V^+/PI^-), late apoptotic cells (annexin-V^+/PI^+) and necrotic cells (annexin-V^-/PI^+). (C) and RT-qPCR analysis (D) confirmed that

thiostrepton reduce FOXM1 expression. Data are presented as mean ± SD of three independent experiments. Statistical analysis was performed using Student's t-tests against the control sample (untreated). ** $p \leq 0.01$

Moreover flow cytometric analysis carried out after different times of treatment indicate that thiostrepton induce apoptosis as demonstrated by the appearance of a large percentage of annexin-V positive cells in both cell lines (Figures 4B and 5B). It important to note that apoptosis occur in a concentration- and time-dependent manner. FOXM1 downregulation was confirmed by western blot analysis (**Figure 4C and 5C**) and by RT-qPCR (**Figure 4D and 5D**). It is also notable that in both cell lines FOXM1 protein levels along with its downstream target genes, were decreased after treatment with thiostrepton in a similar manner to that observed for FOXM1 silencing.

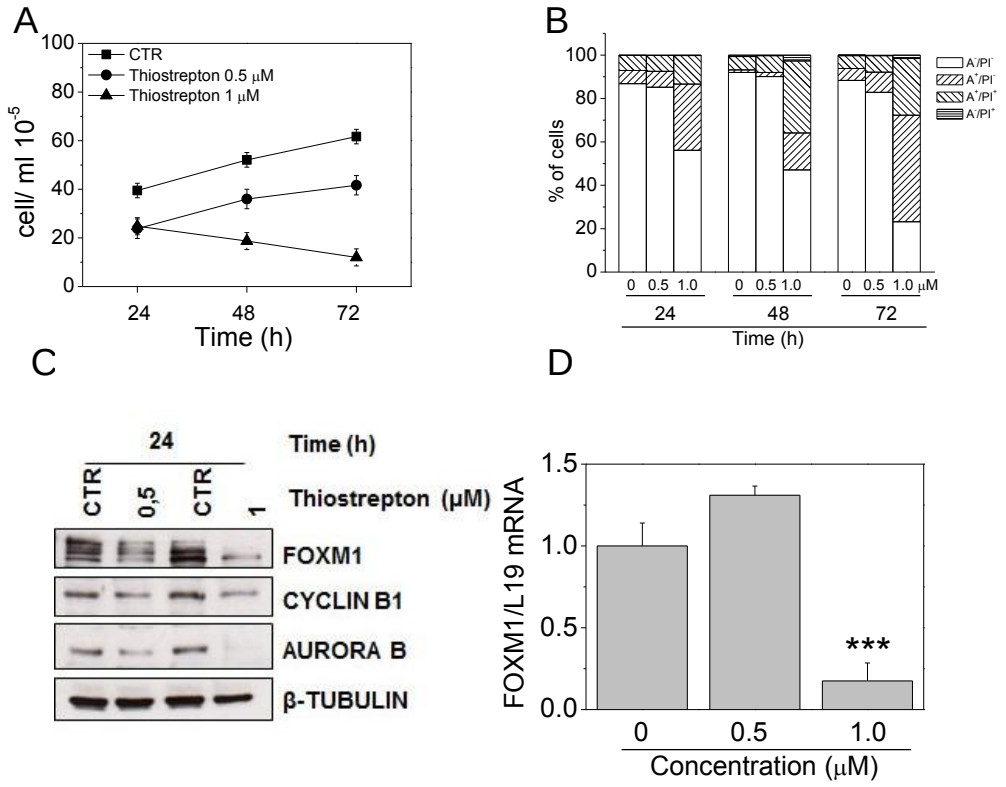

Figure 5. FOXM1 inhibition in REH cells by thiostrepton treatment induce apoptosis. REH cells were treated with thiostrepton at the concentration of 0.5 μM or 1 μM, for 24, 48 and 72 h. Cell viability analysis was performed by tripan blue assay (A) whereas induction of apoptosis was assessed by flow cytometry after staining of the cells with Annexin-V-FITC and propidium iodide (B). Dual staining permits discrimination between live cells (annexin-V^-/PI^-), early apoptotic cells (annexin-V^+/PI^-), late apoptotic cells (annexin-V^+/PI^+) and necrotic cells (annexin-V^-/PI^+). (C) and RT-qPCR analysis (D) confirmed that thiostrepton

reduce FOXM1 expression. Data are presented as mean ± SD of three independent experiments. Statistical analysis was performed using Student's t-tests against the control sample (untreated). ** $p \leq 0.01$

We also analyzed the cell-cycle phase distribution in REH and NALM-6 cells following the treatment with both 0.5 μM and 1 μM concentrations of thiostrepton at 24, 48, and 72 h. The results (**Figure 6A and 6B**) showed that in a similar manner, thiostrepton treatment induced an arrest in G2/M cell-cycle phase along with a decrease of the S phase.

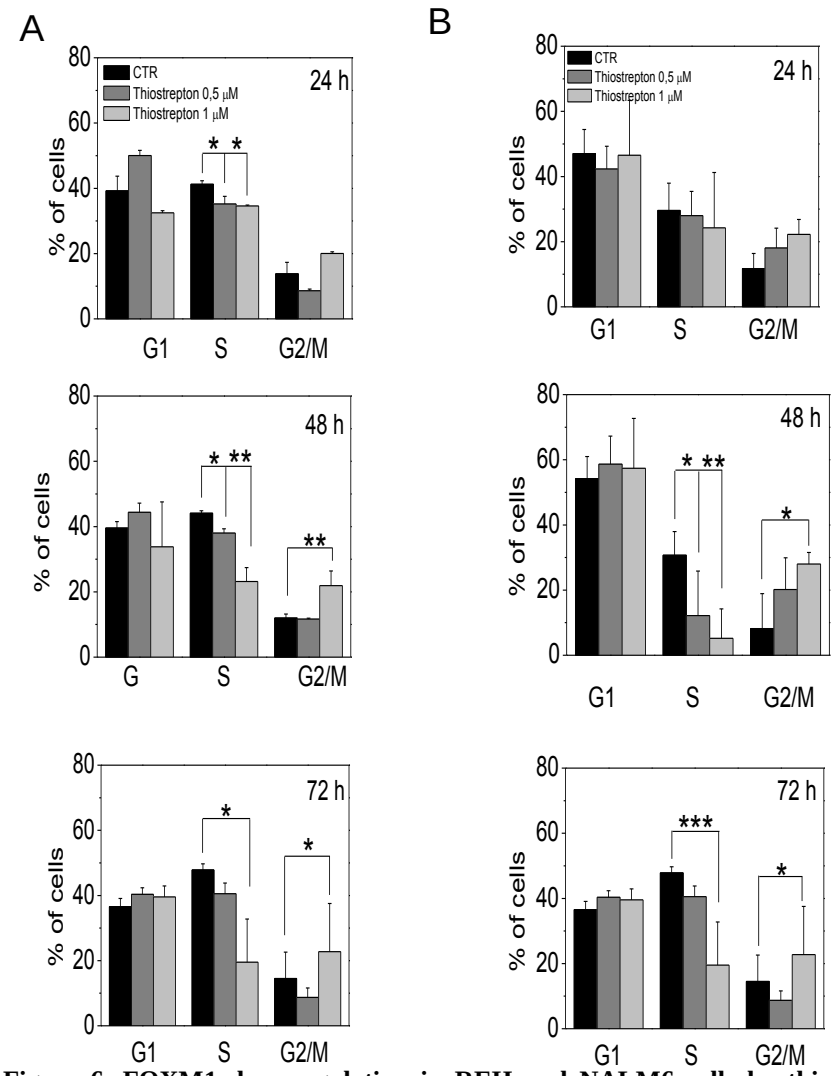

Figure 6. FOXM1 downregulation in REH and NALM6 cells by thiostrepton treatment induces a G2/M cell cycle arrest. NALM-6 (A) and REH cell (B) lines were treated with the indicated concentration of thiostrepton. After 24, 48 and 72 h of treatment, cell cycle analysis was performed to investigate the effect of FOXM1 inhibition in cell cycle-phase progression. Results are the average ± SD of three independent experiments in triplicate. Statistical analysis was performed using Student's t-tests against the untreated cells. *, $p \leq 0.05$: **, $p \leq 0.01$, ***$p \leq 0.001$.

Thiostrepton synergises with conventional chemotherapeutic agents in inhibiting B-ALL proliferation

Since FOXM1 downregulation led to a decrease in B-ALL cell proliferation, we next tested if thiostrepton can be used in combination with the most commonly used chemotherapeutics in B-ALL treatment. To this end, four different B-ALL cell lines, two glucocorticoid-resistant (REH, SEM) and two glucocorticoid-sensitive (NALM-6, RS4;11) were then treated for 48 h with thiostrepton in combination with chemotherapeutic agents (i.e. dexamethasone, asparaginase, daunorubicin, vincristine and Ara-C) used normally to treat pediatric B-ALL patients. More specifically, thiostrepton was combined with different drugs at fixed molar combination ratio, and cell viability analyzed by MTT assay (**Figure 7A and figures S6-S8**).

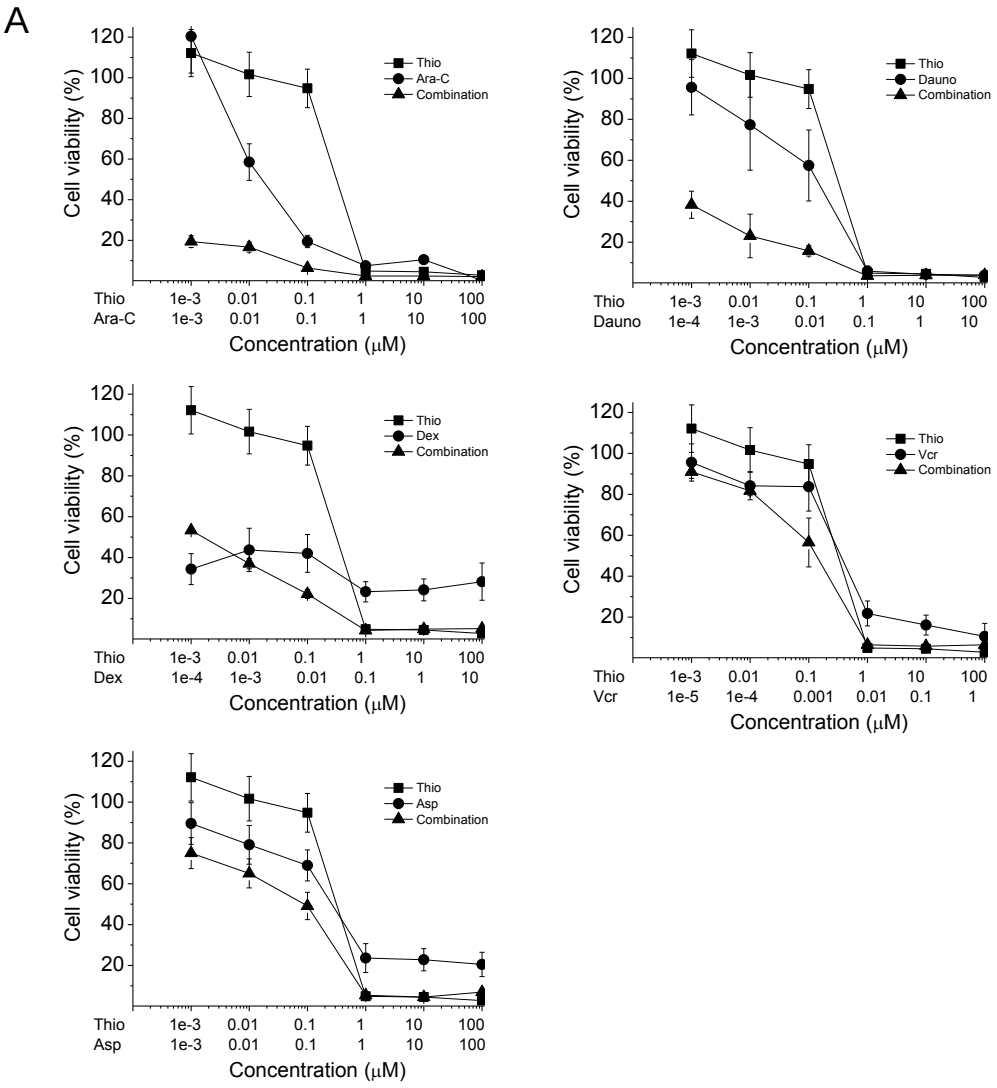

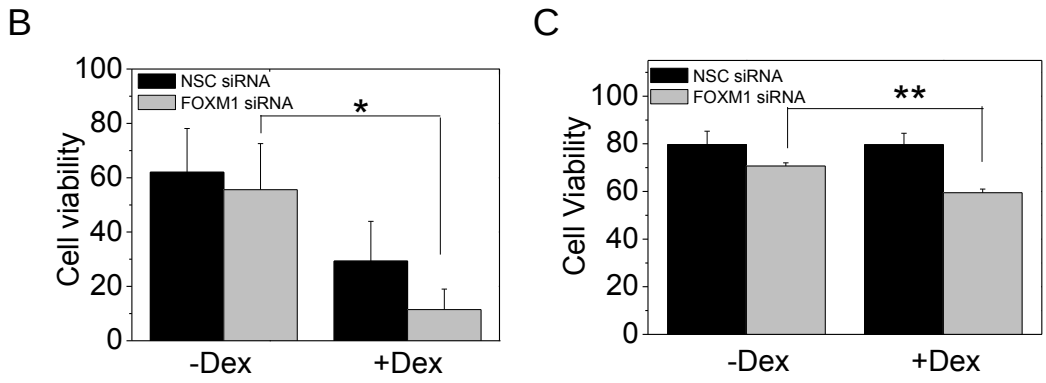

Figure 7. Effect of thiostrepton treatment alone and in combination with different chemotherapic drugs in NALM-6 cells (A). Cells were treated at the indicated concentration and at fixed combination ratio and viability was assessed by MTT test after 48 hof incubation. Data are expressed as mean ± SEM of three independent experiments. NALM-6 (B) and REH (C) cells were knocked down for FOXM1 and after 48 h were further treated for 48 h with dexamethasone at the concentration of 1 µM. Cell viability was analyzed by flow cytometry after double staining of the cells with Annexin-V-FITC and PI. Result are expressed as mean ± SD of three independent experiments. Statistical analysis was performed using Student's t-tests against the cells transfected with the non-specific (NSC) siRNA. *, $p \leq 0.05$: **, $p \leq 0.01$

As described above, thiostrepton alone has a significant cytotoxicity when used as single agent. More importantly, when used in combination with chemotherapic drugs, we observed a synergistic increase of their cytotoxicity as demonstrated by the values of combination index (CI) according to Chou and Talalay.(Chou, 2006, 2010) As depicted in **Table 1** which reports CI values calculated at GI_{50}, GI_{75} and GI_{90}, revealed that in almost all cell lines tested, thiostrepton and chemotherapeutic drugs acted in a synergistic fashion (CI<1). Our results therefore show that in general, the pharmacological downregulation of FOXM1 caused by thiostrepton, can significantly increase the cell death effects provoked by the treatment with the conventional chemotherapeutic agents used alone.

Table 1. Combination index values (CI) in B-ALL cell lines treated with thiostrepton in combination with chemotherapic drugs.

	GI_{50} [b]	GI_{75} [b]	GI_{90} [b]
Dauno (1:10)[a]			
RS4;11	2.4	0.17	0.01
SEM	0.27	0.28	0.35
NALM-6	0.06	0.12	0.25
REH	0.84	1.1	1.1
Ara-C (1:1) [a]			
RS4;11	0.07	0.02	0.006
SEM	0.33	0.35	0.42
NALM-6	0.0017	0.001	0.09
REH	0.16	0.29	0.54
Dex (1:10) [a]			
RS4;11	0.10	0.9	8.0
SEM	0.18	0.15	0.13
NALM-6	0.8	0.044	0.24
REH	1.1	0.97	0.85
Vcr (1:1000) [a]			
RS4;11	0.04	0.02	9.5
SEM	1.1	0.75	0.6
NALM-6	0.64	0.44	0.74
REH	0.09	0.02	0.01
Asp (1:1) [a]			
RS4;11	0.5	0.2	0.1
SEM	1.6	0.8	0.4
NALM-6	0.10	0.13	0.5
REH	1.3	0.05	0.15

[a] Molar ratio with thiostrepton. [b] Growth inhibition determined after 48 h of treatment by MTT test. Abbreviations: Ara-C, cytarabine; CI, combination index; Dex, dexamethasone; Dauno, daunorubicin; Vcr, vincristine. Synergy, additivity and antagonism are defined by a CI<1, CI=1 or CI>1, respectively.

To further prove this last assumption, we knocked down FOXM1 in REH and NALM-6 cells using siRNA and treated them with dexamethasone. After 48 h of treatment we analyzed cell viability by flow cytometry staining with Annexin-V and propidium iodide (PI). The result showed (**Figure 7A and 7B**) a significant decrease in cell viability after 48 h of treatment in FOXM1 silenced cells compared to the controls, in particular in

glucocorticoid resistant cells, indicating that FOXM1 can be an important therapeutic target for overcoming glucocorticoid resistance in B-ALL.

1.4.5 DISCUSSION

FOXM1 is an important regulator of the cell cycle and plays a crucial role in tumorigenesis. Its overexpression has been also found in many different human cancers. Very little is known about its function in haematological malignancies. Our aim was to investigate the role of FOXM1 in B-ALL, the most common pediatric leukaemia. RT-PCR analysis performed on ten B-ALL patient samples showed that FOXM1 mRNA, is highly overexpressed in comparison to lymphocytes derived from healthy donors. Accordingly, this pattern was closely related to an increase in transcript levels of Cyclin B1 and Aurora B, two G2/M phase regulators directly regulated by FOXM1. Immunoblot analysis also demonstrated similar overexpression of FOXM1 and its downstream targets in samples from blast's patients, suggesting that FOXM1 is also aberrant overexpressed in B-ALL as in many other cancer types. In agreement, five B-ALL cell lines analyzed also overexpressed FOXM1 and its downstream targets, confirming the results obtained in patients. An important finding from our study is that depletion of FOXM1 by siRNA caused a significant reduction in cell proliferation in B-ALL cell lines, suggesting a role for FOXM1 in the oncogenesis of B-ALL. Moreover, knockdown of FOXM1 led to a cell cycle arrest in G2/M, suggesting that FOXM1 promotes cell proliferation through modulation of cell cycle progression, as also reported by Nakamura at al. in acute myeloid leukemia cells.(Nakamura *et al*, 2010) Knockdown of FOXM1 in B-ALL cell lines led to a downregulation of proteins involved regulation of mitotic progression, consistent with previous data.(Nakamura *et al*, 2010) We also showed that FOXM1 silencing is accompanied by a decreased expression of $p27^{Kip1}$ and $p21^{Cip1/Waf1}$ proteins, which are known to assemble different Cyclin/Cdk complexes. More precisely they are phosphorylated by the Cdk2-cyclin E complex are recognized by the specificity subunits Skp2 and Cks1 of the SCF ubiquitin ligase complex, which targets them for ubiquitin-mediated proteasome degradation. (Carrano *et al*, 1999; Hara *et al*, 2001; Lu & Hunter, 2010).

Thus it is also possible to speculate that their decreases reflect an accelerate ubiquitinylation and subsequent degradation. Thiostrepton is a thiazole antibiotic that inhibits the transcriptional activity of FOXM1. It also downregulates FOXM1 mRNA expression as FOXM1 also positively autoregulates it own transcription.(Kwok *et al*, 2008; Koo *et al*, 2012) Indeed, both the mRNA and protein expression of FOXM1 was downregulated by thiostrepton in B-ALLs. In this study, we also found that thiostrepton remarkably reduces the cell viability of different B-ALL cell lines causing apoptosis in a concentration and time dependent manner, and induces a G2/M arrest of the cell cycle, consistent with the result obtained with the siRNA-mediated knockdown of FOXM1.

Standard treatment options for newly diagnosed childhood B-ALL are predominantly chemotherapy. Importantly, patients that respond poorly to the chemotherapy treatment are predicted to undergo relapse in the future, so an understanding of the biological mechanisms which underlie this poor responsiveness is therefore crucial for the development of more effective therapies. Consistent with this, Bhatla *et al.* have identified in a cohort of relapsed B-ALL pediatric patients a series of up-regulated genes which also includes FOXM1.(Bhatla *et al*, 2012)

In light of these results we examined if combining thiostrepton with the chemotherapeutics used in B-ALL therapy could increase their efficacy. Our results clearly indicate a strong synergistic effect (CI<1) between thiostrepton and drugs with different mechanisms of action in the four B-ALL cell lines tested. In particular, it is important to note that thiostrepton is able to partially reverse the glucocorticoid resistance in REH cells. Furthermore, these results were confirmed, in a more specific way, in the same cell lines silenced for FOXM1 (**Figure 7**). Given that patients that respond poorly to glucocorticoid therapy when diagnosed are usually predicted to undergo relapse in the future, our findings suggest that FOXM1 inhibition could be a potential useful strategy in clinical therapy to optimize the efficacy of existing therapeutics for B-ALL, although further studies are needed to better understand the molecular mechanism(s) involved in these synergistic effects. In summary, we show that FOXM1 has a role in both the oncogenesis and the development of drug resistance in B-ALL, and the targeting of FOXM1 can be a useful means for treating B-ALL and for overcoming drug resistance.

1.4.6 REFERENCES

Accordi B, Galla L, Milani G, Curtarello M, Serafin V, Lissandron V, Viola G, te Kronnie G, De Maria R, Petricoin EF, Liotta L a, Indraccolo S, Basso G (2013) AMPK inhibition enhances apoptosis in MLL-rearranged pediatric B-acute lymphoblastic leukemia cells. *Leukemia* **27**: 1019–1027.

Bektas N, Haaf A ten, Veeck J, Wild PJ, Lüscher-Firzlaff J, Hartmann A, Knüchel R, Dahl E (2008) Tight correlation between expression of the Forkhead transcription factor FOXM1 and HER2 in human breast cancer. *BMC Cancer* **8**: 42.

Bertoli C, Skotheim JM, de Bruin RAM (2013) Control of cell cycle transcription during G1 and S phases. *Nat Rev Mol Cell Biol* **14**: 518–528.

Bhatla T, Wang J, Morrison DJ, Raetz E a, Burke MJ, Brown P, Carroll WL (2012) Epigenetic reprogramming reverses the relapse-specific gene expression signature and restores chemosensitivity in childhood B-lymphoblastic leukemia. *Blood* **119**: 5201–5210.

Bortolozzi R, Viola G, Porcù E, Consolaro F, Marzano C, Pellei M, Gandin V, Basso G (2014) A novel copper (I) complex induces ER-stress-mediated apoptosis and sensitizes B-acute lymphoblastic leukemia cells to chemotherapeutic agents. *Oncotarget* **5**: 5978-5991.

Carrano AC, Eytan E, Hershko A, Pagano M (1999) SKP2 is required for ubiquitin-mediated degradation of the CDK inhibitor p27. *Nat Cell Biol* **1**: 193–199.

Chou T (2006) Theoretical basis, experimental design, and computerized simulation of synergism and antagonism in drug combination studies. *Pharmacol Rev* **58**: 621-681.

Chou T-C (2010) Drug combination studies and their synergy quantification using the Chou-Talalay method. *Cancer Res* **70**: 440–446.

Chu X-Y, Zhu Z-M, Chen L-B, Wang J-H, Su Q-S, Yang J-R, Lin Y, Xue L-J, Liu X-B, Mo X-B (2012) FOXM1 expression correlates with tumor invasion and a poor prognosis of colorectal cancer. *Acta Histochem* **114**: 755–762.

Gemenetzidis E, Elena-Costea D, Parkinson EK, Waseem A, Wan H, Teh M-T (2010) Induction of human epithelial stem/progenitor expansion by FOXM1. *Cancer Res* **70**: 9515–9526.

Hara T, Kamura T, Nakayama K, Oshikawa K, Hatakeyama S (2001) Degradation of p27(Kip1) at the G(0)-G(1) transition mediated by a Skp2-independent ubiquitination pathway. *J Biol Chem* **276**: 48937–48943.

Hegde NS, Sanders DA, Rodriguez R, Balasubramanian S (2011) The transcription factor FOXM1 is a cellular target of the natural product thiostrepton. *Nat Chem* **3**: 725–731.

Hui RC-Y, Gomes AR, Constantinidou D, Costa JR, Karadedou CT, Fernandez de Mattos S, Wymann MP, Brosens JJ, Schulze A, Lam EW-F (2008) The forkhead transcription factor FOXO3a increases phosphoinositide-3 kinase/Akt activity in drug-resistant leukemic cells through induction of PIK3CA expression. *Mol Cell Biol* **28**: 5886–5898.

Huynh KM, Soh J-W, Dash R, Sarkar D, Fisher PB, Kang D (2011) FOXM1 expression mediates growth suppression during terminal differentiation of HO-1 human metastatic melanoma cells. *J Cell Physiol* **226**: 194–204.

Khongkow P, Karunarathna U, Khongkow M, Gong C, Gomes AR, Yagüe E, Monteiro LJ, Kongsema M, Zona S, Man EPS, Tsang JW-H, Coombes RC, Wu K-J, Khoo U-S, Medema RH, Freire R, Lam EW-F (2013) FOXM1 targets NBS1 to regulate DNA damage-induced senescence and epirubicin resistance. *Oncogene* **33:** 4144-4155.

Koo C-Y, Muir KW, Lam EW-F (2012) FOXM1: From cancer initiation to progression and treatment. *Biochim Biophys Acta* **1819**: 28–37.

Kwok JM-M, Myatt SS, Marson CM, Coombes RC, Constantinidou D, Lam EW-F (2008) Thiostrepton selectively targets breast cancer cells through inhibition of forkhead box M1 expression. *Mol Cancer Ther* **7**: 2022–2032.

Lam EW-F, Brosens JJ, Gomes AR, Koo C-Y (2013) Forkhead box proteins: tuning forks for transcriptional harmony. *Nat Rev Cancer* **13**: 482–495.

Laoukili J, Alvarez M, Meijer L a T, Stahl M, Mohammed S, Kleij L, Heck AJR, Medema RH (2008) Activation of FoxM1 during G2 requires cyclin A/Cdk-dependent relief of autorepression by the FoxM1 N-terminal domain. *Mol Cell Biol* **28**: 3076–3087.

Laoukili J, Kooistra MRH, Brás A, Kauw J, Kerkhoven RM, Morrison A, Clevers H, Medema RH (2005) FoxM1 is required for execution of the mitotic programme and chromosome stability. *Nat Cell Biol* **7**: 126–136.

Li X, Qiu W, Liu B, Yao R, Liu S, Yao Y, Liang J (2013) Forkhead box transcription factor 1 expression in gastric cancer: FOXM1 is a poor prognostic factor and mediates resistance to docetaxel. *J Transl Med* **11**: 204.

Liu M, Dai B, Kang S-H, Ban K, Huang F-J, Lang FF, Aldape KD, Xie T, Pelloski CE, Xie K, Sawaya R, Huang S (2006) FoxM1B is overexpressed in human glioblastomas and critically regulates the tumorigenicity of glioma cells. *Cancer Res* **66**: 3593–3602.

Lu Z, Hunter T (2010) Ubiquitylation and proteasomal degradation of the p21(Cip1), p27(Kip1) and p57(Kip2) CDK inhibitors. *Cell Cycle* **9**: 2342–2352.

Martin KJ, Patrick DR, Bissell MJ, Fournier M V (2008) Prognostic breast cancer signature identified from 3D culture model accurately predicts clinical outcome across independent datasets. *PLoS One* **3**: e2994.

Mencalha AL, Binato R, Ferreira GM, Du Rocher B, Abdelhay E (2012) Forkhead box M1 (FoxM1) gene is a new STAT3 transcriptional factor target and is essential for proliferation, survival and DNA repair of K562 cell line. *PLoS One* **7**: e48160.

Monteiro LJ, Khongkow P, Kongsema M, Morris JR, Man C, Weekes D, Koo C-Y, Gomes AR, Pinto PH, Varghese V, Kenny LM, Charles Coombes R, Freire R, Medema RH, Lam EW-F (2013) The Forkhead Box M1 protein regulates BRIP1 expression and DNA damage repair in epirubicin treatment. *Oncogene* **32**: 4634–4645.

Nakamura S, Hirano I, Okinaka K, Takemura T, Yokota D, Ono T, Shigeno K, Shibata K, Fujisawa S, Ohnishi K (2010) The FOXM1 transcriptional factor promotes the proliferation of leukemia cells through modulation of cell cycle progression in acute myeloid leukemia. *Carcinogenesis* **31**: 2012–2021.

Nilsson I, Hoffmann I (2000) Cell cycle regulation by the Cdc25 phosphatase family. *Prog Cell Cycle Res* **4**: 107–114.

Uddin S, Hussain AR, Ahmed M, Siddiqui K, Al-Dayel F, Bavi P, Al-Kuraya KS (2012) Overexpression of FoxM1 offers a promising therapeutic target in diffuse large B-cell lymphoma. *Haematologica* **97**: 1092–1100.

Wang I-C, Chen Y-J, Hughes D, Petrovic V, Major ML, Park HJ, Tan Y, Ackerson T, Costa RH (2005) Forkhead box M1 regulates the transcriptional network of genes essential for mitotic progression and genes encoding the SCF (Skp2-Cks1) ubiquitin ligase. *Mol Cell Biol* **25**: 10875–10894.

Wang Z, Park HJ, Carr JR, Chen Y, Zheng Y, Li J, Tyner AL, Costa RH, Bagchi S, Raychaudhuri P (2011) FoxM1 in tumorigenicity of the neuroblastoma cells and renewal of the neural progenitors. *Cancer Res* **71**: 4292–4302.

Wang Z, Zheng Y, Park HJ, Li J, Carr JR, Chen YJ, Kiefer MM, Kopanja D, Bagchi S, Tyner AL, Raychaudhuri P (2013) Targeting FoxM1 effectively retards p53-null lymphoma and sarcoma. *Mol Cancer Ther* **12**: 759–767.

Xia L, Huang W, Tian D, Zhu H, Zhang Y, Hu H, Fan D, Nie Y, Wu K (2012) Upregulated FoxM1 expression induced by hepatitis B virus X protein promotes tumor metastasis and indicates poor prognosis in hepatitis B virus-related hepatocellular carcinoma. *J Hepatol* **57**: 600–612.

Zhao B, Barrera LA, Ersing I, Willox B, Schmidt SCS, Greenfeld H, Zhou H, Mollo SB, Shi TT, Takasaki K, Jiang S, Cahir-McFarland E, Kellis M, Bulyk ML, Kieff E, Gewurz BE (2014) The NF-κB Genomic Landscape in Lymphoblastoid B Cells. *Cell Rep* 1–12.

1.4.7 SUPPLEMENTARY INFORMATION

Table S1. Characteristics of patients sample.

B-ALL sample	Gender	Age at diagnosis	% of blast in BM	Cytogenetics
#1	F	6	82	9q22
#2	M	16	91	9q22
#3	F	5	77	12q21
#4	M	3	90	12q21
#5	F	3	63	12q21)
#6	F	8	97	Normal
#7	M	1	89	Normal
#8	F	8	90	Normal
#9	M	4	90	Normal
#10	M	2	89	Normal
#11	F	3	92	9q22
#12	F	5	89	Normal
#13	F	1	87	Normal
#14	F	2	93	Normal
#15	M	6	83	Normal
#16	M	10	86	Normal
#17	F	2	90	Normal
#18	M	3	89	Normal
#19	F	7	82	Normal
#20	M	2	85	Normal

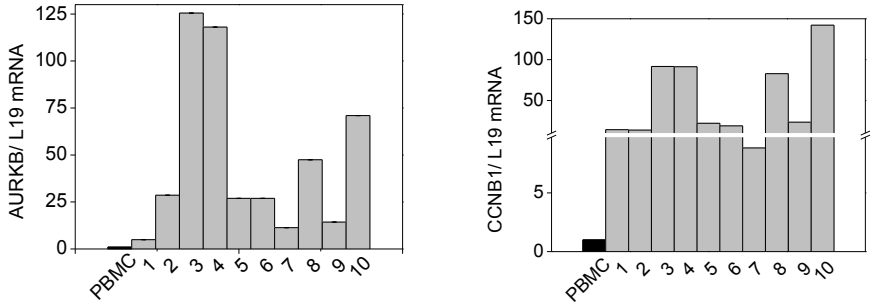

Figure S1. Basal AURKB and CCNB1 mRNA levels were analyzed in ten samples of B-ALL patient's and compared to peripheral blood mononuclear cells (PBMC) of healthy donors by RT-qPCR. The results were normalised with L19 mRNA levels using the DDCt method. The median of threshold cycles (Ct) values was normalized to the median of Ct values of the L19 mRNA levels. Results are the average ± SD of three independent experiments in triplicate.

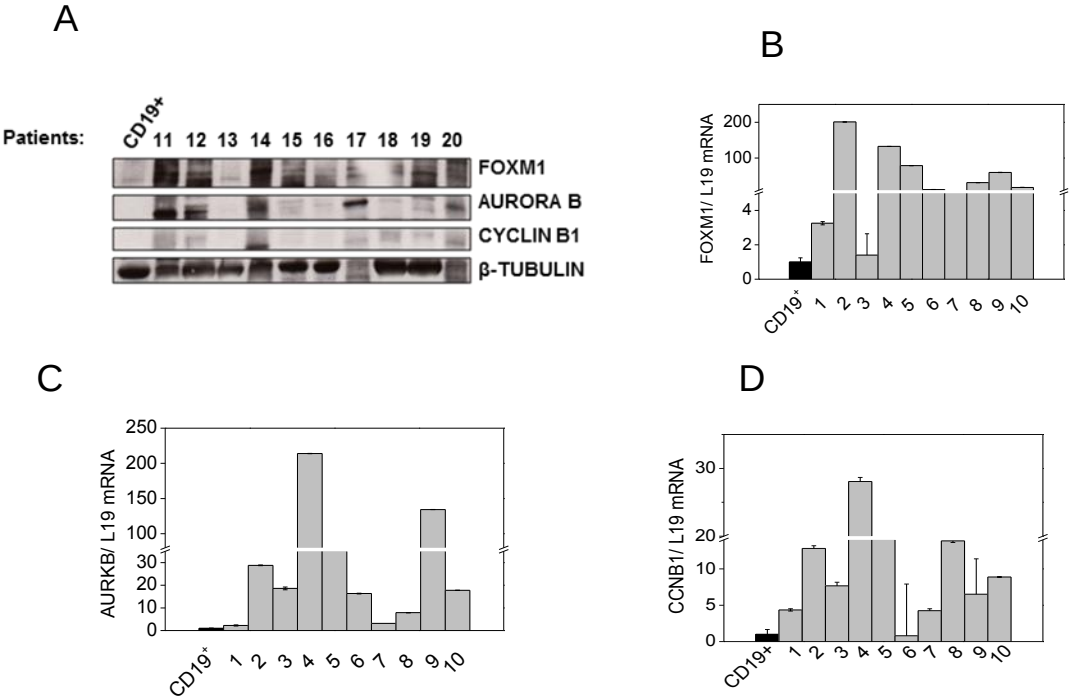

Figure S2. FOXM1 is highly expressed in B-ALL patients compared to CD19 positive cells ($CD19^+$) from healthy donors. **A)** Cell lysates were obtained from ten B-ALL patients and analyzed for the expression of FOXM1 and its downstream target genes Cyclin B1 and Aurora B in comparison to $CD19^+$ **B-D)** Basal FOXM1, AURKB and CCNB1 mRNA levels were analyzed in ten samples of B-ALL patients and compared to $CD19^+$ from healthy donors by RT-qPCR. Results are the average ± SD of three independent experiments in triplicate.

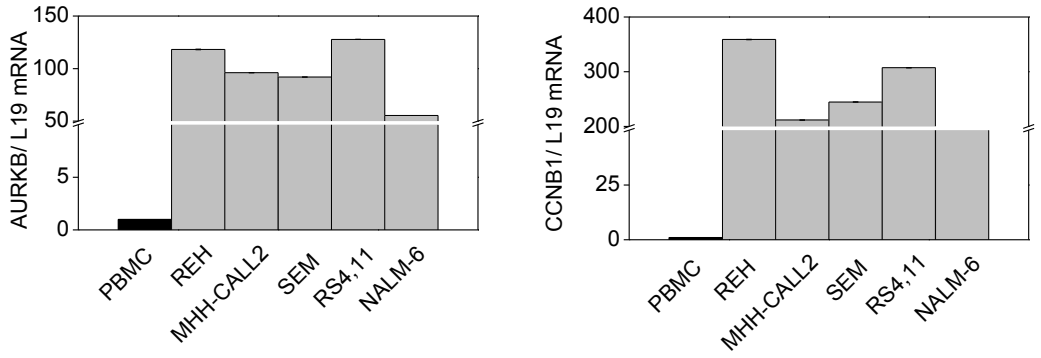

Figure S3. Basal AURKB and CCNB1 mRNA levels were analyzed in five B-ALL cell lines (REH, MHH-CALL2, SEM, RS4;11, NALM-6) and compared to peripheral blood mononuclear cells (PBMC) of healthy donors by RT-qPCR. The results were normalised with L19 mRNA levels using the DDCt method. Results are the average ± SD of three independent experiments in triplicate.

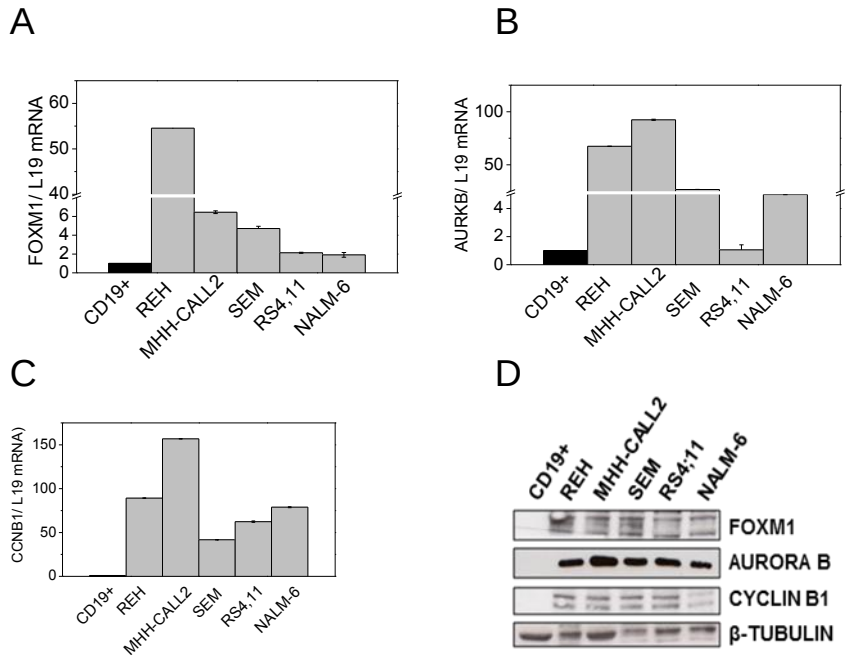

Figure S4. A-C) FOXM1 and its downstream target genes are overexpressed in B-ALL cell lines. Total RNA from five B-ALL cell lines (REH, MHH-CALL2, SEM, RS4;11, NALM-6) was extracted and FOXM1 mRNA levels were analyzed and compared to $CD19^+$ from healthy donors by RT-qPCR. The results were normalised with L19 mRNA levels using the DDCt method. **D)** REH, MHH-CALL2, SEM, RS4;11, NALM-6 cell lysates were collected at basal conditions for subsequent western blot analysis for the indicated antibodies.

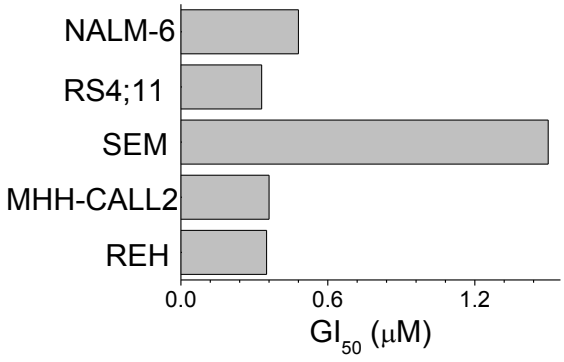

Figure S5. GI_{50} values after incubation of the indicated B-cell lines with thiostrepton. Cell viability was analyzed after 72 h of incubation by MTT test. Data are expressed as the mean ± SE from the dose-response curves of at least three independent experiments.

RS4;11

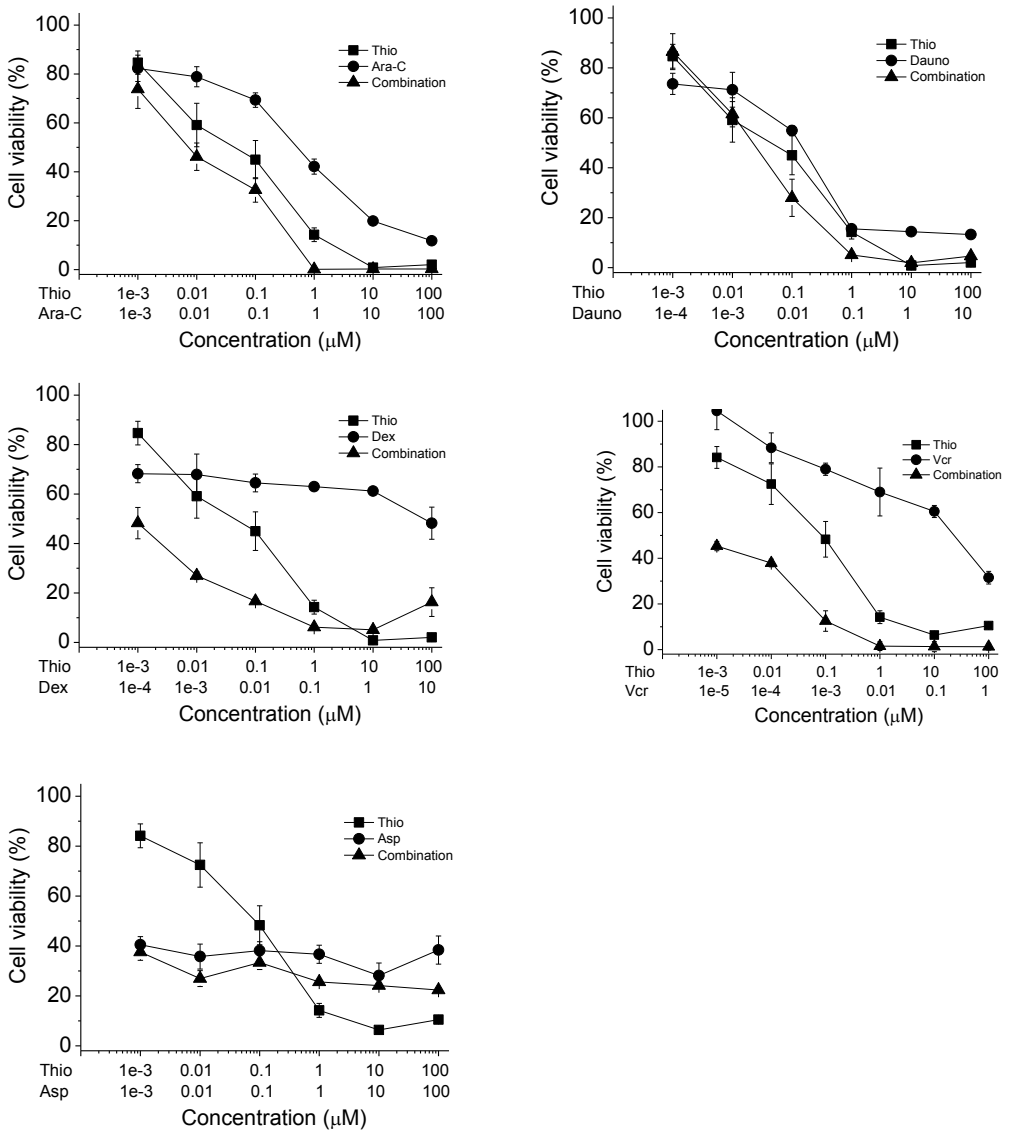

Figure S6. Dose-response curves obtained in RS4;11 cells treated with thiostrepton and the indicated concentration of drugs at fixed molar combination ratio. Cell viability was obtained after 48 h of incubation by MTT test. Data are expressed as mean± SE of two independent experiment performed in triplicate.

SEM

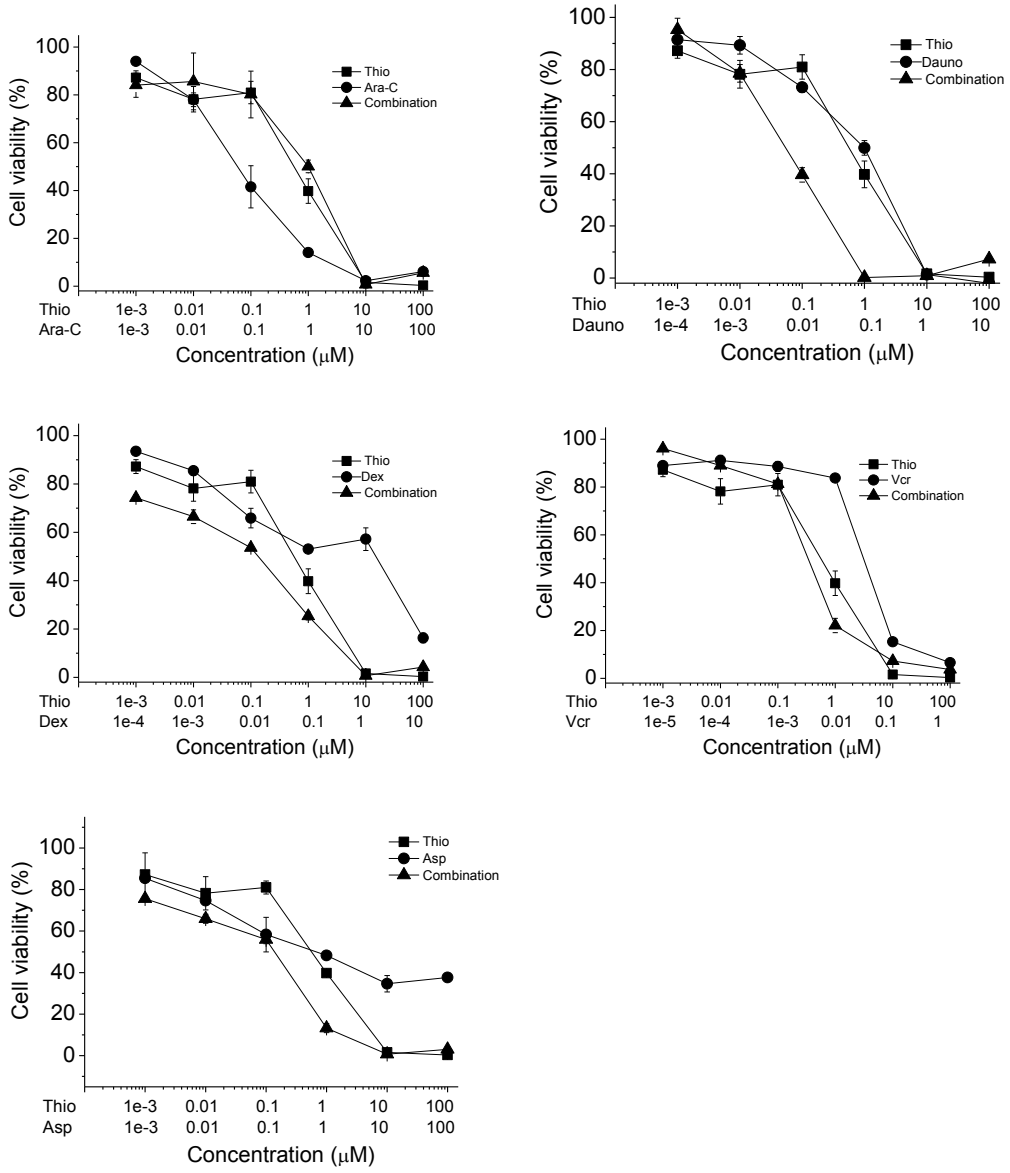

Figure S7. Dose-response curves obtained in SEM cells treated with thiostrepton and the indicated concentration of drugs at fixed molar combination ratio. Cell viability was obtained after 48 h of incubation by MTT test. Data are expressed as mean± SE of two independent experiment performed in triplicate.

REH

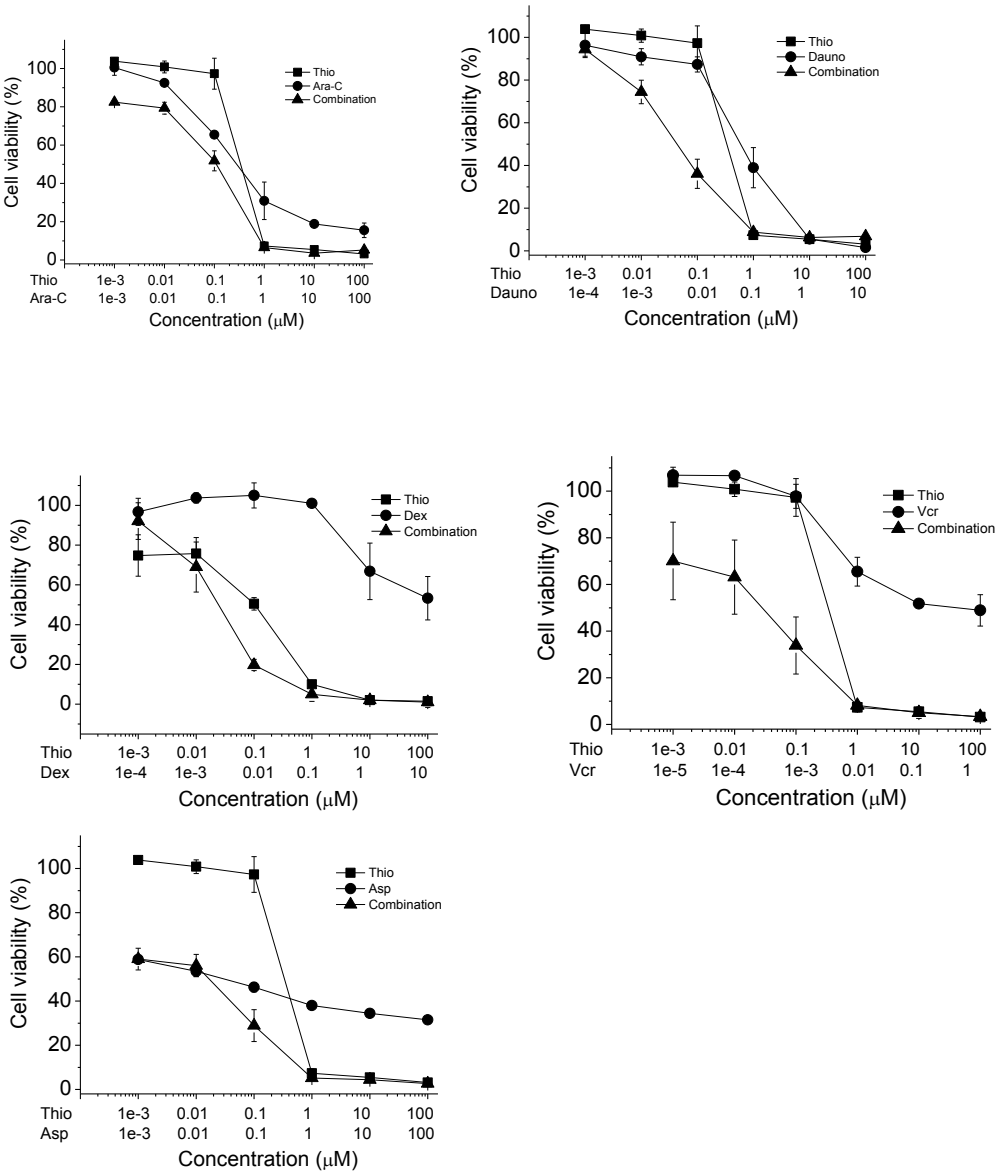

Figure S8. Dose-response curves obtained in REH cells treated with thiostrepton and the indicated concentration of drugs at fixed molar combination ratio. Cell viability was obtained after 48 h of incubation by MTT test. Data are expressed as mean± SE of two independent experiment performed in triplicate.

1.5 RESULTS

FOXO3a and post-translational modifications: mediators of glucocorticoid sensitivity in acute B acute lymphoblastic leukaemia

Francesca Consolaro[1,2^], Sadaf Ghaem-Maghami[1^], Roberta Bortolozzi[2], Mattaka Khongkow[1], Giuseppe Basso[2], Giampietro Viola[2*], Eric W-F Lam[1*]

[1]*Department of Surgery and Cancer, Imperial College London, Imperial Centre for Translational and Experimental Medicine (ICTEM), London, UK, W12 0NN*

[2]*Dipartimento di Salute della Donna e del Bambino, Laboratorio di Oncoematologia, University of Padova, Italy*

*Co-corresponding authors

^Joint first authors.

Short title: FOXO3a mediates glucocorticoid function in B-ALL

Keywords. FOXO3a; B-ALL ; B acute lymphoblastic leukaemia; glucocorticoid, drug resistance phosphorylation, acetylation

1.5.1 ABSTRACT

Background: Glucocorticoids are widely used to treat B acute lymphoblastic leukaemia (B-ALL); however, the molecular mechanisms underlying glucocorticoid response and resistance remain poorly understood. In this study, we investigated the role and regulation of FOXO3a in mediating the dexamethasone response in B-ALL.

Methods: B-ALL cell lines and patient samples, MTT assay, propidium iodide and annexin V staining, flow cytometry, immunoblotting and precipitation, real-time PCR, siRNA depletion, SIRT inhibitors were used in this study to investigate the function, regulation and expression of FOXO3a in B-ALL.

Results: Our results showed that FOXO3a mediates the cytotoxic function of dexamethasone. In response to dexamethasone, we found that FOXO3a translocates into the nucleus, where it induces the expression of downstream targets, including $p27^{Kip1}$ and Bim, important for proliferative arrest and cell death in the sensitive RS4;11 and SUP-B15 B-ALL cells. Our data showed that FOXO3a activation by dexamethasone is mediated through the suppression of the PI3K-Akt signalling cascade. Furthermore, we also uncovered two post-translational modifications, phosphorylation on Ser-7 and acetylation on Lys-242/5, associated with FOXO3a activation by dexamethasone. Western blot analysis showed that the FOXO3a phosphorylation on Ser-7 is associated with p38/JNK activation, whereas the acetylation on Lys-242/5 is correlated with the downregulation of SIRT1/2/6 and the induction of the acetyltransferase CBP/p300.

Conclusion: Collectively, our results suggest that FOXO3a and its post-translational regulation are essential for dexamethasone response and that targeting FOXO3a and sirtuins can enhance the dexamethasone function in B-ALL cells.

1.5.2 INTRODUCTION

B acute lymphoblastic leukaemia (B-ALL) is one of the most common clonal malignant diseases in children, and it stems from unchecked proliferation of lymphoid progenitor cells. Glucocorticoids are the most effective and commonly used agents for treatment of B-ALL; however, their efficacy is often hampered by the development of resistance (Gaynon and Carrel, 1999). In fact, glucocorticoid sensitivity at diagnosis has a major bearing on the eventual clinical outcome for patients with childhood B acute lymphoblastic leukaemia (B-ALL) (Gaynon and Carrel, 1999). In consequence, uncovering the mechanisms that underlie dexamethasone responsiveness will not only help to identify reliable biomarkers for early diagnosis and for predicting disease relapse but also aid the design of targeted therapies to overcome glucocorticoid resistance in B-ALL. Despite this, the molecular mechanisms underlying glucocorticoid response and resistance remain poorly understood (Gaynon and Carrel, 1999).

FOXO3a (previously known as FKHR-L1) is a member of the Forkhead family of transcription factors, which share a distinct forkhead DNA-binding domain (Lam *et al.*, 2013). FOXO3a plays an important role in proliferation, apoptosis, autophagy, metabolism, inflammation, differentiation, and stress resistance (Nestal de Moraes *et al.*, 2014; Ho *et al.*, 2008). The stability, subcellular localization, the DNA binding affinity, and the transcriptional activity of FOXO3a are primarily regulated by a complex array of posttranslational modifications (Wang *et al.*, 2014). FOXO3a is primarily regulated by the PI3K-Akt(PKB) signalling pathway (Tzivion *et al.*, 2011; X. Zhang *et al.*, 2011; Kops *et al.*, 2002). In the presence of growth factors, the PI3K-Akt axis is activated and Akt phosphorylates the FOXO3a at three sites, Thr-32, Ser-253 and Ser-315, triggering the 14-3-3 protein binding, nuclear export and subsequent degradation via the ubiquitynation-mediated proteasome pathway (Tzivion *et al.*, 2011; X. Zhang *et al.*, 2011; Kops *et al.*, 2002). The Ser-315 residue locates within the nuclear export domain and its phosphorylation has been shown to be important for FOXO3a nuclear export (Boccitto and Kalb, 2011). The MAPK kinase ERK has also been shown to phosphorylate FOXO3a on Ser-294, Ser-344 and Ser-425, driving its proteasomal degradation via ubiquitin E3 ligase, MDM2 (Yang *et al.*, 2008). Conversely, the phosphorylation mediated by the other two MAPKs, p38 and JNK (c-jun-NH2-kinase), promotes FOXO3a nuclear localization and

transcriptional activity. The stress-activated protein kinase p38 phosphorylates FOXO3a on Ser-7 promoting its nuclear localization, whereas JNK phosphorylates the FOXO3a-related FOXO4 at Thr-447 and Thr-451 (Ho *et al.*, 2012; Essers *et al.*, 2004). Furthermore, JNK can also activate FOXO3a indirectly by repressing the PI3K-Akt activity (Sunters *et al.*, 2006). Resembling phosphorylation, acetylation can both promote and decrease the transcriptional activity of FOXO3a. FOXO acetylation is controlled coordinately by the histone/lysine acetyltransferase and deacetylases. Co-precipitation analysis revealed that the acetyltransferase CBP/p300 binds the first 52 amino acids of the N-terminal region of FOXO3a (Mahmud *et al.*, 2002). Interestingly, p300 also directly acetylates FOXO transcription factors at several conserved lysine residues, Lys-242, Lys-245 and Lys-262 of FOXO3a (Daitoku *et al.*, 2004; Dansen *et al.*, 2009; Matsuzaki *et al.*, 2005). However, p300-dependent acetylation has been shown to have a dual function in FOXO-mediated transcription; it can either attenuate FOXO-transcriptional activity or it can promote the recruitment and assembly of the transcriptional machinery, increasing their DNA-binding ability and transcriptional activity (Perrot and Rechler, 2005; Senf *et al.*, 2011). FOXO3a acetylation status is further modulated by class III histone/lysine deacetylases (sirtuins), including SIRT1, SIRT2, SIRT3 and SIRT6 (Olmos *et al.*, 2011). For example, it has been demonstrated that SIRT1 can antagonise the p300-mediated acetylation and activation of FOXO3a (Motta *et al.*, 2004). In agreement, studies conducted in breast cancer have also showed that SIRT6 overexpression correlates with FOXO3a inactivation and that SIRT6 depletion sensitizes breast cancer cells to both paclitaxel and epirubicin treatments (Khongkow *et al.*, 2013).

FOXO3a functions primarily as a tumour suppressor in a number of haematological malignancies, playing a crucial role in controlling cell cycle arrest, apoptosis and self-renewal of haematopoietic progenitor cells (Nordigarden *et al.*, 2009; Miyamoto *et al.*, 2008). For example, hyperphosphorylation of FOXO3a has been shown to be correlated with adverse prognosis in AML (Kornblau *et al.*, 2010). FOXO3a activation can induce apoptotic cell death in therapy-resistant T-ALL cells (Ausserlechner *et al.*, 2013). Furthermore, deletion of FOXO1/3a/4 in mice has been found to lead to the development of T-cell lymphoma (Paik *et al.*, 2007). Hitherto, the involvement of FOXO3a in B-ALL and its role in treatment response has remained undefined. Nevertheless, it has been shown

that in glucocorticoid resistant B-ALL patients, Bim, a downstream FOXO3a target (Essafi *et al.*, 2005), is downregulated compared to their sensitive counterparts (Bachmann *et al.*, 2005). Moreover, FOXO3a expression has also been demonstrated to predict bortezomib sensitivity and patient remission in B-ALL (Dewar *et al.*, 2011). Together these findings led us to hypothesize that FOXO3a has a key role in glucocorticoid sensitivity in B-ALL. In this study, we investigated the role and regulation of FOXO3a in mediating the dexamethasone response in B-ALL. More specifically, we intended to determine how phosphorylation and acetylation, two major FOXO3a post-translational modifications, influence FOXO3a subcellular localization and function.

1.5.3 MATERIALS AND METHODS

Cells, patient samples and cell cultures

B-ALL patient samples were obtained after informed consent according to the tenets of the Declaration of Helsinki. The study was approved by the Italian Association of Pediatric Onco-Hematology (AIEOP). All analyzed BCP-ALL samples were collected at the time of diagnosis before treatment, after Ficoll-Hypaque (Pharmacia, Uppsala, Sweden) separation of mononuclear cells as described previously (Accordi *et al.*, 2013). For details, see Supplementary Materials and Methods

Drug treatment and MTT proliferative assay

See Supplementary Materials and Methods

Flow cytometric analysis of cell cycle distribution and Apoptosis assay

See Supplementary Materials and Methods

Subcellular fractionation, Immunoprecipitation (IP), Immunoblotting (IB) and immunofluorescent staining

These procedures were performed as previously described (Myatt *et al.*, 2014). For details, see Supplementary Materials and Methods.

Real time-quantitative PCR (RT-qPCR)

Total RNA was isolated from frozen cell pellets using the RNeasy Mini kit (Qiagen, UK) according to manufactures' instructions.

Also see Supplementary Materials and Methods

Statistical Analysis

Results are presented as the mean ± SD. The differences between different conditions were analyzed using the two-sided Student's t test. P values lower than 0.05 were considered significant. *, $p \leq 0.05$: **, $p \leq 0.01$, ***$p \leq 0.001$.

1.5.4 RESULTS

Dexamethasone treatment induces FOXO3a activation in B-ALL sensitive cells

Deregulation of the PI3K-Akt-FOXO3a pathway has been shown to be involved in cancer development and contribute to therapy resistance in different haematological malignancies (Vecchio *et al.*, 2013; Kawauchi *et al.*, 2009; Y. Zhang *et al.*, 2011; Myatt and Lam, 2007). To explore the potential role played by FOXO3a in dexamethasone response, we first examined the expression of both total and phosphorylated forms of FOXO3a in one dexamethasone-resistant B-ALL cell line (REH) and two dexamethasone-sensitive cell lines (RS4;11 and SUP-B15) following treatment with 1 μM dexamethasone for 24 h

(Figure 1A). Dose-response curves were previously obtained by treating cells for 72 h with a range of dexamethasone concentrations (0-100 μM) and the results confirmed the dexamethasone-sensitivity of the B-ALL cells (Figure 1B; Figure S1, supplementary data). Western blot analysis showed that baseline FOXO3a is more hyperphosphorylated at Akt-targeted sites, inducing Thr-32 and Ser-315, in the dexamethasone-resistant REH cells compared to the sensitive counterparts, RS4;11 and SUP-B15 (Figure 1A). The resistant REH cells expressed comparable levels of FOXO3a, P-FOXO3a (S315), P-FOXO3a (T32), P-FOXO3a (S253) before and after dexamethasone treatment. In contrast, in the sensitive cells, RS4;11 and SUP-B15, dexamethasone caused the down-regulation of FOXO3a phosphorylation at Thr-32, Ser-253 and Ser-315, indicative of FOXO3a nuclear relocation and activation (Myatt and Lam, 2007; Ho *et al.*, 2008). In response to dexamethasone, FOXO3a activation in the sensitive cells was further confirmed by the increased expression of the FOXO3a target Bim and the consequent activation of apoptosis, as evidenced by caspase-3 , -7 and -9 cleavage and activation. In concordance, the expression of another FOXO3a downstream target $p27^{Kip1}$ was also increased in sensitive cells following dexamethasone treatment. Notably, the $p27^{Kip1}$ and Bim mRNA levels were also induced by dexmethasone in the sensitive and not the resistant cells, further supporting their transcriptional induction by FOXO3a (Fig. 1C). Interestingly, unlike FOXO3a the expression of the other FOXO family members, FOXO1 and FOXO4 were expressed at low levels in the sensitive cells before and after dexamethasone, suggesting that FOXO1 and FOXO4 are unlikely to have a crucial part to play in dexamethasone response (Figure 1A). Together, these results suggest that after treatment FOXO3a becomes hypophosphorylated at Akt-dependent sites and consequently, activated in the sensitive B-ALL cells. Conversely, in the resistant cells FOXO3a remained phosphorylated and inactive. We next analyzed the expression of the components of PI3K-Akt signalling pathway after dexamethasone treatment (Figure 1D). In sensitive cells the Akt activator mTOR became dephosphorylated (at S2448), thus less active, after dexamethasone treatment. Accordingly, these data show that dexamethasone treatment leads to PI3K-Akt inactivation in sensitive cells, and as a consequence, FOXO3a becomes hypophosphorylated and activated. In contrast, FOXO3a remains phosphorylated and inactive in the resistant REH cells.

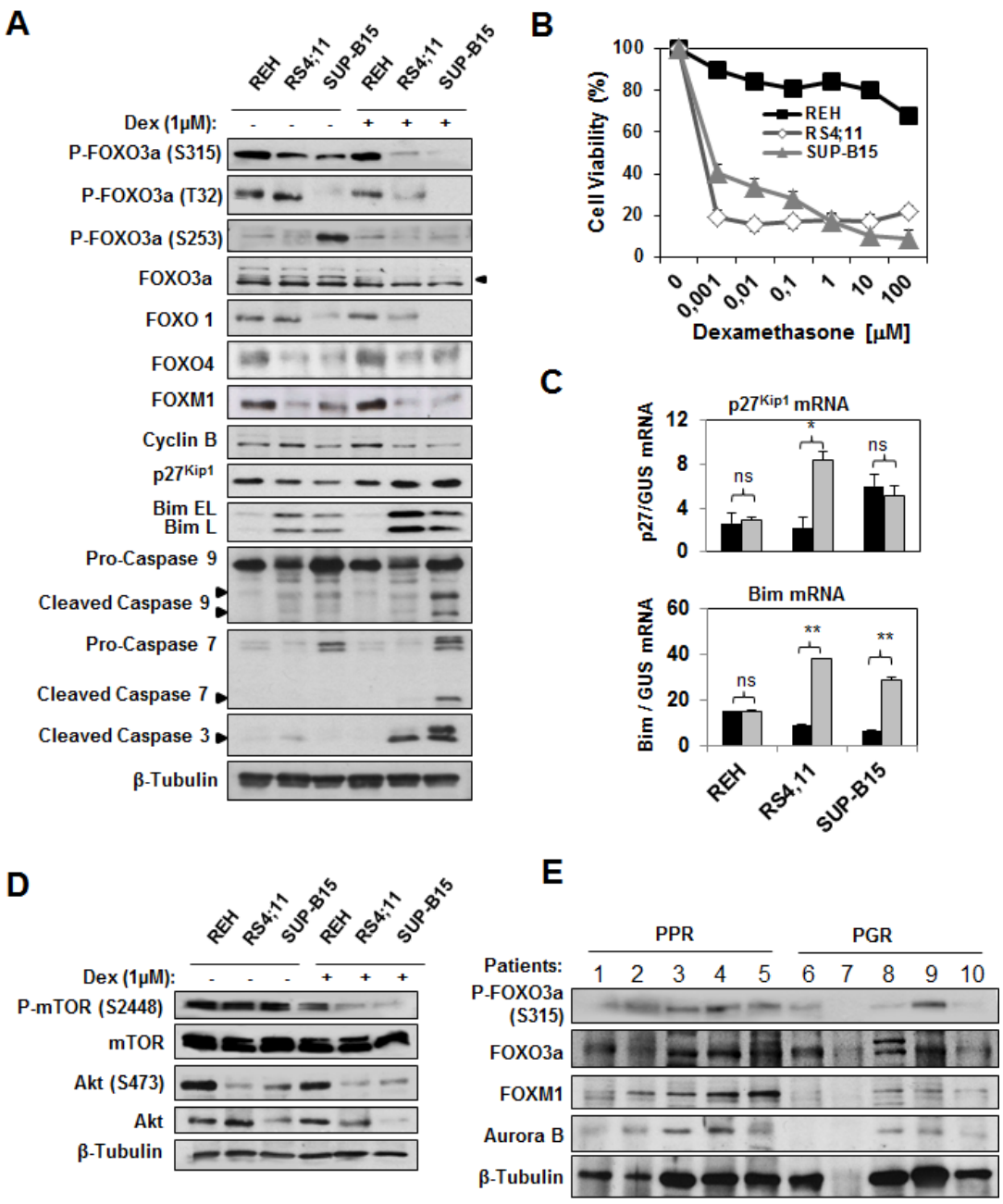

Figure 1. Dexamethasone induces FOXO3a activation and proliferative arrest in sensitive but not resistant B-ALL cells. The REH, RS4;11 and SUP-B15 B-ALL cell lines were treated with 1 μM dexamethasone for 0 and 24 h. A) Cell lysates were collected for western blot analysis for the indicated proteins. B) MTT assay was performed on REH, RS4;11 and SUP-B15 cells. Results are the average ± SD of 3 independent experiments in triplicate. Statistical analysis performed using Students t-tests showed dexamethasone **very significantly reduced RSA;11 and SUP-B15 at all concentrations studied, whereas dexamethasone only *significantly inhibited REH proliferation at >10 μM dexamethasone (t-test: 0.0001-100 μM verses 0 μM dexamethasone of the same cell line; *significant $p<0.05$, ** very significant $p<0.01$, and ns

not significant). C) Bim and $p27^{Kip1}$ mRNA levels were analyzed by RT-qPCR analysis and results were normalised to L19 mRNA levels. Error bars show the standard deviations. Results are the average ± SD of 3 independent experiments in triplicate. Statistical analysis was performed using Students t-tests (*t*-test: 0 h verses 24 h treatment; *significant $p<0.05$, and ns: not significant). D) Protein expression of P-mTOR (S2448), mTOR, Akt (S473), Akt and β-Tubulin was analyzed in the dexamethasone treated B-ALL cells. E) Protein expression of FOXO3a, P-FOXO3a (S315), FOXM1, Aurora B and β-Tubulin was analyzed at baseline conditions in five poor responder patients (PPR) and five glucocorticoid good responder patients (PGR) by western blot analysis.

FOXO3a is hyperphosphorylated at Ser-315 in poor responder patients (PPR)

To confirm the physiological relevance of our findings from the B-ALL cell lines, bone marrow cells from 10 pediatric B-ALL patients of good (PGR) and poor response (PPR) to prednisone therapy were studied by western blotting. In agreement with the data obtained from the cell culture models (Figure 1E), western blot results showed that while there was little difference in FOXO3a levels between the two groups. FOXO3a was generally more phosphorylated on the Akt-targeted Ser-315 residue in PPR individuals (1-5) compared to PGR patients (6-10) (Figure 1E). Collectively, these data indicated that FOXO3a at baseline conditions is more phosphorylated and therefore, less active in PPR patients, providing further evidence that FOXO3a has a role in modulating dexamethasone sensitivity.

Dexamethasone treatment leads to cell cycle arrest and cell death in drug sensitive B-ALL cells.

To explore further the potential role of FOXO3a in dexamethasone treatment and resistance, we next studied the effects of dexamethasone on the B-ALLs by propidium iodide staining and flow cytometry. Consistent with the proliferation assays, the cell cycle analysis showed that whereas there were no significant shifts in cell cycle distribution of REH cells in response to dexamethasone, considerable cell cycle phase changes indicative of cell proliferative arrest and cell death were observed for the sensitive RS4;11 and SUP-B15 cells (Figure 2A, 2B and 2C)**.** Accordingly, in response to dexamethasone, there were also increases in sub-G1 cell population for the sensitive and not the resistant cells (Figure 2B). We also detected a significant increase in G2/M population in SUP-B15 cells

following treatment (Figure 2C). Upon dexamethasone, we also observed a significant decrease in RS4;11 cells in S phase with a corresponding increase in G2/M phase cells (Figure 2C). The G2/M arrest observed can be due to the fact that FOXO3a negatively regulates the expression of genes, including cyclin B and FOXM1 (Figure 1A) important for G2/M progression (Myatt and Lam, 2007; Lam *et al.*, 2013). Collectively, these data suggest that dexamethasone arrests cell cycle progression, particularly in G2/M phase, and induces cell death in the sensitive but not resistant B-ALL cells. It is also notable that this cell cycle arrest and cell death induced by dexamethasone in the sensitive cells correlated with FOXO3a activation (Figure 1), providing further evidence of a role of FOXO3a in the cytostatic and cytotoxic function of dexamethasone in B-ALLs.

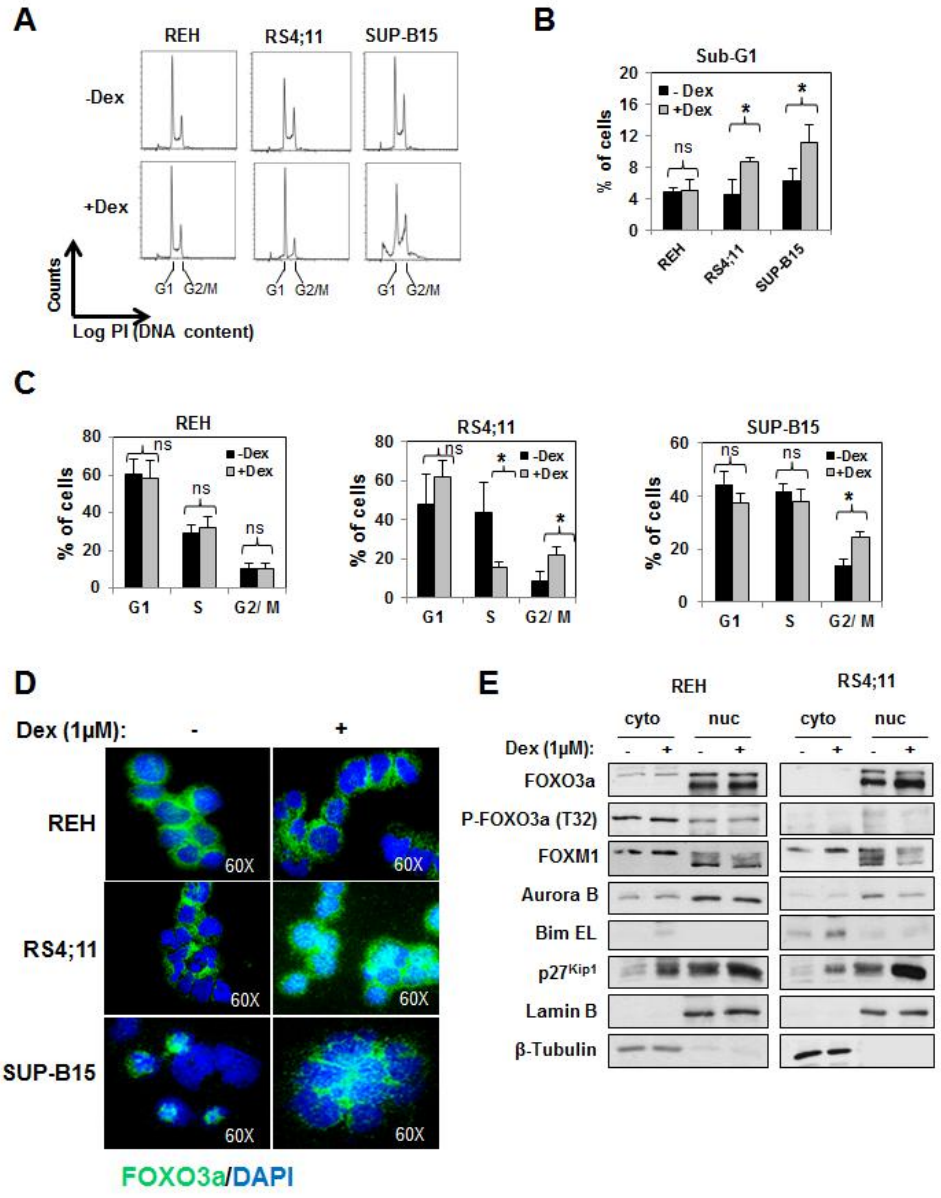

Figure 2. Dexamethasone treatment perturbs cell proliferation and induces FOXO3a nuclear translocation in sensitive B-ALL cells. A) REH, RS4;11 and SUP-B15 cells treated with dexamethasone (1μM) for 0 and 24 h were subjects to flow cytometric analysis after propidium iodide staining. Representative cell cycle profiles with and without dexamethasone treatment are shown. B) and C) Cell cycle analysis of sub-G1 and G1-S-G2/M populations was performed on these dexamethasone-treated REH, RS4;11 and SUP-B15 cells. Error bars show the standard deviations. Results are the average ± SD of 3 independent experiments in triplicate. Statistical analysis was performed using Students t-tests (*t*-test: 0 h verses 24 h treatment; *significant $p<0.05$, ** very significant $p<0.01$, and ns: not significant). D) After 0 and 24 h of dexamethasone treatment (1 μM), immunofluorescent staining was performed on the REH, RS4;11 and SUP-B15 cells using the mouse FOXO3a antibody and DAPI. All of the images shown are typical results obtained from at least 10 different fields. FOXO3a localization was detected using a secondary Alexa conjugated antibody. Nuclei were stained with DAPI. Images were obtained using a video-confocal microscope (Vico, Ecliple Ti80, Nikon), equipped with a digital camera. E) After treatment, cells were collected, and cytosolic (Cyto)/nuclear fractionation (Nuclear) procedures were performed. The resultant fractions were standardized according to protein content, followed by Western blot analyses using the indicated antibodies.

FOXO3a translocates to the nucleus after dexamethasone treatment in sensitive B-ALL cells

As Akt-phosphorylation of FOXO3a promotes its relocation to the cytoplasm, we next analyzed whether dexamethasone treatment also influences FOXO3a subcellular localization. To this end, B-ALL cells were either untreated or treated with dexamethasone for 24 h, fixed and stained with a specific FOXO3a fluorescent-conjugated antibody. The results showed that upon dexamethasone treatment, FOXO3a translocated from cytoplasm into nucleus in the sensitive cell lines RS4;11 and SUP-B15, but not in the resistant REH cells (Figure 2D). To confirm this further, we examined the expression of FOXO3a in the cytoplasmic and nuclear fractions of the sensitive RS4;11 and resistant REH B-ALL cells in response to dexamethasone treatment. In agreement, the western blotting results showed that dexamethasone treatment increased the nuclear FOXO3a and $p27^{Kip1}$ expression, the cytoplasmic Bim expression, but reduced the nuclear P-FOXO3a, FOXM1 and Aurora B expression substantially in the sensitive and not the resistant cells (Figure 2E). Together these results reinforce the idea that FOXO3a is activated in the dexamethasone-sensitive and not in the resistant B-ALL cells.

FOXO3a is a critical mediator of dexamethasone-induced apoptosis in B-ALL

To test if FOXO3a is essential for the cytotoxic function of dexamethasone in B-ALL, we depleted its expression using a smart pool of FOXO3a siRNA and assayed for the ability of dexamethasone to induce cell death in the sensitive RS4;11 cells. After 48 h of transfection with FOXO3a siRNA or non-silencing control (NSC) siRNA, cells were treated for another 24 h with dexamethasone before they were collected for subsequent cell death analysis. The knockdown of FOXO3a in RS4;11 was confirmed at mRNA and protein levels using real-time quantitative (RTq)-PCR (Figure 3A) and Western blot analysis (Figure 3B), respectively. Importantly, the expression of two FOXO3a-targets, Bim and $p27^{Kip1}$, also decreased substantially in the FOXO3a-silenced cells, confirming a depletion of FOXO3a activity. As shown in Figure 3C and 3D, dexamethasone failed to induce apoptosis in RS4;11 cells with FOXO3a knockdown, indicating that FOXO3a depletion conferred dexamethasone resistance to the RS4;11 cells and therefore suggesting that FOXO3a plays a central role in mediating the cytotoxic function of dexamethasone in B-ALL.

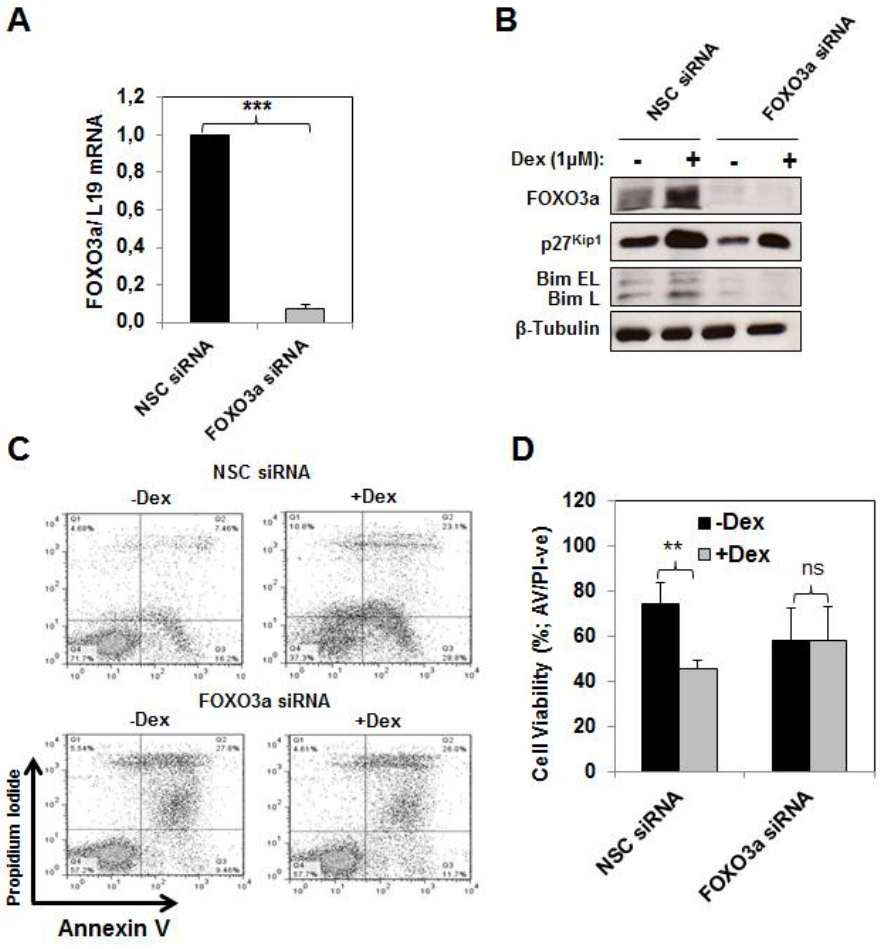

Figure 3. Depletion of FOXO3a promotes resistance to dexamethasone in B-ALL cells. RS4;11 cells were transfected with NS (non-silencing) siRNA or FOXO3a siRNA. A) FOXO3a mRNA levels were analyzed 72 h after transfection by RT-qPCR analysis and results were normalised to L19 mRNA levels. B) Forty-eight hours after transfection, cells were treated for 24 h with dexamethasone and then subjected for western blot analysis for FOXo3a, p27Kip1 and Bim expression. C) The dexamethasone treated RS4;11 cells were assayed for cell viability by Annexin V (AV) and propidium iodide staining. Representative flow cytometric analysis was shown. D) The results represent average of three independent cell death experiments ± SD. Statistical significance was determined by Student's t-test: **P ≤ 0.01; ns, not significant).

Dexamethasone promotes FOXO3a phosphorylation on Ser-7

In addition to Akt, MAPK kinases also phosphorylate and modulate FOXO3a activity (Ho *et al.*, 2008). In particular, it has been reported that p38 and JNK regulates FOXO3a nuclear localization and that p38 and JNK also phosphorylates FOXO3a on Ser-7 (Ho *et al.*, 2012). To explore the molecular mechanisms by which dexamethasone modulates FOXO3a function, we next analyzed the expression patterns of FOXO3a and MAPK kinases, including ERK, p38, and JNK, in REH, RS4;11 and SUP-B15 B-ALL cells in response to dexamethasone treatment. The results showed that the FOXO3a Ser-7 phosphorylation level increased in sensitive but not resistant cells following dexamethasone treatment (Figure 4A). Furthermore, while there was an induction in activity of the two canonical MAPKs, p38 and JNK, as revealed by the phosphorylation specific antibodies, ERK expression and activity remained relatively constant in RS4;11 and SUP-B15 cells after dexamethasone (Figure 4A). Conversely, in REH cells the JNK activity decreased whereas ERK activity increased marginally (Figure 4A). These results indicate that p38 and JNK may have a role in mediating dexamethasone function in B-ALL. To test this conjecture, we next assessed if inhibition of JNK, p38 or ERK kinases using small molecule inhibitors can influence dexamethasone sensitivity. More specifically, REH and RS4;11 cells were treated for 48 h with 1 μM of dexamethasone combined with a range of concentrations (0-100 μM) of JNK, p38 and ERK inhibitors, SP600125, SB202190 and PD98059, respectively, and cell viability analyzed by MTT assay (Figure 4B and Supplementary Figure S1). Interestingly, we observed a significant decrease in the cytotoxicity of dexamethasone when administered with the JNK inhibitor, SP600125, in both RS4;11 and REH cells (Figure 4B). By comparison, the dexamethasone cytotoxicity did not alter significantly when combined with either the p38 or ERK inhibitors (Figure S1, Supplementary data).

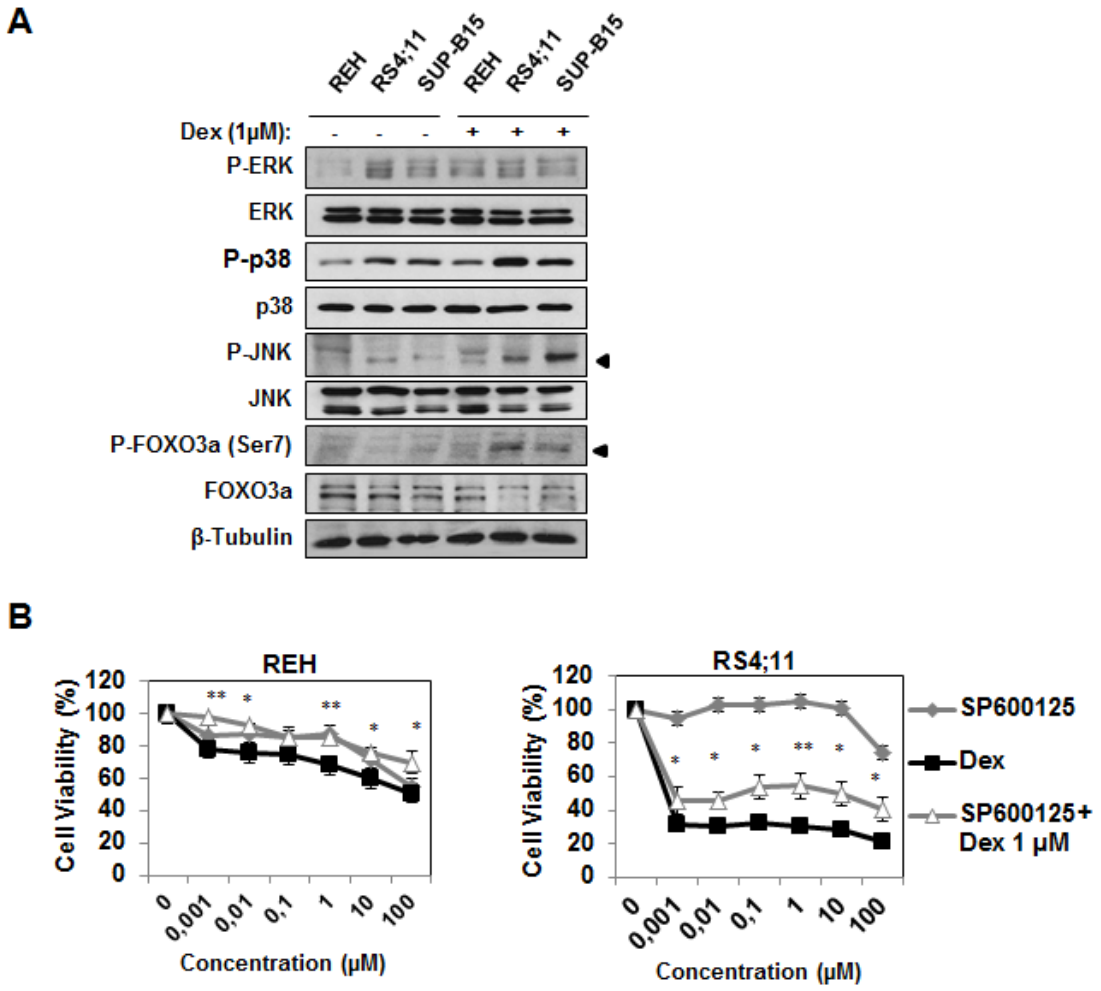

Figure 4. Dexamethasone enhances FOXO3a Ser-7, JNK and p38 phosphorylation in sensitive and not resistant B-ALL cell lines. A) REH, RS4;11 and SUP-B15 cells were treated with dexamethasone (1μM) for 0 and 24 h. Cells were collected after treatment and were subjects to western blot analysis with antibodies shown. B) REH and RS4;11 cells were treated with the a range of concentrations of (0-100μM) SP600125 and/or dexamethasone. Cell viability analysis was performed after 48 h using MTT assay. (t-test: SP600125 with 1μM dexamethasone verses dexamethasone at 1μM) *significant $p<0.05$, ** very significant $p<0.01$ and no marker: not significant .

FOXO3a nuclear localisation is associated with phosphorylation on Ser-7 and acetylation on Lys-242/245 in B-ALL cells

Acetylation has been described to modulate the transcriptional activity of FOXO3a (Shiota *et al.*, 2010; Khongkow *et al.*, 2013). In addition, a recent study has also demonstrated that JNK-phosphorylation can promote FOXO1 acetylation and activation (Vahtola *et al.*, 2010). These findings have led us to propose that dexamethasone activates JNK to mediate FOXO3a phosphorylation and consequently, acetylation. To examine if dexamethasone induces FOXO3a acetylation, immunoprecipitation experiments were performed on REH, RS4;11 and SUP-B15 cells using anti-FOXO3a antibodies. Western blot results using pan-acetylation antibodies showed that in response to dexamethasone there was a net increase in FOXO3a acetylation levels in the drug sensitive RS4;11 and SUP-B15 but not in the resistant REH cells (Figure 5A). By contrast, when the Western blots were reprobed with a monoclonal anti-FOXO3a, the results indicated that the FOXO3a acetylation observed was not a result of the expression patterns of FOXO3a following dexamethasone treatment (Figure 5A). Similar results were obtained, when the reverse immunoprecipitation and western blotting was performed using a pan-acetylation and a FOXO3a antibody, demonstrating that dexamethasone induces FOXO3a acetylation in sensitive and not resistant B-All cells (Figure 5B). We next used the FOXO3a (S7) antibody to immunoprecipate the FOXO3a complex and probed with a pan-FOXO3a antibody. The western blot results showed that FOXO3a Ser-7 phosphorylation demonstrated similar expression patterns as FOXO3a acetylation in both the sensitive and resistant B-ALL cells in response to dexamethasone (Figure 5C), implicating that dexamethasone mediates both FOXO3a Ser-7 phosphorylation and acetylation in B-ALL.

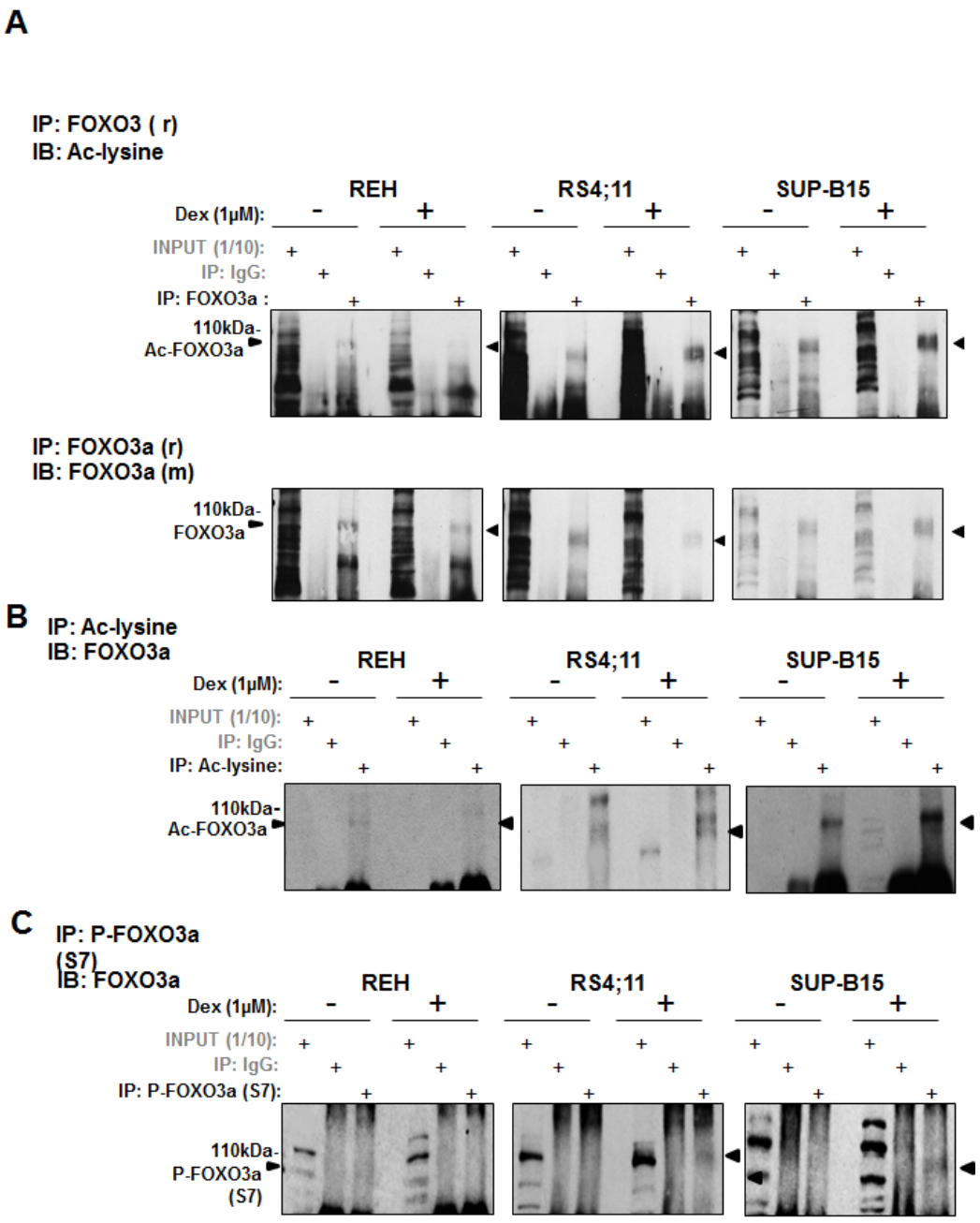

Figure 5. Dexamethasone enhances FOXO3a acetylation and Ser-7 phosphorylation in sensitive and not resistant B-ALL cell lines. A) REH and RS4;11 cells were treated with dexamethasone (1μM) for 0 and 24 h. Co-immunoprecipitation (co-IP) was performed with a FOXO3a antibody (rabbit) and probed (IB) for Ac-Lysine and FOXO3a (mouse). B) Reverse co-immunoprecipitation (co-IP) was performed with the Ac-Lysine antibody and probed with a FOXO3a antibody (rabbit). C) Co-IP was performed with the FOXO3a (S7) antibody and probed with a FOXO3a antibody (rabbit). Inputs (1/10 of IP), and IP products with IgG and specific antibodies were resolved on western blot and analyzed with IB antibodies as indicated.

FOXO3a Lys-242 and Lys-245 acetylation is associated with nuclear localisation, Ser-7 phosphorylation and JNK activation

The residues Lys-242 and Lys-245 (K242/5) located within the overlapping DNA-binding and nuclear localization signal (NLS) domains of FOXO3a have been demonstrated to be CBP-acetylation sites (Tsai *et al.*, 2007; Lam *et al.*, 2013)}. It is possible that these post-translational modifications could alter FOXO3a DNA-binding and/or nuclear localization ability and thereby, impact its transcriptional activity. To investigate FOXO3a acetylation further, we generated an acetylation-specific antibody that recognizes the Lys-242 and Lys-245 acetylated FOXO3a. Using this Ac-FOXO3a (K242/5) specific antibody in western blot analysis, we found that FOXO3a increased in Lys-242/5 acetylation upon dexamethasone treatment in the sensitive but not resistant cells in a short time course (Figure 6A). The western blot results also revealed that the expression patterns of FOXO3a Lys-242/5 acetylation were similar to that of Ser-7 phosphorylation and JNK phosphorylation, providing further evidence that JNK phosphorylation is associated FOXO3a Ser-7 phosphorylation and acetylation on Lys-242/5 (Figure 6A). To test this idea further, we next examined the expression of total-acetylated, Lys-242/5 acetylated and Ser-7 phosphorylated FOXO3a in the cytoplasmic and nuclear fractions of the sensitive and resistant B-ALL cells in response to treatment with dexamethasone following immunoprecipitation with the anti-FOXO3a (Figure 6B). The results showed that the total acetylated, the Lys-242/5 acetylated, and the Ser-7 phosphorylated FOXO3a resided predominantly in the nuclei. In addition, Western blot results clearly showed that in the sensitive cells FOXO3a became more acetylated and phosphorylated after dexamethasone treatment. On the contrary, FOXO3a acetylation (total and Lys-242/245) and phosphorylation (Ser-7) decreased marginally following dexamethasone in the resistant REH cells. Collectively, these data suggest that Lys-242/245 acetylation and Ser-7 phosphorylation is associated with dexamethasone-mediated nuclear relocalization and activation of FOXO3a (Figure 6B). In agreement, previous studies have shown that Ser-7 phosphorylation and Lys-242/245 acetylation promote nuclear relocalization and activation of FOXO3a and FOXO1, respectively (Ho *et al.*, 2012; Matsuzaki *et al.*, 2005).

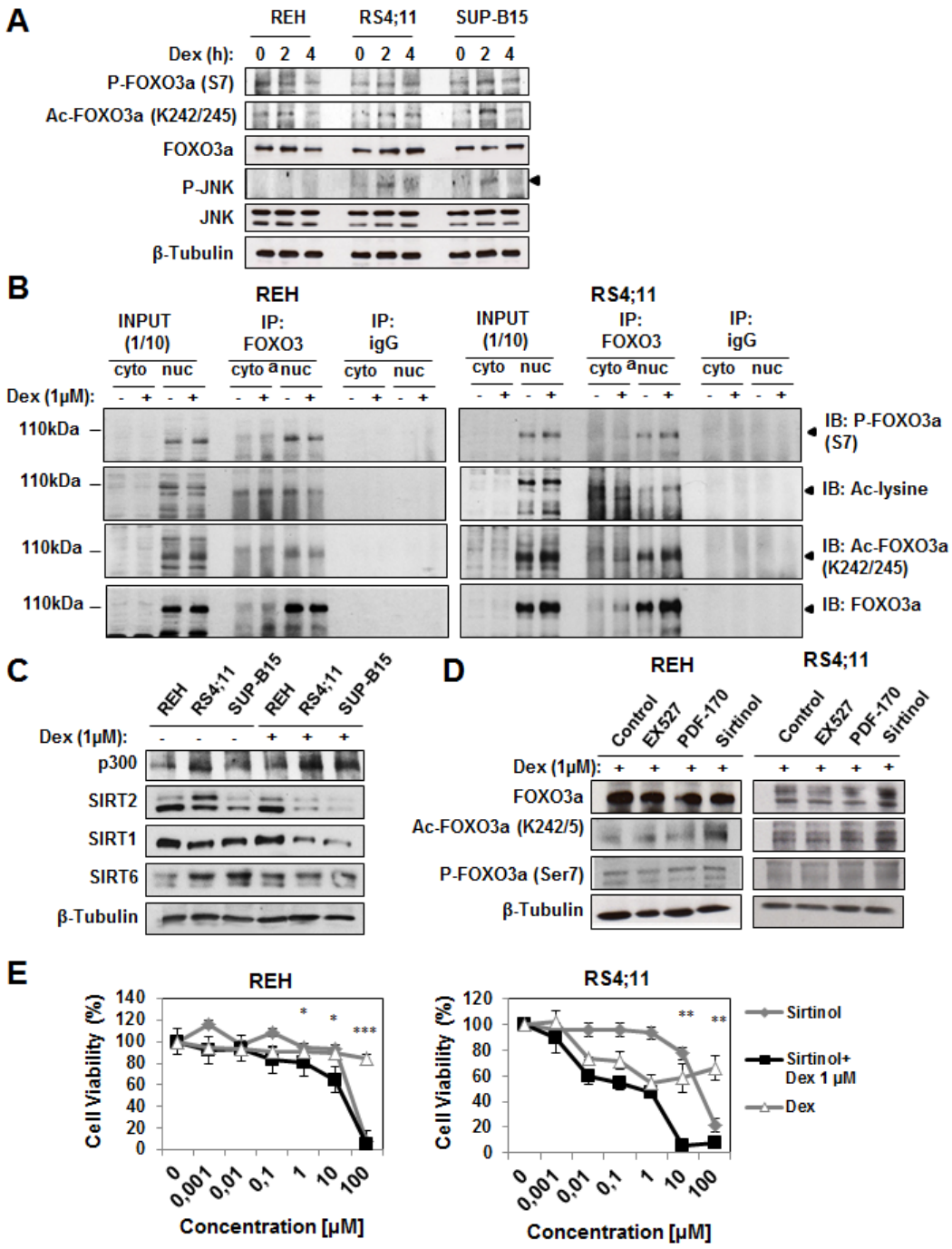

Figure 6. Dexamethasone enhances FOXO3a acetylation on Lys 242/245 in sensitive and not resistant B-ALL cell lines via Sirtuins A) REH, RS4;11 and SUP-B15 cells were treated with dexamethasone (1μM) for 0, 2 and 4 h. Cells were collected after treatment and were subjects to western blot analysis with antibodies shown. B) REH and RS4;11 cells were treated with dexamethasone (1μM) for 0 and 24 h. Co-immunoprecipitation (co-IP) was performed on the respective nuclear and cytoplasmic lysates with a FOXO3a antibody (rabbit) and probed for P-FOXO3a (S7), Ac-Lysine, Ac-FOXO3a (K242/K245), and

FOXO3a (mouse). Inputs (1/10 of IP), and IP products with IgG and specific antibodies were resolved on western blot and probed for proteins as indicated. C) REH, RS4;11 and SUP-B15 cells were treated with dexamethasone (1μM) for 0 and 24 h. The treated cells were collected and subjected to western blot analysis for the proteins indicated. D) REH and RS4;11 cells were either untreated or treated with the SIRT inhibitors indicated in the presence of 1μM dexamethasone for 24 h and subjected to immunoblotting with antibodies indicated. E) REH and RS4;11 cells were treated with the a range of concentrations of (0-100μM) Sirtinol and/or dexamethasone. Cell viability analysis was performed after 24 h using MTT assay. (t-test: Sirtinol with 1μM dexamethasone verses dexamethasone at 1μM) *significant $p<0.05$, ** very significant $p<0.01$ and no marker: not significant .

FOXO3a acetylation is associated with p300 activation and SIRT1/2/6 downregulation

To investigate the mechanisms underlying FOXO3a acetylation, we studied the expression patterns of known mediators of FOXO3a acetylation, including the acetyl transferase CBP/p300 and the histone/lysine deacetylases SIRT1, SIRT2 and SIRT6, in response to dexamethasone in the B-ALL cell lines. Specifically, p300/CBP has been shown to mediate the FOXO3a acetylation on Lys-242, Lys-245 and Lys-262 residues, whereas SIRT1, -2 and-6 have been shown to target FOXO3a for deacetylation (van der Heide and Smidt, 2005; Wang *et al.*, 2012; Peck *et al.*, 2010; Di Fruscia *et al.*, 2014; Khongkow *et al.*, 2013). Western blot analysis showed that dexamethasone treatment upregulated CBP/p300 and downregulated SIRT1, -2 and -6 expression in the drug sensitive RS4;11 and SUP-B15 cells (Figure 6C). By contrast, dexamethasone treatment did not affect CBP/p300 expression as well as SIRT1, -2 and -6 levels after dexamethasone treatment in the resistant REH cells. Taken together, these data suggest that the dexamethasone-induced FOXO3a acetylation in B-ALL is mediated by mechanisms involving the downregulation of SIRT1/2 and upregulation of CBP/p300 and that these control mechanisms are deregulated in resistant cells. As we had already shown that FOXO3a has a role in B-ALL dexamethasone sensitivity, we next tested if SIRT1, SIRT2 or general SIRT inhibition can re-sensitize the drug resistant B-ALL cells to dexamethasone. To this end, we treated both the drug sensitive RS4;11 and resistant REH cells with 1 μM of dexamethasone and a range of concentrations (0-100 μM) of EX-527 (a SIRT1 inhibitor) (Peck *et al.*, 2010), PDF-170 (a SIRT2 inhibitor) (Di Fruscia *et al.*, 2012) and Sirtinol (a pan SIRT1/2/6 inhibitor) (Peck *et al.*, 2010) (Figure 6D and 6E). MTT proliferation assay revealed that only Sirtinol, but not EX-527 or PDF-170, enhanced the antiproliferative effects of

dexamethasone in both the sensitive (RS4;11) and the resistant (REH) cell lines (Figure 6E). These data suggest that sirtuins have a key role in modulating dexamethasone sensitivity and that the inhibition of at least SIRT1 and -2 simultaneously is required for overcoming dexamethasone resistance. We next tested if these SIRT inhibitors can combine with dexamethasone to restore FOXO3a acetylation (K242/5) in the resistant cells. Consistent with the proliferation assay results, western blot results showed that only Sirtinol and neither EX-527 nor PDF-170 could further enhance FOXO3a acetylation induced by dexamethasone in the resistant cells. Notably, FOXO3a acetylation (K242/5) was not enhanced by the SIRT inhibitors in the sensitive RS4;11 cells (Figure 6 D), and it is likely to be due to the fact that FOXO3a acetylation was already strongly induced by dexamethasone in these cells.

1.5.5 DISCUSSION

It is well established that Akt (PKB)-mediated phosphorylation and inactivation of FOXO3a culminates in cytoplasmic localization and cell proliferation (Lam *et al.*, 2013; Nestal de Moraes *et al.*, 2014). Herein, we showed that in the sensitive B-ALL cell lines, RS4;11 and SUP-B15, FOXO3a became dephosphorylated on Akt-targeted sites, Ser253, Thr315 and Thr32 upon dexamethasone treatment, but its phosphorylation was unaffected by dexamethasone in the resistant REH cells. These findings suggest that FOXO3a has a central role in mediating dexamethasone response. In agreement with this, FOXO3a activation by dexamethasone is confirmed by the increased expression of two FOXO3a-targets, $p27^{Kip1}$ and Bim, important for cell cycle arrest and cell death. Dexamethasone-treatment also caused cleavage of caspase-3, -7 and -9, indicative of apoptosis in the sensitive B-ALL. FOXO3a can also suppress the expression of targets important for the G2/M phase transition, including Cyclin B, Aurora B and FOXM1, (Lam *et al.*, 2013), and this may explain the G2/M arrest observed after FOXO3a induction by dexamethasone. The dexamethasone-induced FOXO3a dephosphorylation at the Akt sites was accompanied by its translocation to the nucleus in the sensitive cells, whereas FOXO3a remained phosphorylated and retained in the cytoplasm in resistant cells, as revealed by immunofluorescence staining. The physiological relevance of this finding is confirmed in B-ALL patient samples where we found that FOXO3a is predominantly more phosphorylated on the Ser-315 residue in patients of good response (PGR) compared to poor responders (PPR) to prednisone therapy. Crucially, depletion of FOXO3a in the sensitive RS4;11 cells rendered these B-ALL cells significantly less responsive to dexamethasone treatment, confirming further the central role played by this transcription factor in dexamethasone response.

Our findings also suggest that besides Akt-mediated phosphorylation, FOXO3a is differentially regulated by other post-translational mechanisms in dexamethasone sensitive and resistant B-ALL cells. More specifically, our data indicate that dexamethasone induces activation of JNK and p38 MAPKs and the phosphorylation of FOXO3a on Ser-7 in the sensitive but not the resistant B-ALL cells. Consistent with this, we have previously demonstrated that DNA damaging agents, such as doxorubicin, also activate the p38 MAPK, which in turn will phosphorylate FOXO3a on Ser-7 to promote its nuclear

localization and activation to mediate cell cycle arrest (Ho *et al.*, 2012). Surprisingly, our proliferative analysis shows that JNK, but not ERK or p38, inhibitor can combine effectively with dexamethasone to impair sensitive and resistant B-ALL proliferation. Consistently, our previous work has shown that JNK kinases can promote FOXO3a activity and expression by repressing Akt activity and also by direct phosphorylation in breast cancer cells (Sunters *et al.*, 2003; Sunters *et al.*, 2006). In this context, JNK induces FOXO3a nuclear relocalisation and the activation of its targets, including $p27^{Kip1}$ and Bim, important for cell cycle arrest and cell death (Sunters *et al.*, 2003; Sunters *et al.*, 2006). Consistent with this, we also observed upon dexamethasone treatment, the activation of JNK and p38 MAPKs, which are associated with FOXO3a nuclear translocation, dephosphorylation at Akt-sites, induction of $p27^{Kip1}$ and Bim expression and cell proliferative arrest in the sensitive and not the resistant B-ALL cells. Our observations, in conjunction with the results of previous studies, suggest that dexamethasone targets FOXO3a via JNK and Akt to mediate its cytotoxic and cytostatic function in B-ALL.

We also found that FOXO3a is acetylated in the sensitive and not the resistant B-ALL cells and that FOXO3a acetylation can be further enhanced upon dexamethasone treatment. In these cases, our acetylation-specific FOXO3a antibody revealed that dexamethasone also causes FOXO3a to be acetylated at Lys242/5 in the sensitive and not the resistant cells. In attempting to explore the mechanism involved, we found that the expression of CREB-binding protein (CBP) is increased, whereas SIRT-1 and -2 levels are suppressed by dexamethasone treatment. In agreement, previous research has shown that FOXO1/3a acetylation at Lys-242 and Lys-245 is mediated through the antagonistic action of cAMP-response element-binding protein (CREB)-binding protein and the NAD-dependent histone/lysine deacetylase sirtuins (Matsuzaki *et al.*, 2005; Tsai *et al.*, 2007). However, the authors of these studies also predict that acetylation at Lys-242 and Lys-245 attenuates the DNA-binding activity and thereby impairs transcriptional activity of FOXO proteins (Matsuzaki *et al.*, 2005; Tsai *et al.*, 2007). On the contrary, our results indicate that FOXO3a acetylation, particularly at Lys-242/5, is associated with nuclear localization, induction of downstream anti-proliferative targets, cell proliferative arrest and sensitivity to dexamethasone. Hence, the analogy between this and our study is not perfect. However, in support of our findings, SIRT6 has recently been shown to regulate gluconeogenesis by

promoting FOXO1 nuclear exclusion (Zhang *et al.*, 2014). Moreover, another recent study on pancreatic cancer also demonstrates that JNK-phosphorylation can promote FOXO1 acetylation and activation as well as Bim expression (Pramanik *et al.*, 2014). In this case, FOXO1 acetylation is also accompanied by increased expression of CREB-binding protein (CBP) and reduced SIRT1 expression (Pramanik *et al.*, 2014). Furthermore, deacetylation of FOXO3a by SIRT1 or SIRT2 leads to Skp2-mediated FOXO3 ubiquitination and degradation (Wang *et al.*, 2012). Critically, we showed that the pan-SIRT inhibitor sirtinol, but not the specific SIRT1 (EX527) or SIRT2 (PDF-170) inhibitor, can combine with dexamethasone to restrict both sensitive and resistant B-ALL cell proliferation, suggesting at least both SIRT1 and -2 have to be suppressed simultaneously to exert the anti-proliferative effects of dexamethasone. This observation is in concordance with our earlier results showing that both SIRT1 and SIRT2 were both downregulated in response to dexamethasone in the sensitive but not the resistant B-ALL cells. Together these data suggest a role for both SIRT1 and -2 in restricting the cytotoxic and cytostatic function of dexamethasone and that dexamethasone mediates its action through downregulating SIRT1 and SIRT2 expression in B-All. Aptly, the pan-SIRT inhibitor sirtinol, but not the SIRT1 or -2 inhibitor, can function in combination with dexamethasone to induce FOXO3a acetylation at Lys-242/5 in B-ALL cells. Collectively, ours and others' results have led us to propose a signalling mechanism whereby dexamethasone can induce JNK to inhibit FOXO3a phosphorylation at Akt-sites and induce phosphorylation at Ser-7 and acetylation at Lys-242/5 to promote nuclear localization and thereby, transcription activity. As we have shown that FOXO3a has a essential role in dexamethasone responsiveness, it is therefore tempting to speculate that the sensitivity to dexamethasone is at least in part determined by acetylation and phosphorylation status of FOXO3a. However, to draw informed definitive conclusions on this model, additional in-depth experimental work is required to identify all the phosphorylation and acetylation sites involved and to define the regulation and function of these post-translational modifications.

Nevertheless, our findings are of significance because they reveal a potential novel therapeutic strategy to treat B-ALL and to overcome dexamethasone resistance by concurrent upregulation of JNK and/or antagonism of sirtuins with dexamethasone. Evidently, our data suggest that pan-SIRT inhibitors, such as sirtinol, have substantial synergistic potential with dexamethasone and can be used to improve the efficacy of

dexamethasone and to overcome dexamethasone resistance. Our data also provide evidence that FOXO3a phosphorylation at Ser-7, phosphorylation at Akt-targeted sites, and acetylation at Lys-242/5 can be reliable biomarkers for predicting and for monitoring dexamethasone response in B-ALL patients in the clinic.

1.5.6 REFERENCES

Accordi, B., Galla, L., Milani, G., Curtarello, M., Serafin, V., Lissandron, V., Viola, G., te Kronnie, G., De Maria, R., Petricoin, E.F., 3rd, Liotta, L.A., Indraccolo, S., Basso, G. (2013) AMPK inhibition enhances apoptosis in MLL-rearranged pediatric B-acute lymphoblastic leukemia cells. *Leukemia* **27** (5): 1019-27.

Ausserlechner, M.J., Salvador, C., Deutschmann, A., Bodner, M., Viola, G., Bortolozzi, R., Basso, G., Hagenbuchner, J., Obexer, P. (2013) Therapy-resistant acute lymphoblastic leukemia (ALL) cells inactivate FOXO3 to escape apoptosis induction by TRAIL and Noxa. *Oncotarget* **4** (7): 995-1007.

Bachmann, P.S., Gorman, R., Mackenzie, K.L., Lutze-Mann, L., Lock, R.B. (2005) Dexamethasone resistance in B-cell precursor childhood acute lymphoblastic leukemia occurs downstream of ligand-induced nuclear translocation of the glucocorticoid receptor. *Blood* **105** (6): 2519-26.

Boccitto, M., Kalb, R.G. (2011) Regulation of Foxo-dependent transcription by post-translational modifications. *Curr Drug Targets* **12** (9): 1303-10.

Daitoku, H., Hatta, M., Matsuzaki, H., Aratani, S., Ohshima, T., Miyagishi, M., Nakajima, T., Fukamizu, A. (2004) Silent information regulator 2 potentiates Foxo1-mediated transcription through its deacetylase activity. *Proc Natl Acad Sci U S A* **101** (27): 10042-7.

Dansen, T.B., Smits, L.M., van Triest, M.H., de Keizer, P.L., van Leenen, D., Koerkamp, M.G., Szypowska, A., Meppelink, A., Brenkman, A.B., Yodoi, J., Holstege, F.C., Burgering, B.M. (2009) Redox-sensitive cysteines bridge p300/CBP-mediated acetylation and FoxO4 activity. *Nat Chem Biol* **5** (9): 664-72.

Dewar, R., Chen, S.T., Yeckes-Rodin, H., Miller, K., Khosravi-Far, R. (2011) Bortezomib treatment causes remission in a Ph+ALL patient and reveals FoxO as a theranostic marker. *Cancer Biol Ther* **11** (6): 552-8.

Di Fruscia, P., Ho, K.K., Laohasinnarong, S., Khongkow, M., Kroll, S.H., Islam, S.A., Sternberg, M.J., Schmidtkunz, K., Jung, M., Lam, E.W., Fuchter, M.J. (2012) The Discovery of Novel 10,11-Dihydro-5H-dibenz[b,f]azepine SIRT2 Inhibitors. *Medchemcomm* (3).

Di Fruscia, P., Zacharioudakis, E., Liu, C., Moniot, S., Laohasinnarong, S., Khongkow, M., Harrison, I.F., Koltsida, K., Reynolds, C.R., Schmidtkunz, K., Jung, M., Chapman, K.L., Steegborn, C., Dexter, D.T., Sternberg, M.J., Lam, E.W., Fuchter, M.J. (2014) The Discovery of a Highly Selective

5,6,7,8-Tetrahydrobenzo[4,5]thieno[2,3-d]pyrimidin-4(3H)-one SIRT2 Inhibitor that is Neuroprotective in an in vitro Parkinson's Disease Model. *ChemMedChem*.

Essafi, A., Fernandez de Mattos, S., Hassen, Y.A., Soeiro, I., Mufti, G.J., Thomas, N.S., Medema, R.H., Lam, E.W. (2005) Direct transcriptional regulation of Bim by FoxO3a mediates STI571-induced apoptosis in Bcr-Abl-expressing cells. *Oncogene* **24** (14): 2317-29.

Essers, M.A., Weijzen, S., de Vries-Smits, A.M., Saarloos, I., de Ruiter, N.D., Bos, J.L., Burgering, B.M. (2004) FOXO transcription factor activation by oxidative stress mediated by the small GTPase Ral and JNK. *EMBO J* **23** (24): 4802-12.

Gaynon, P.S., Carrel, A.L. (1999) Glucocorticosteroid therapy in childhood acute lymphoblastic leukemia. *Adv Exp Med Biol* **457**: 593-605.

Ho, K.K., McGuire, V.A., Koo, C.Y., Muir, K.W., de Olano, N., Maifoshie, E., Kelly, D.J., McGovern, U.B., Monteiro, L.J., Gomes, A.R., Nebreda, A.R., Campbell, D.G., Arthur, J.S., Lam, E.W. (2012) Phosphorylation of FOXO3a on Ser-7 by p38 promotes its nuclear localization in response to doxorubicin. *J Biol Chem* **287** (2): 1545-55.

Ho, K.K., Myatt, S.S., Lam, E.W. (2008) Many forks in the path: cycling with FoxO. *Oncogene* **27** (16): 2300-11.

Kawauchi, K., Ogasawara, T., Yasuyama, M., Otsuka, K., Yamada, O. (2009) The PI3K/Akt pathway as a target in the treatment of hematologic malignancies. *Anticancer Agents Med Chem* **9** (5): 550-9.

Khongkow, M., Olmos, Y., Gong, C., Gomes, A.R., Monteiro, L.J., Yague, E., Cavaco, T.B., Khongkow, P., Man, E.P., Laohasinnarong, S., Koo, C.Y., Harada-Shoji, N., Tsang, J.W., Coombes, R.C., Schwer, B., Khoo, U.S., Lam, E.W. (2013) SIRT6 modulates paclitaxel and epirubicin resistance and survival in breast cancer. *Carcinogenesis* **34** (7): 1476-86.

Kops, G.J., Dansen, T.B., Polderman, P.E., Saarloos, I., Wirtz, K.W., Coffer, P.J., Huang, T.T., Bos, J.L., Medema, R.H., Burgering, B.M. (2002) Forkhead transcription factor FOXO3a protects quiescent cells from oxidative stress. *Nature* **419** (6904): 316-21.

Kornblau, S.M., Singh, N., Qiu, Y., Chen, W., Zhang, N., Coombes, K.R. (2010) Highly phosphorylated FOXO3A is an adverse prognostic factor in acute myeloid leukemia. *Clin Cancer Res* **16** (6): 1865-74.

Lam, E.W., Brosens, J.J., Gomes, A.R., Koo, C.Y. (2013) Forkhead box proteins: tuning forks for transcriptional harmony. *Nat Rev Cancer* **13** (7): 482-95.

Mahmud, D.L., M, G.A., Deb, D.K., Platanias, L.C., Uddin, S., Wickrema, A. (2002) Phosphorylation of forkhead transcription factors by erythropoietin and stem cell factor prevents acetylation and their interaction with coactivator p300 in erythroid progenitor cells. *Oncogene* **21** (10): 1556-62.

Matsuzaki, H., Daitoku, H., Hatta, M., Aoyama, H., Yoshimochi, K., Fukamizu, A. (2005) Acetylation of Foxo1 alters its DNA-binding ability and sensitivity to phosphorylation. *Proc Natl Acad Sci U S A* **102** (32): 11278-83.

Miyamoto, K., Miyamoto, T., Kato, R., Yoshimura, A., Motoyama, N., Suda, T. (2008) FoxO3a regulates hematopoietic homeostasis through a negative feedback pathway in conditions of stress or aging. *Blood* **112** (12): 4485-93.

Motta, M.C., Divecha, N., Lemieux, M., Kamel, C., Chen, D., Gu, W., Bultsma, Y., McBurney, M., Guarente, L. (2004) Mammalian SIRT1 represses forkhead transcription factors. *Cell* **116** (4): 551-63.

Myatt, S.S., Kongsema, M., Man, C.W., Kelly, D.J., Gomes, A.R., Khongkow, P., Karunarathna, U., Zona, S., Langer, J.K., Dunsby, C.W., Coombes, R.C., French, P.M., Brosens, J.J., Lam, E.W. (2014) SUMOylation inhibits FOXM1 activity and delays mitotic transition. *Oncogene* **33** (34): 4316-29.

Myatt, S.S., Lam, E.W. (2007) The emerging roles of forkhead box (Fox) proteins in cancer. *Nat Rev Cancer* **7** (11): 847-59.

Nestal de Moraes, G., Bella, L., Zona, S., Burton, M.J., Lam, E.W. (2014) Insights into a Critical Role of the FOXO3a-FOXM1 Axis in DNA Damage Response and Genotoxic Drug Resistance. *Curr Drug Targets*.

Nordigarden, A., Kraft, M., Eliasson, P., Labi, V., Lam, E.W., Villunger, A., Jonsson, J.I. (2009) BH3-only protein Bim more critical than Puma in tyrosine kinase inhibitor-induced apoptosis of human leukemic cells and transduced hematopoietic progenitors carrying oncogenic FLT3. *Blood* **113** (10): 2302-11.

Olmos, Y., Brosens, J.J., Lam, E.W. (2011) Interplay between SIRT proteins and tumour suppressor transcription factors in chemotherapeutic resistance of cancer. *Drug Resist Updat* **14** (1): 35-44.

Paik, J.H., Kollipara, R., Chu, G., Ji, H., Xiao, Y., Ding, Z., Miao, L., Tothova, Z., Horner, J.W., Carrasco, D.R., Jiang, S., Gilliland, D.G., Chin, L., Wong, W.H., Castrillon, D.H., DePinho, R.A. (2007) FoxOs are lineage-restricted redundant tumor suppressors and regulate endothelial cell homeostasis. *Cell* **128** (2): 309-23.

Peck, B., Chen, C.Y., Ho, K.K., Di Fruscia, P., Myatt, S.S., Coombes, R.C., Fuchter, M.J., Hsiao, C.D., Lam, E.W. (2010) SIRT inhibitors induce cell death and p53 acetylation through targeting both SIRT1 and SIRT2. *Mol Cancer Ther* **9** (4): 844-55.

Perrot, V., Rechler, M.M. (2005) The coactivator p300 directly acetylates the forkhead transcription factor Foxo1 and stimulates Foxo1-induced transcription. *Mol Endocrinol* **19** (9): 2283-98.

Pramanik, K.C., Fofaria, N.M., Gupta, P., Srivastava, S.K. (2014) CBP-mediated FOXO-1 acetylation inhibits pancreatic tumor growth by targeting SirT. *Mol Cancer Ther* **13** (3): 687-98.

Senf, S.M., Sandesara, P.B., Reed, S.A., Judge, A.R. (2011) p300 Acetyltransferase activity differentially regulates the localization and activity of the FOXO homologues in skeletal muscle. *Am J Physiol Cell Physiol* **300** (6): C1490-501.

Shiota, M., Yokomizo, A., Kashiwagi, E., Tada, Y., Inokuchi, J., Tatsugami, K., Kuroiwa, K., Uchiumi, T., Seki, N., Naito, S. (2010) Foxo3a expression and acetylation regulate cancer cell growth and sensitivity to cisplatin. *Cancer Sci* **101** (5): 1177-85.

Sunters, A., Fernandez de Mattos, S., Stahl, M., Brosens, J.J., Zoumpoulidou, G., Saunders, C.A., Coffer, P.J., Medema, R.H., Coombes, R.C., Lam, E.W. (2003) FoxO3a transcriptional regulation of Bim controls apoptosis in paclitaxel-treated breast cancer cell lines. *J Biol Chem* **278** (50): 49795-805.

Sunters, A., Madureira, P.A., Pomeranz, K.M., Aubert, M., Brosens, J.J., Cook, S.J., Burgering, B.M., Coombes, R.C., Lam, E.W. (2006) Paclitaxel-induced nuclear translocation of FOXO3a in breast cancer cells is mediated by c-Jun NH2-terminal kinase and Akt. *Cancer Res* **66** (1): 212-20.

Tsai, K.L., Sun, Y.J., Huang, C.Y., Yang, J.Y., Hung, M.C., Hsiao, C.D. (2007) Crystal structure of the human FOXO3a-DBD/DNA complex suggests the effects of post-translational modification. *Nucleic Acids Res* **35** (20): 6984-94.

Tzivion, G., Dobson, M., Ramakrishnan, G. (2011) FoxO transcription factors; Regulation by AKT and 14-3-3 proteins. *Biochim Biophys Acta* **1813** (11): 1938-45.

Vahtola, E., Louhelainen, M., Forsten, H., Merasto, S., Raivio, J., Kaheinen, P., Kyto, V., Tikkanen, I., Levijoki, J., Mervaala, E. (2010) Sirtuin1-p53, forkhead box O3a, p38 and post-infarct cardiac remodeling in the spontaneously diabetic Goto-Kakizaki rat. *Cardiovasc Diabetol* **9**: 5.

van der Heide, L.P., Smidt, M.P. (2005) Regulation of FoxO activity by CBP/p300-mediated acetylation. *Trends Biochem Sci* **30** (2): 81-6.

Vecchio, L., Seke Etet, P.F., Kipanyula, M.J., Krampera, M., Nwabo Kamdje, A.H. (2013) Importance of epigenetic changes in cancer etiology, pathogenesis, clinical profiling, and treatment: what can be learned from hematologic malignancies? *Biochim Biophys Acta* **1836** (1): 90-104.

Wang, F., Chan, C.H., Chen, K., Guan, X., Lin, H.K., Tong, Q. (2012) Deacetylation of FOXO3 by SIRT1 or SIRT2 leads to Skp2-mediated FOXO3 ubiquitination and degradation. *Oncogene* **31** (12): 1546-57.

Wang, Y., Zhou, Y., Graves, D.T. (2014) FOXO transcription factors: their clinical significance and regulation. *Biomed Res Int* **2014**: 925350.

Yang, J.Y., Zong, C.S., Xia, W., Yamaguchi, H., Ding, Q., Xie, X., Lang, J.Y., Lai, C.C., Chang, C.J., Huang, W.C., Huang, H., Kuo, H.P., Lee, D.F., Li, L.Y., Lien, H.C., Cheng, X., Chang, K.J., Hsiao, C.D., Tsai, F.J., Tsai, C.H., Sahin, A.A., Muller, W.J., Mills, G.B., Yu, D., Hortobagyi, G.N., Hung, M.C. (2008) ERK promotes tumorigenesis by inhibiting FOXO3a via MDM2-mediated degradation. *Nat Cell Biol* **10** (2): 138-48.

Zhang, P., Tu, B., Wang, H., Cao, Z., Tang, M., Zhang, C., Gu, B., Li, Z., Wang, L., Yang, Y., Zhao, Y., Wang, H., Luo, J., Deng, C.X., Gao, B., Roeder, R.G., Zhu, W.G. (2014) Tumor suppressor p53 cooperates with SIRT6 to regulate gluconeogenesis by promoting FoxO1 nuclear exclusion. *Proc Natl Acad Sci U S A* **111** (29): 10684-9.

Zhang, X., Tang, N., Hadden, T.J., Rishi, A.K. (2011) Akt, FoxO and regulation of apoptosis. *Biochim Biophys Acta* **1813** (11): 1978-86.

Zhang, Y., Gan, B., Liu, D., Paik, J.H. (2011) FoxO family members in cancer. *Cancer Biol Ther* **12** (4): 253-9.

1.5.7 SUPPLEMENTARY INFORMATION

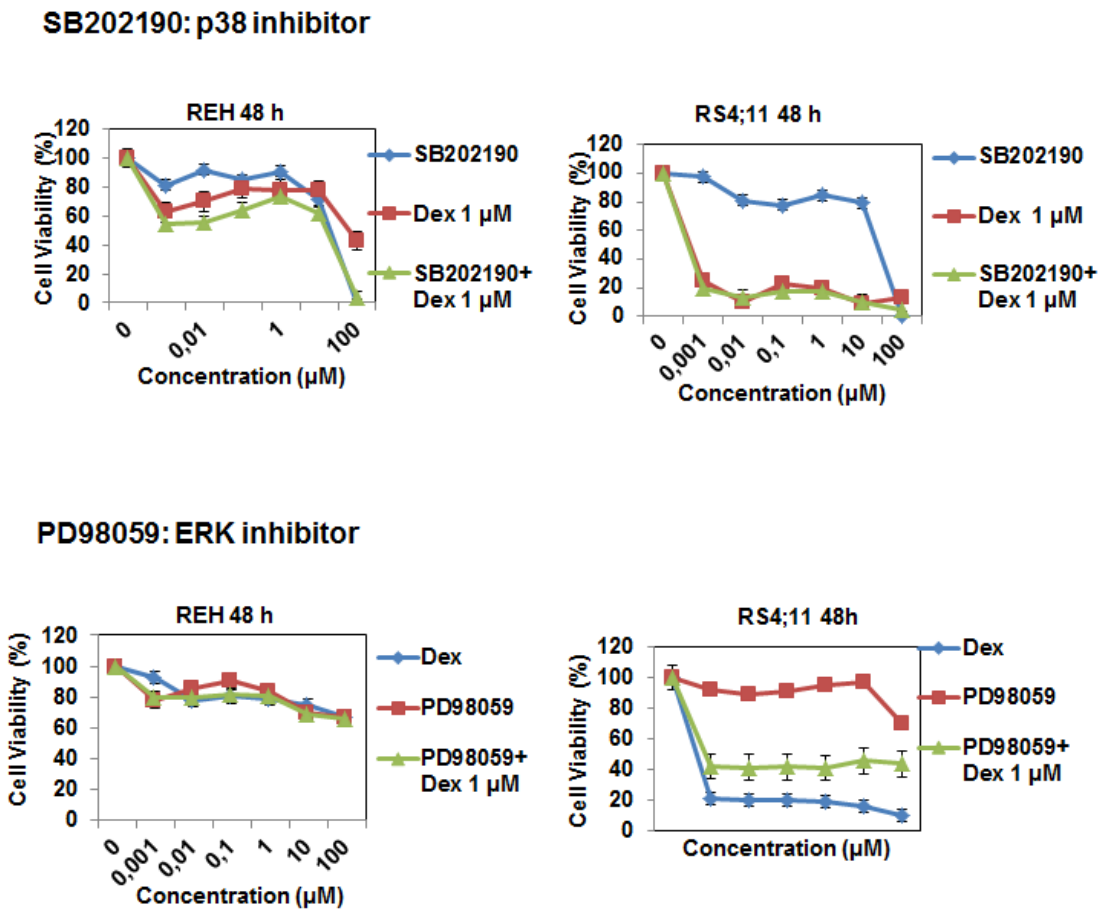

Supplementary Figure S1

p38 and ERK inhibitors do not inhibit the cytotoxic and cytostatic function of dexamethasone in B-ALL cell lines. REH and RS4;11 cells were treated with the a range of concentrations of (0-100μM) of p38 and ERK inhibitors, SB202190 and PD98059 and/or dexamethasone. Cell viability analysis was performed after 48 h using MTT assay.

SIRTs inhibitor: Sirtinol

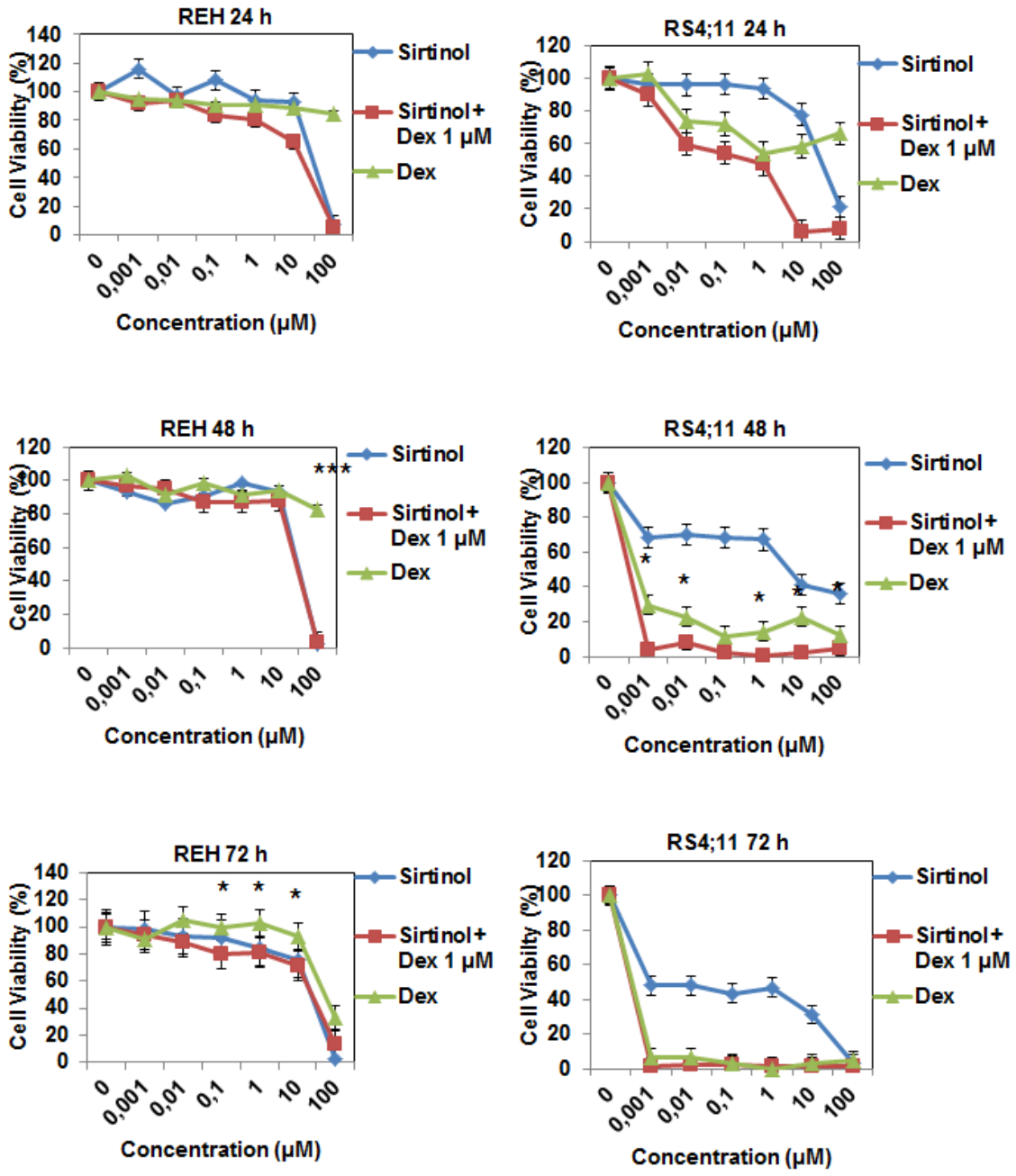

SIRT1 inhibitor: EX-527

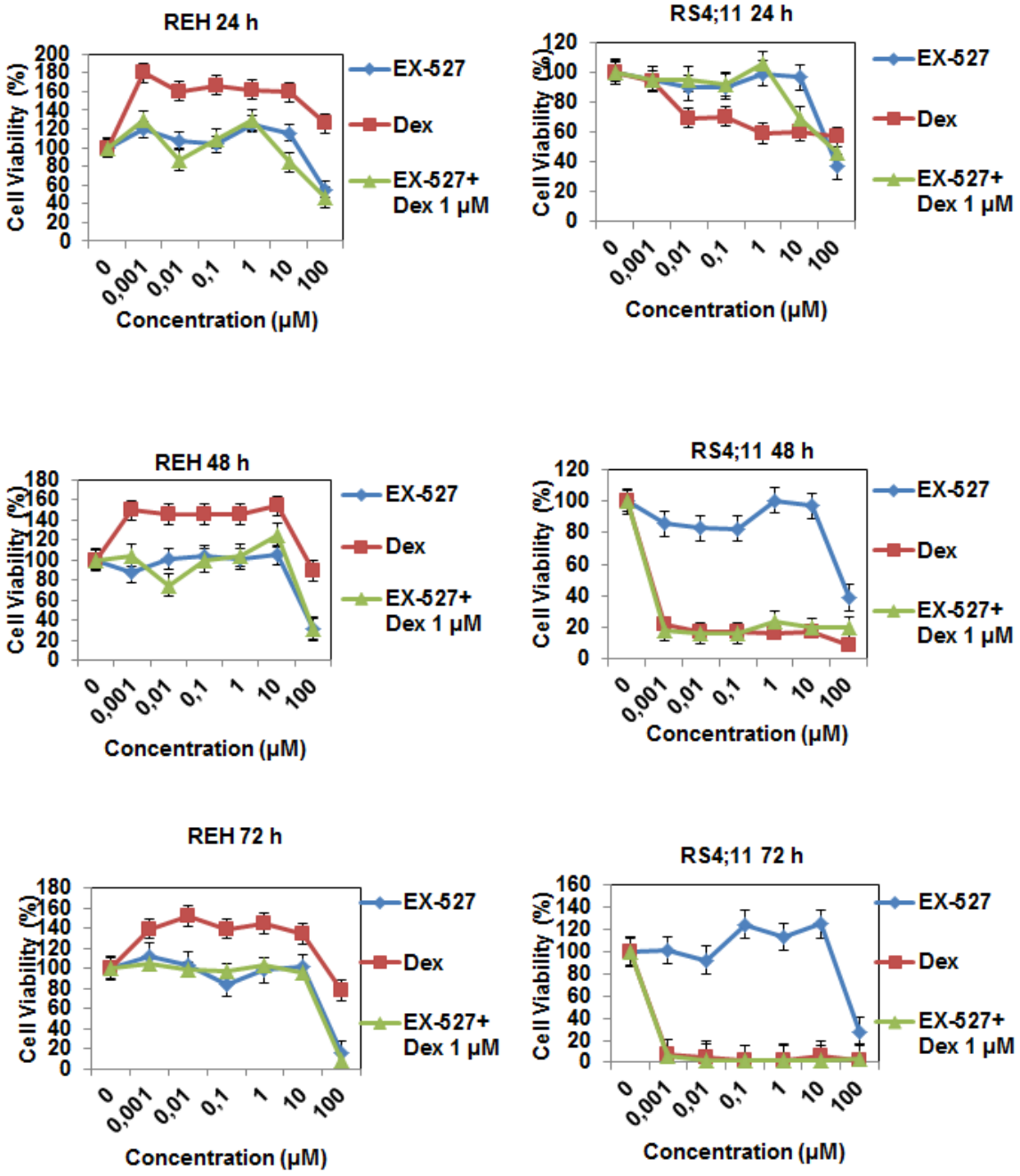

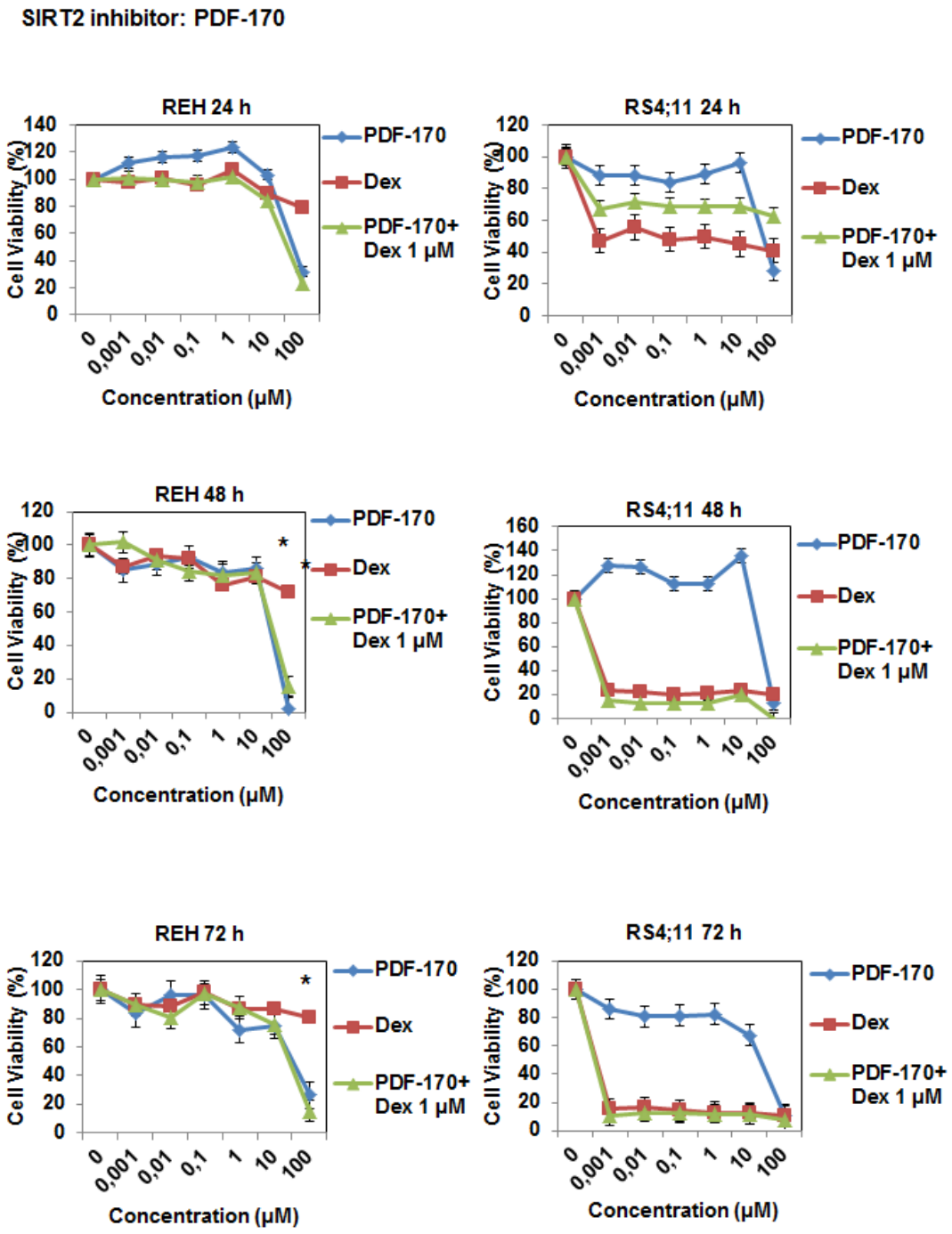

Supplementary Figure S2

Sirtinol but not EX527 or PDF-170 significantly enhances ithe cytotoxic and cytostatic function of dexamethasone in B-ALL cell lines. REH and RS4;11 cells were treated with the a range of concentrations of SIRT inhibitors (0-100μM) and/or dexamethasone. Cell viability analysis was performed after 24, 48 and 72 h using MTT assay. A) Sintinol (SIRT1/2/6 inhibitor); B) EX527 (SIRT1 inhibitor); C) PDF-170 (SIRT2 inhibitor). (t-test: Sirtinol with 1μM dexamethasone verses dexamethasone at 1μM) *significant $p<0.05$, ** very significant $p<0.01$ and no marker: not significant .

1.6 CONCLUSIONS

B-ALL is one of the most common childhood cancer. Over the years, several evidences confirmed the importance on finding the molecular mechanisms underlying dexamethasone resistance at diagnosis. In fact, this condition is often associated with bad prognosis and future relapse conditions.

In this study we aimed to clarify whether the transcription factors FOXM1 and FOXO3a, two members of Forkhead box (FOX) family, are involved in B-ALL. More specifically, we investigated if FOXM1 is involved in B-ALL tumor proliferation and drug resistance, and whether FOXO3a activation is fundamental for dexamethasone sensitiveness. We further analysed how FOXO3a activity might be regulated by post-translational modifications such as phosphorylation and acetylation.

We firstly observed that protein and mRNA levels of FOXM1 were higher in ten B-ALL patient's and five B-ALL cell lines (REH, MHH-CALL2, SEM, RS4;11, NALM-6) compared to peripheral blood mononuclear cells (PBMC) of healthy donors. To then investigate if FOXM1 is involved in cell proliferation and cell cycle progression we inhibited its expression through knockdown and thiostrepton treatment in one glucocorticoid-sensitive cell line, NALM-6, and one glucocorticoid-resistant cell line, REH. Results showed that FOXM1 downregulation causes a significant reduction on cell proliferation, cell cycle arrest in G2/M and increase on sub-G1 cells. More importantly, FOXM1 knockdown also leads to a downregulation of proteins involved in the regulation of mitotic progression and increases cell sensitiveness to dexamethasone treatment in both NALM-6 and REH. To then test if FOXM1 inhibition might improve chemotherapeutic agents efficiency we treated four different B-ALL cell lines with thiostrepton in combination with chemotherapeutic agents (i.e. dexamethasone, asparaginase, daunorubicin, vincristine and Ara-C). Combination index values (CI) calculated according to the Chou-Talalay method revealed that thiostrepton synergises with conventional chemotherapeutic agents in B-ALL reinforcing the hypothesis that FOXM1 might be a key target to optimize the efficacy of existing therapeutics for B-ALL and to overcome drug resistance.

Studying the role of FOXO3a in B-ALL and in particular in glucocorticoid sensitiveness, we observed that in the sensitive B-ALL cell lines, RS4;11 and SUP-B15, the Akt

signaling pathway becomes downregulated following treatment leading then to the consequent FOXO3a activation. In fact we observed that in the sensitive B-ALL cell lines, RS4;11 and SUP-B15, FOXO3a becomes dephosphorylated on Akt-targeted sites, Ser253, Thr315 and Thr32 upon dexamethasone treatment, but its phosphorylation is unaffected by dexamethasone in the resistant REH cells. In agreement with this, FOXO3a activation by dexamethasone was confirmed by the increased expression of two FOXO3a-targets, $p27^{Kip1}$ and Bim, and cell cycle arrest and apoptotis signatures. Furthermore immunostaining data confirmed that following dexamethasone treatment, FOXO3a translocates from cytoplasm to the nucleus only in sensitive cells whereas knockdown experiments showed that FOXO3a expression is essential for dexamethasone- induced cytotoxicity. These findings suggest that FOXO3a has a central role in mediating dexamethasone response. On trying to clarify why FOXO3a is differently regulated in resistant and sensitive cell lines, we analyzed if some other post-translational modifications might be involved in FOXO3a regulation. Interestingly western blot and Immunoprecipitation data showed that, upon dexamethasone treatment, FOXO3a becomes more phosphorylated at Ser7 and more acetylated at Lys 242 and Lys 245 residues only in sensitive cells. Moreover we also observed that the expression patterns of FOXO3a phosphorylation at Ser7 were similar to that of Lys 242/5 acetylation and JNK activation, providing evidence that dexamethasone induces JNK activation which is associated to FOXO3a Ser7 phosphorylation and Lys242/245 acetylation. In addiction our results clearly showed that the total acetylated, the Lys-242/5 acetylated and the Ser7 phosphorylated FOXO3a resided predominantly in the nuclei. In addition FOXO3a in sensitive cells becomes more acetylated and phosphorylated after dexamethasone treatment. On the contrary, FOXO3a acetylation (total and Lys-242/245) and phosphorylation (Ser-7) decreased marginally following dexamethasone in the resistant REH cells. Collectively, these data suggest that Lys-242/245 acetylation and Ser-7 phosphorylation are associated with dexamethasone-mediated nuclear relocalization and activation of FOXO3a. We also found that FOXO3a acetylation is associated with p300 activation and SIRT1/2/6 downregulation. Furthermore, MTT and western blot analysis revealed that only the pan-SIRT1/2/6 inhibitor (Sirtinol), but not the SIRT1 or -2 inhibitor (EX-527 and PDF-170), increases the antiproliferative effect of dexamethasone in both sensitive and resistant cell lines further enhancing the FOXO3a acetylation induced by dexamethasone. Therefore our

data suggest that sirtuins have a key role on modulating dexamethsone sensitivity and that the inhibition oft least SIRT1, and -2 simultaneously is required for overcoming dexamethasone resistance. Moreover our findings reveal a potential novel therapeutic strategy to treat B-ALL and to overcome dexamethasone resistance by concurrent upregulation of JNK and/or antagonism of sirtuins with dexamethasone. Our data also provide evidence that FOXO3a phosphorylation at Ser-7, phosphorylation at Akt-targeted sites, and acetylation at Lys-242/5 can be reliable biomarkers for predicting and for monitoring dexamethasone response in B-ALL patients in the clinic. Furthermore, it might be interesting to clarify the interplay between FOXO3a and FOXM1 in B-ALL. It is well known that FOXO3a can also exert its tumor suppressor function also by blocking FOXM1 expression and activity: FOXO3a can represses the expression of genes implicated in tumour initiation, including FOXM1[20]. Recent research also showed that FOXO3a and FOXM1 antagonize each other's activity by competitively binding to the same target genes, which are involved in chemotherapeutic drug sensitivity and resistance. Therefore, we could assume that the FOXO3a-FOXM1 axis might be involved in dexamethasone responsiveness. Western blot data in fact showed that the FOXO3a activation, observed in glucocorticoid-sensitive cells, is also associated to the FOXM1 downregulation and consequent arrest in G2/M cell cycle phase. Therefore, understanding if there is an interplay between these two transcription factors, FOXO3 and FOXM1, will provide insight into chemotherapeutic drug action and will help to identify novel therapeutic approaches.

1.7 REFERENCES

1. Myatt SS, Lam EW-F. The emerging roles of forkhead box (Fox) proteins in cancer. *Nat. Rev. Cancer* 2007;7:847-859.

2. Gomes AR, Zhao F, Lam EWF. Role and regulation of the forkhead transcription factors FOXO3a and FOXM1 in carcinogenesis and drug resistance. *Chin. J. Cancer* 2013;32:365-370.

3. Lam EW-F, Brosens JJ, Gomes AR, Koo C-Y. Forkhead box proteins: tuning forks for transcriptional harmony. *Nat. Rev. Cancer* 2013;13(7):482-95.

4. Mullighan CG. The molecular genetic makeup of acute lymphoblastic leukemia. *Hematology Am. Soc. Hematol. Educ. Program* 2012;2012:389-96.

5. Cobaleda C, Sánchez-García I. B-cell acute lymphoblastic leukaemia: Towards understanding its cellular origin. *BioEssays* 2009;31:600-609.

6. Woo JS, Alberti MO, Tirado C a. Childhood B-acute lymphoblastic leukemia: a genetic update. *Exp. Hematol. Oncol.* 2014;3:16.

7. Dördelmann M, Reiter A, Borkhardt A, et al. *Prednisone Response Is the Strongest Predictor of Treatment Outcome in Infant Acute Lymphoblastic Leukemia.*; 1999:1209-1217.

8. Inaba H, Pui C-H. Glucocorticoid use in acute lymphoblastic leukaemia. *Lancet Oncol.* 2010;11:1096-1106.

9. Kaspers GJ, Pieters R, Klumper E, De Waal FC, Veerman AJ. Glucocorticoid resistance in childhood leukemia. *Leuk. Lymphoma* 1994;13:187-201.

10. Jackson BC, Carpenter C, Nebert DW, Vasiliou V. Update of human and mouse forkhead box (FOX) gene families. *Hum. Genomics* 2010;4:345-352.

11. Van Der Heide LP, Smidt MP. Regulation of FoxO activity by CBP/p300-mediated acetylation. *Trends Biochem. Sci.* 2005;30:81-86.

12. Wang F, Marshall CB, Li GY, Yamamoto K, Mak TW, Ikura M. Synergistic interplay between promoter recognition and CBP/p300 coactivator recruitment by FOXO3a. *ACS Chem. Biol.* 2009;4:1017-1027. doi:10.1021/cb900190u.

13. McGovern UB, Francis RE, Peck B, et al. Gefitinib (Iressa) represses FOXM1 expression via FOXO3a in breast cancer. *Mol. Cancer Ther.* 2009;8:582-591.

14. Hui RC-Y, Francis RE, Guest SK, et al. Doxorubicin activates FOXO3a to induce the expression of multidrug resistance gene ABCB1 (MDR1) in K562 leukemic cells. *Mol. Cancer Ther.* 2008;7:670-678.

15. Tran H, Brunet A, Grenier JM, et al. DNA repair pathway stimulated by the forkhead transcription factor FOXO3a through the Gadd45 protein. *Science* 2002;296:530-534.

16. Wilson MSC, Brosens JJ, Schwenen HDC, Lam EW-F. FOXO and FOXM1 in cancer: the FOXO-FOXM1 axis shapes the outcome of cancer chemotherapy. *Curr. Drug Targets* 2011;12:1256-1266.

17. Wierstra I, Alves J. Despite its strong transactivation domain, transcription factor FOXM1c is kept almost inactive by two different inhibitory domains. In: *Biological Chemistry*.Vol 387.; 2006:963-976.

18. Wierstra I. The transcription factor FOXM1 (Forkhead box M1): Proliferation-specific expression, transcription factor function, target genes, mouse models, and normal biological roles. *Adv. Cancer Res.* 2013;118:97-398.

19. Laoukili J, Stahl M, Medema RH. FoxM1: At the crossroads of ageing and cancer. *Biochim. Biophys. Acta - Rev. Cancer* 2007;1775:92-102.

20. Koo CY, Muir KW, Lam EWF. FOXM1: From cancer initiation to progression and treatment. *Biochim. Biophys. Acta - Gene Regul. Mech.* 2012;1819(1):28-37.

21. Bella L, Zona S, Nestal de Moraes G, Lam EWF. FOXM1: A key oncofoetal transcription factor in health and disease. *Seminars in Cancer Biology*. 2014.

22. Schwenen, Helma D. C; Monteiro, Lara J.; Wilson, Miranda S. C.; Lam EW-F. FOXM1. *Transcr. factor Encycl.* 2009:2-5.

23. Costa RH. FoxM1 dances with mitosis. *Nat. Cell Biol.* 2005;7:108-110.

24. Tan Y, Raychaudhuri P, Costa RH. Chk2 mediates stabilization of the FoxM1 transcription factor to stimulate expression of DNA repair genes. *Mol. Cell. Biol.* 2007;27:1007-1016.

25. Bashir T, Dorrello NV, Amador V, Guardavaccaro D, Pagano M. Control of the SCF(Skp2-Cks1) ubiquitin ligase by the APC/C(Cdh1) ubiquitin ligase. *Nature* 2004;428:190-193.

26. Park YY, Jung SY, Jennings NB, et al. FOXM1 mediates Dox resistance in breast cancer by enhancing DNA repair. *Carcinogenesis* 2012;33:1843-1853.

27. Zona S, Bella L, Burton MJ, Nestal de Moraes G, Lam EW-F. FOXM1: An emerging master regulator of DNA damage response and genotoxic agent resistance. *Biochim. Biophys. Acta* 2014;1839(11):1316-1322.

28. Quan M, Wang P, Cui J, Gao Y, Xie K. The roles of FOXM1 in pancreatic stem cells and carcinogenesis. *Mol. Cancer* 2013;12:159.

29. Gong A, Huang S. FoxM1 and Wnt/β-catenin signaling in glioma stem cells. *Cancer Res.* 2012;72:5658-5662.

30. Zhang Y, Zhang N, Dai B, et al. FoxM1B transcriptionally regulates vascular endothelial growth factor expression and promotes the angiogenesis and growth of glioma cells. *Cancer Res.* 2008;68:8733-8742.

31. Huang C, Qiu Z, Wang L, et al. A novel FoxM1-caveolin signaling pathway promotes pancreatic cancer invasion and metastasis. *Cancer Res.* 2012;72:655-665.

32. Bao B, Wang Z, Ali S, et al. Over-expression of FoxM1 leads to epithelial-mesenchymal transition and cancer stem cell phenotype in pancreatic cancer cells. *J. Cell. Biochem.* 2011;112:2296-2306.

33. Raychaudhuri P, Park HJ. FoxM1: A master regulator of tumor metastasis. *Cancer Res.* 2011;71:4329-4333.

34. Wang Z, Banerjee S, Kong D, Li Y, Sarkar FH. Down-regulation of Forkhead Box M1 transcription factor leads to the inhibition of invasion and angiogenesis of pancreatic cancer cells. *Cancer Res.* 2007;67:8293-8300.

35. Dai B, Kang S-H, Gong W, et al. Aberrant FoxM1B expression increases matrix metalloproteinase-2 transcription and enhances the invasion of glioma cells. *Oncogene* 2007;26:6212-6219.

36. Halasi M, Gartel AL. A novel mode of FoxM1 regulation: Positive auto-regulatory loop. *Cell Cycle* 2009;8:1966-1967.

37. Kwok JM-M, Myatt SS, Marson CM, Coombes RC, Constantinidou D, Lam EW-F. Thiostrepton selectively targets breast cancer cells through inhibition of forkhead box M1 expression. *Mol. Cancer Ther.* 2008;7(7):2022-32.

38. Nakamura S, Hirano I, Okinaka K, et al. The FOXM1 transcriptional factor promotes the proliferation of leukemia cells through modulation of cell cycle progression in acute myeloid leukemia. *Carcinogenesis* 2010;31(11):2012-21.

39. Tzivion G, Dobson M, Ramakrishnan G. FoxO transcription factors; Regulation by AKT and 14-3-3 proteins. *Biochim. Biophys. Acta - Mol. Cell Res.* 2011;1813:1938-1945.

40. Zhao B, Barrera LA, Ersing I, et al. The NF-κB Genomic Landscape in Lymphoblastoid B Cells. *Cell Rep.* 2014:1-12. doi:10.1016/j.celrep.2014.07.037.

41. Tran H, Brunet A, Griffith EC, Greenberg ME. The many forks in FOXO's road. *Sci. STKE* 2003;2003:RE5.

42. Ho KK, McGuire VA, Koo CY, et al. Phosphorylation of FOXO3a on Ser-7 by p38 promotes its nuclear localization in response to doxorubicin. *J. Biol. Chem.* 2012;287:1545-1555.

43. Eijkelenboom A, Burgering BMT. FOXOs: signalling integrators for homeostasis maintenance. *Nat. Rev. Mol. Cell Biol.* 2013;14:83-97.

44. Huang H, Regan KM, Wang F, et al. Skp2 inhibits FOXO1 in tumor suppression through ubiquitin-mediated degradation. *Proc. Natl. Acad. Sci. U. S. A.* 2005;102:1649-1654.

45. Boccitto M, Kalb RG. Regulation of Foxo-dependent transcription by post-translational modifications. *Curr. Drug Targets* 2011;12:1303-1310.

46. Barthel A, Schmoll D, Unterman TG. FoxO proteins in insulin action and metabolism. *Trends Endocrinol. Metab.* 2005;16:183-189.

47. Yang J-Y, Zong CS, Xia W, et al. ERK promotes tumorigenesis by inhibiting FOXO3a via MDM2-mediated degradation. *Nat. Cell Biol.* 2008;10:138-148.

48. Essers MAG, Weijzen S, de Vries-Smits AMM, et al. FOXO transcription factor activation by oxidative stress mediated by the small GTPase Ral and JNK. *EMBO J.* 2004;23:4802-4812.

49. Huang H, Tindall DJ. Regulation of FOXO protein stability via ubiquitination and proteasome degradation. *Biochim. Biophys. Acta - Mol. Cell Res.* 2011;1813:1961-1964.

50. Zhao Y, Wang Y, Zhu WG. Applications of post-translational modifications of FoxO family proteins in biological functions. *J. Mol. Cell Biol.* 2011;3:276-282.

51. Mahmud DL, G-Amlak M, Deb DK, Platanias LC, Uddin S, Wickrema A. Phosphorylation of forkhead transcription factors by erythropoietin and stem cell factor prevents acetylation and their interaction with coactivator p300 in erythroid progenitor cells. *Oncogene* 2002;21:1556-1562.

52. Dansen TB, Smits LMM, van Triest MH, et al. Redox-sensitive cysteines bridge p300/CBP-mediated acetylation and FoxO4 activity. *Nat. Chem. Biol.* 2009;5:664-672.

53. Perrot V, Rechler MM. The coactivator p300 directly acetylates the forkhead transcription factor Foxo1 and stimulates Foxo1-induced transcription. *Mol. Endocrinol.* 2005;19:2283-2298.

54. Senf SM, Sandesara PB, Reed SA, Judge AR. p300 Acetyltransferase activity differentially regulates the localization and activity of the FOXO homologues in skeletal muscle. *Am. J. Physiol. Cell Physiol.* 2011;300:C1490-C1501.

55. Motta MC, Divecha N, Lemieux M, et al. Mammalian SIRT1 Represses Forkhead Transcription Factors. *Cell* 2004;116:551-563

56. Khongkow M, Olmos Y, Gong C, et al. SIRT6 modulates paclitaxel and epirubicin resistance and survival in breast cancer. *Carcinogenesis* 2013;34:1476-1486.

57. Xie Q, Hao Y, Tao L, et al. Lysine methylation of FOXO3 regulates oxidative stress-induced neuronal cell death. *EMBO Rep.* 2012;13:371-377.

58. Calnan DR, Webb AE, White JL, et al. Methylation by Set9 modulates FoxO3 stability and transcriptional activity. *Aging (Albany. NY).* 2012;4:462-479.

59. Greer EL, Brunet A. FOXO transcription factors at the interface between longevity and tumor suppression. *Oncogene* 2005;24:7410-7425.

60. Kornblau SM, Singh N, Qiu Y, Chen W, Zhang N, Coombes KR. Highly phosphorylated FOXO3A is an adverse prognostic factor in acute myeloid leukemia. *Clin. Cancer Res.* 2010;16:1865-1874.

61. Ausserlechner MJ, Salvador C, Deutschmann A, et al. Therapy-resistant acute lymphoblastic leukemia (ALL) cells inactivate FOXO3 to escape apoptosis induction by TRAIL and Noxa. *Oncotarget* 2013;4:995-1007.

62. Paik JH, Kollipara R, Chu G, et al. FoxOs Are Lineage-Restricted Redundant Tumor Suppressors and Regulate Endothelial Cell Homeostasis. *Cell* 2007;128:309-323.

63. Naka K, Hoshii T, Muraguchi T, et al. TGF-beta-FOXO signalling maintains leukaemia-initiating cells in chronic myeloid leukaemia. *Nature* 2010;463:676-680.

64. Bachmann PS, Gorman R, Papa RA, et al. Divergent mechanisms of glucocorticoid resistance in experimental models of pediatric acute lymphoblastic leukemia. *Cancer Res.* 2007;67:4482-4490.

65. Dewar R, Chen ST, Yeckes-Rodin H, Miller K, Khosravi-Far R. Bortezomib treatment causes remission in a Ph+ALL patient and reveals FoxO as a theranostic marker. *Cancer Biol. Ther.* 2011;11:552-558.

66. Zhao F, Lam EWF. Role of the forkhead transcription factor FOXO-FOXM1 axis in cancer and drug resistance. *Front. Med. China* 2012;6:376-380.

67. Madureira PA, Varshochi R, Constantinidou D, et al. The Forkhead box M1 protein regulates the transcription of the estrogen receptor alpha in breast cancer cells. *J. Biol. Chem.* 2006;281:25167-25176.

CHAPTER 2

ANTITUBULINIC AND OXIDATIVE STRESS-INDUCING AGENTS

SUMMARY

Over the years the biomedical research was focused on the development of new anticancer agents able to selectively target cancer cells at low concentration efficacy. Based on the idea that oncogenes and tumour suppressor genes are a critical force in the malignant transformation of cells, research efforts have focused on developing drugs that directly target these genes.

Moreover, because cancer cells frequently have multiple genetic alterations, recent studies suggest that targeting the unique biochemical alterations which distinguish cancer cells from normal cells might be a feasible approach to achieve therapeutic activity and selectivity, and perhaps to prevent the development of drug resistance[12].

The most common features of human cancer is the cell cycle deregulation that leads to hyper proliferation pattern. In fact tumor cells accumulate mutations that result in unscheduled proliferation as a consequence of unresponsiveness to growth inhibitory signals, self-sufficiency in growth factors or both[3]. Therefore several therapeutic strategies have been proposed for targeting the tubulin polymerization in cancer. Tubulin binding agents constitute an important class of compounds with broad activity in both solid and in hematologic neoplasia. They can act either promoting the microtubules polymerization and stabilization (i.e. taxanes, epothilones), or inducing microtubules depolymerization and instability (i.e. colchicine, vinca alkaloids, combretastatins)[4]. These agents are believed to block cell division by interfering with the function of the mitotic spindle, blocking cells at the metaphase/anaphase junction of mitosis. Moreover literature shows that tubulin-binding agents may play their antitumoral effect also by disrupting the vascular structure[5].

In this work we evaluated the antiproliferative activity, interactions with tubulin and cell cycle effects of a new class of compounds that incorporated the structural motif of the 1-(3',4',5'-trimethoxtbenzoyl)-3-arylamino-5-amino-1,2,4-triazole molecular skeleton. Furthermore the effects of the most active agent, **3c** were compared to the combretastatin molecule CA-4. Our data showed that this compound clearly induces apoptosis through caspase-9 and -3 activation. Furthermore the vascular disrupting activity was evaluated in HUVEC cells with compound **3c** that showed an activity comparable to that of CA-4. In addition, compound **3c** significantly reduced *in vivo* the growth of syngeneic hepatocellular carcinoma in Balb/c mice, suggesting that **3c** could be a new antimitotic agent with clinical potential.

Cancer cells are also characterized by altered metabolic activity which provokes increased levels of intracellular oxidative stress. Therefore cancer cells would be more vulnerable to further oxidative stress induced by Reactive Oxygen Species (ROS)-generating agents and more dependent on the enzymatic antioxidant systems.

Importantly, this dependency might not be shared by many nontransformed cells, whose lower basal ROS levels and/or elevated antioxidant capacity could provide resistance to treatments that impair ROS metabolism. In keeping with this hypothesis, various small molecules, including ones with disulfide, α,β-unsaturated carbonyl, sulfonate, or other electrophilic functional groups, have been shown to elevate ROS levels by blocking the antioxidant enzymatic activity then inducing cancer cell death[6].

In this study we investigated whether a series of α-bromoacryloylamido arylcinnamide derivatives plays as antitumoral molecules by increasing ROS in cancer cells. We observed that the most potent hybrid compounds **4p** caused a decrease in intracellular GSH content in cancer cells. However studies are underway to determine the precise molecular mechanism that leads to the decrease in intracellular GSH levels with the aim of develope new cancer therapeutic strategies

.

2.1 TUBULIN BINDING AGENTS

2.1.1 GENERAL INTRODUCTION

Resistance to chemotherapy is a major problem facing current cancer research. Over the years the biomedical research was focused on the development of new anticancer agents able to selectively target cancer cells at low concentration efficacy and to overcome drug resistance. Since malignant transformation is frequently driven by multiple genetic alterations in cancer cells, recent studies suggested that targeting the unique biochemical alterations, which distinguish cancer cells from normal cells might be a feasible approach to achieve therapeutic activity and selectivity, and perhaps prevent the development of drug resistance.

Compared to the normal counterpart, cancer cells are characterized by the cell cycle deregulation that leads to their hyperproliferative pattern. Tumor cells accumulate mutations that result in unscheduled proliferation, as a consequence of unresponsiveness to growth inhibitory signals, self-sufficiency in growth factors or both[7]. Therefore several antitumoral strategies have been proposed for targeting the cell division cycle in cancer by targeting tubulin polimerization[8].

2.1.1.1 TUBULIN STRUCTURE

The microtubule system of eukaryotic cells is a critical element in a variety of fundamental cellular processes such as cell formation, maintenance of cell shape, regulation of motility, cell signaling, secretion, intracellular transport and mitotic spindle elongation for the correct chromosome segregation[9]. Microtubules are built from subunits, each of which is itself a dimer composed by two very similar globular proteins called α-tubulin and β-tubulin[10]. The tubulin dimers stack together by non-covalent bonding to form the wall of the hollow cylindrical microtubules. This tube like structure is made of 13 parallel protofilaments, which are linear chains of tubulin dimers with α and β-tubulin alternating along its length.

Each protofilament has a structural polarity, with α-tubulin exposed at one end and β-tubulin at the other, and this polarity is the same for all protofilaments, giving a structural polarity to the microtubule as a whole. One end of the microtubule, thought to be the β-tubulin end, is called plus end, and the other, the α tubulin end is called minus end. The

microtubule system has a dynamic behavior, known as "dynamic instability", in which microtubules alternate between period of growing and shrinking through the addition or removal of tubulin monomers. This process is mediated by hydrolysis of GTP.

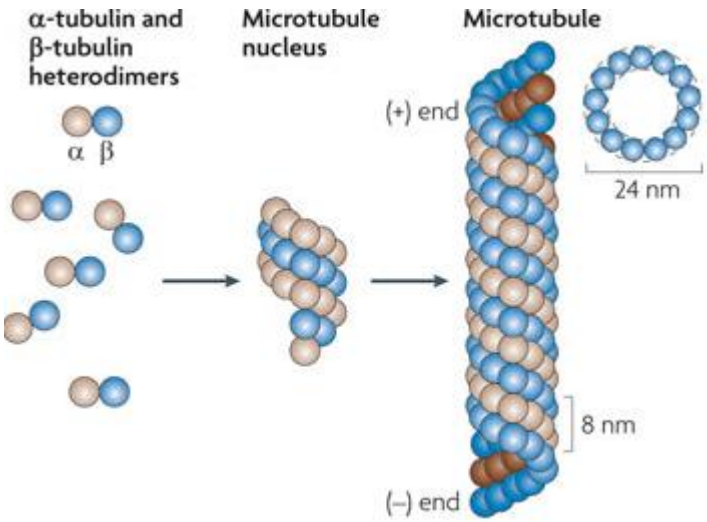

Figure 1: The microtubule's structure is constituted by dimers of α-tubulin and β-tubulin. (Adapted from Ref[8])

2.1.1.2 TUBULIN AND CELL CYCLE PROGRESSION

Microtubules dynamic plays a key role on mitosis progression and thus in cell division and proliferation. The mitosis (also called M phase) is divided into six stages: prophase, prometaphase, metaphase anaphase and telophase. At the onset of mitosis, the interphase microtubular network develop into the mitotic spindle. Microtubules extend in all directions from the two centromeres which are localized on pole of cell. During the prometaphase, an important stage in which there is disassemblation of the nuclear envelope, the spindle microtubules attach chromosomes through specialized protein complexes called kinetochores. With the methaphase the mitotic spindle moves to align at the equator of cell all chromosomes forming the metaphase plate, and finally during the anaphase chromosomes segregate into daughter cells[11].

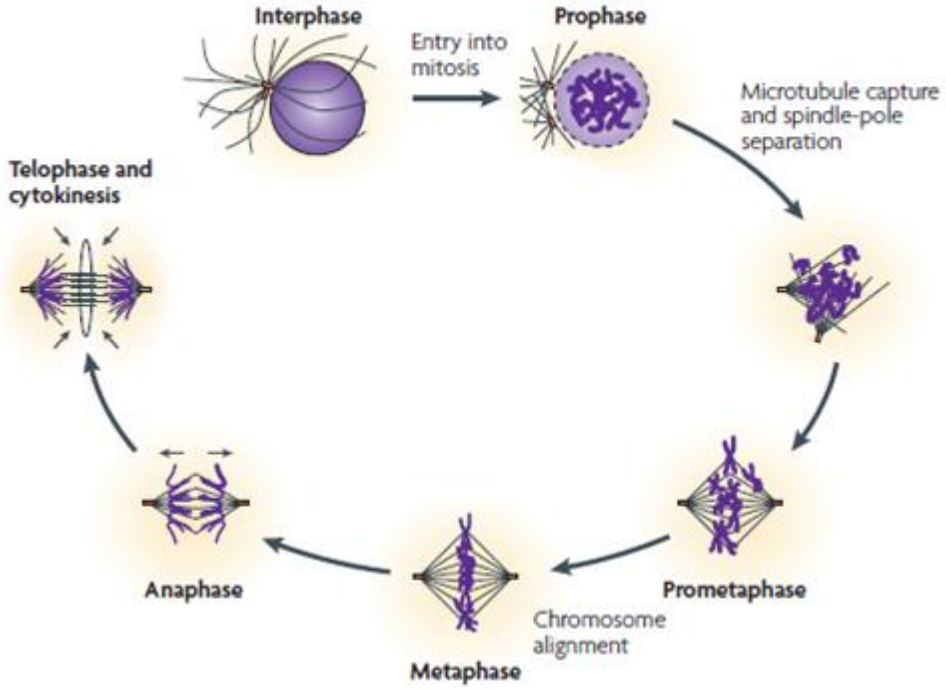

Figure 2: Microtubules involvement in mitotic spindles assemblation during mitosis. (Adapted from Ref[7])

2.1.1.3 TUBULIN TARGETING AGENTS

Because of the central role of microtubules dynamic in mitosis progression and cell proliferation, drugs that affect microtubule assembly are important component in combination chemotherapy for the treatment of pediatric and adult cancer. The impressive success of antimitotic agents in patients is due to their potent antiproliferative effects and to their particular mechanism of action of altering microtubule dynamics. In dividing cells, such as cancer cells, microtubules are highly dynamic and exquisitely sensitive to therapeutic inhibitors. This explains why compounds that alter microtubule function have proved to be highly active in patients with cancer. The microtubule-targeted antimitotic drugs are often classified into two major groups, the microtubule-destabilizing agents and the microtubule-stabilizing agents, according to their effects at high concentrations on microtubule polymer mass[84]. The so-called "destabilizing" agents inhibit microtubule polymerization when present at high concentrations. Most of these agents bind in one of two domains on tubulin, the "vinca" domain and the "colchicine" domain. Vinca site binders include the vinca alkaloids (vinblastine, vincristine, vinorelbine, vindesine, and

vinflunine), the cryptophycins, the dolastatins, eribulin, spongistatin, rhizoxin, maytansinoids and tasidotin. Colchicine-site binders include colchicine and its analogs, podophyllotoxin, combretastatins, CI-980, 2-methoxyestradiol, phenylahistins (diketopiperazine), steganacins, and curacins. Furthermore some of the destabilizing agents, including the hemiasterlins, estramustine, noscapine, herbicides such as carbendazim, psychoactive drugs such as phenytoin, and food components such as sulforaphane found in cruciferous vegetables, bind to novel sites on tubulin[8].

The "microtubule-stabilizing" agents enhance microtubule polymerization at high drug concentrations and include taxol (paclitaxel, Taxol™), docetaxel (Taxotere™), the epothilones, ixabepilone (Ixempra™) and patupilone, discodermolide, eleutherobins, sarcodictyins, cyclostreptin, dictyostatin, laulimalide, rhazinilam, peloruside A, certain steroids and polyisoprenyl benzophenones. Most of the stabilizing agents bind to the same, or an overlapping, taxoid binding site on β-tubulin which is located on the inside surface of the microtubule. However, two of the agents, laulimalide and peloruside A, are not displaced by paclitaxel and for this reason are believed to bind to a novel site on tubulin. Overall several hundred compounds have been reported to arrest mitosis by their effects on microtubules. In all cases where it has been investigated, they do so most potently by suppressing microtubule dynamics.

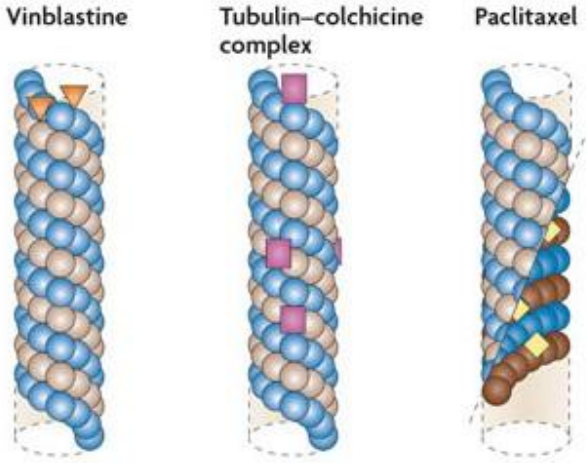

Figure 4: The "destabilizing" agents bind in one of two domains on tubulin, the "vinca" domain and the "colchicine" domain. The stabilizing agents bind to the same, or an overlapping, taxoid binding site on β-tubulin which is located on the inside surface of the microtubule. (Adapted from Ref [8]).

2.1.1.4 CYTOTOXIC EFFECT OF TUBULIN BINDING AGENTS

Both classes of antimitotic drugs suppress microtubule dynamics causing alteration in the spindle organization, with a delay or a block at the metaphase-anaphase transition during mitosis with consequent G_2-M cell cycle arrest. Furthermore activation of spindle assembly checkpoint in G2 phase and prolonged mitotic arrest provoke apoptosis induction[12]. The apoptosis is a programmed cell death characterized by chromatin condensation, DNA fragmentation and activation of caspases[13]. The apoptotic process could be triggered by two pathways called extrinsic and intrinsic pathway. Several works describe that tubulin binding agents induce apoptosis mainly through the intrinsic pathway activation, characterized by the alteration of mitochondrial parameters (such as alteration of membrane potential and ROS production). However, how cell death induction correlates with microtubule destabilization and mitotic arrest still remains unclear and controversial[14].

The intrinsic pathway of apoptosis is mainly initiated by the release of cytochrome *c* from the mitochondrion. Upon release into the cytoplasm, cytochrome *c* associates with dATP, procaspase-9, and the adaptor protein APAF-1, leading to the sequential activation of caspase-9 and effector caspases[15].

The release of apoptosis-inducing proteins from the mitochondria is regulated by pro- and antiapoptotic members of the Bcl-2 family. Antiapoptotic members (Bcl-2, Bcl-XL, and Mcl-1) associate with the mitochondrial outer membrane via their carboxy termini, exposing to the cytoplasm a hydrophobic binding pocket composed of Bcl-2 homology (BH) domains 1, 2, and 3, that is crucial for their activity. Perturbations of normal physiologic processes in specific cellular compartments lead to the activation of BH3-only proapoptotic family members (such as Bad, Bim, Bid, Puma, Noxa, and others). This leads to the altered conformation of the outer-membrane proteins Bax and Bak, which then oligomerize to form pores in the mitochondrial outer membrane resulting in cytochrome *c* release. Therefore the relative levels of expression of antiapoptotic Bcl-2 family members compared to the levels of proapoptotic BH3-only proteins at the mitochondrial membrane determines the activation state of the intrinsic pathway. It has been demonstrated that many microtubules binding agents can induce phosphorylation in serine residues of Bcl2 antiapoptotic proteins, in cell that are blocked in G2-M phase, leading to loss of

prosurvival function and to destabilization of mitochondrial potential. Moreover Bcl2 phosphorylation decreases its binding to the proapoptotic Bax protein, resulting in an increase of free Bax and apoptosis[16].

2.1.1.5 ANTIANGIOGENIC EFFECT OF TUBULIN BINDING AGENTS

Recently it has been described that some microtubule-destabilizing agents might cause blood vessel disruption at no toxic doses thus acting also as antiangiogenic agents[17]. These drugs, binding to tubulin, not only provoke cytoskeleton alterations but are also able to impair endothelial cells functionality. This class of compounds is defined as vascular disrupting agents (VDA)[18]. Preclinical evaluation of tubulin-targeting VDAs showed that these compounds are able to disrupt tumor blood flow, causing tumor hypoxia and necrosis. One of the most important antimitotic agents and vascular disrupting agents (VDA) is Combretastatin A-4 (CA-4)[19,20]. Combretastatin-A4, isolated from the African tree Combretum caffrum, strongly inhibits tubulin polymerization by binding to the colchicine binding site on β-tubulin[21]. Furthermore in advanced clinical trials it was found that the water-soluble derivative of CA-4 (named CA-4P) has potent activity to reduce significantly the tumor blood flow inducing changes in endothelial-cell shape and plasma membrane blebbing, then increasing the permeability of cell monolayers[20]. These changes in endothelial cells result in significant reduction in tumour blood flow, increases in vascular permeability subsequently leading to vascular shutdown.

CA-4

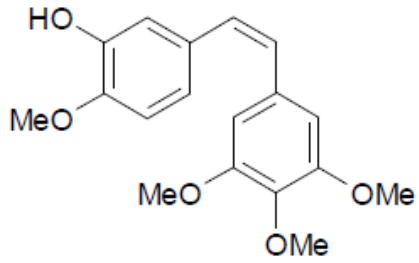

Figure 5: Combretastatin A-4 (CA-4)

2.1.2 AIM OF THE PROJECT

Cancer cells frequently have multiple genetic alterations. However to target the unique biochemical alterations which differentiate cancer cells from normal cells might be a key strategy to selectively target cancer cells overcome drug resistance.

The microtubule system plays an essential role on a variety of cellular processes, such as on maintaining of cell shape, intracellular transport and more importantly on cell cycle division. Therefore over the years several antitumoral compounds have been developed for targeting tubulin polymerization and thus cell cycle progression in cancer. Furthermore, many tubulin binding agents show antivascular effects against tumor endothelium, including the tubuling destabilizing agent CA-4.

In this study we analysed a new series of compounds with general structure **3** synthetized starting from the CA-4 structure with the aim to improve their antimitotic and antiangiogenic activity. The new compounds incorporated the more electron rich structure of compound **2** and the trimethoxyphenyl skeleton that characterized the tubulin inhibitor CA-4 to afford a new series of 1-(3',4',5'-trimethoxybenzoyl)-3-arylamino-5-amino 1,2,4-triazole compounds.

We evaluated *in vitro* the effects of different substituents on benzene of arylamino moiety on antiproliferative activity and tubulin polymerization. The apoptotic and antitubulin activity of **3c** was compared with Combretastatin-A4 (CA-4). Since a high antitumoral activity was observed, we also evaluated their efficacy to act as vascular disrupting agents (VDA) in endothelial cells as model, HUVEC. More importantly the **3c** anticancer activity and then its potential clinical use was further evaluated with *in vivo* experiments by treating a syngenic model of mouse.

2.1.3 RESULTS

Synthesis, Antimitotic and Antivascular Activity of 1-(3',4',5'-Trimethoxybenzoyl)-3-Arylamino-5-Amino-1,2,4-Triazoles

Romeo Romagnoli*[†], Pier Giovanni Baraldi*[†], Maria Kimatrai Salvador[†], Filippo Prencipe[†], Valerio Bertolasi[†], Michela Cancellieri[§], Andrea Brancale[§], Ernest Hamel[‡], Ignazio Castagliuolo[§§], Francesca Consolaro[††], Elena Porcù[††], Giuseppe Basso[††], Giampietro Viola*[††]

J MED CHEM. 2014 Aug 14;57(15):6795-808. doi: 10.1021/jm5008193.

2.1.3.1 ABSTRACT

A new class of compounds that incorporated the structural motif of the 1-(3',4',5'-trimethoxtbenzoyl)-3-arylamino-5-amino-1,2,4-triazole molecular skeleton was synthesized and evaluated for their antiproliferative activity *in vitro* and *in vivo*, interactions with tubulin and cell cycle effects, and the most active agent, **3c**, was evaluated for antitumor activity *in vivo*. Structure-activity relationships were elucidated with various substituents on the phenyl ring of the anilino moiety at the C-3 position of the 1,2,4-triazole ring. The best results for inhibition of cancer cell growth were obtained with the *p*-Me, *m*, *p*-diMe and *p*-Et phenyl derivatives **3c**, **3e** and **3f**, respectively, and, overall, these compounds were more or as active as CA-4. Their vascular disrupting activity was evaluated in HUVEC cells, with compound **3c** showing activity comparable with that of CA-4. Compound **3c** almost eliminated the growth of syngeneic hepatocellular carcinoma in Balb/c mice, suggesting that **3c** could be a new antimitotic agent with clinical potential.

2.1.3.2 INTRODUCTION

The cellular microtubule system, established by an equilibrium between the polymerization and depolymerization of αβ-tubulin heterodimers, is essential in a variety of cellular processes, including maintenance of cell shape, regulation of motility, intracellular transport of vesicles and organelles and cell division.[1] Due to their role in eukaryotic cells, microtubules are a successful target for the development of numerous small natural and synthetic molecules that inhibit the formation of the mitotic spindle.[2-4] Among the naturally occurring antimicrotubule agents, one of the most active is the *cis*-stilbene combretastatin A-4 (CA-4, **1a**, Chart 1), isolated from the African cape bushwillow *Combretum caffrum*.[5] CA-4 inhibits tubulin assembly by strongly binding to the colchicine site on β-tubulin.[6] Its water soluble prodrug, CA-4 disodium phosphate (CA-4P, **1b**),[7] is in advanced clinical trials,[8] and it was found to have potent activity in reducing tumor blood flow, thus acting as a vascular disrupting agent (VDA).[9] Among the synthetic inhibitors of tubulin polymerization, we previously described a series of 2-arylamino-4-amino-5-(3',4',5'-trimethoxybenzoyl)thiazoles with general structure **2** that showed strong antiproliferative activity against a panel of five cancer cell lines.[10] These compounds also caused accumulation of HeLa cells in the G2/M phase of the cell cycle, as is typical for antimicrotubule agents. Derivatives **2a** (R_1=H) and **2b** (R_1=4'-Me) were the most active as inhibitors of tumor cell growth, with IC_{50} values of 6-23 and 15-86 nM, respectively, in the five cell lines.

Ring bioisosterism is widely used as a rational approach for the discovery of new anticancer agents, especially for finding agents with optimal pharmacological properties.[11] Continuing our search strategy for novel and potent antimicrotubule agents, we have underway a pharmacophore exploration and optimization effort based on compounds with general formula **2**. Here we describe replacing the thiazole nucleus with the more electron-rich 1,2,4-triazole bioisosteric ring,[12,13] to afford a new series of 1-(3',4',5'-trimethoxybenzoyl)-3-arylamino-5-amino 1,2,4-triazole analogues with general structure **3**. Our goal was to evaluate the steric and electronic effects of different substituents on the benzene portion of the arylamino moiety. Besides hydrogen (compound **3a**), the examined substituents included fluorine (**3b**) and electron donating alkyl and alkoxy groups (compounds **3c-h** and **3i-n**, respectively).

Chart 1. Inhibitors of Tubulin Polymerization

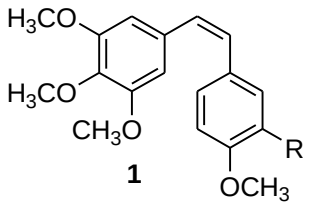

1

R=OH, Combretastatin A-4 (CA-4), **1a**
R=OPO_3Na_2, CA-4P, **1b**

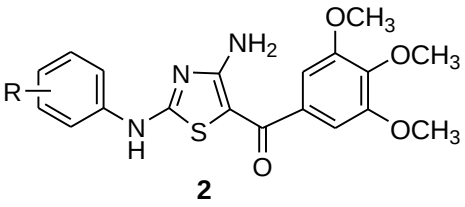

2

R=H, F, Cl, CH_3 and OCH_3
2a, R=H
2b, R=*p*-CH_3

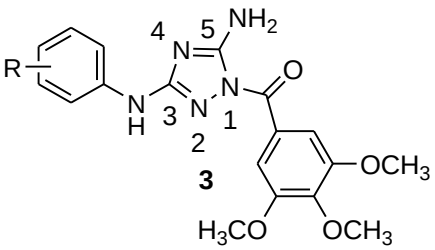

3

3a, R=H
3b, R=p-F
3c, R=p-CH_3
3d,R=m-CH_3
3e, R=m,p-$(CH_3)_2$
3f, R=p-C_2H_5
3g, R=p-$CH(CH_3)_2$
3h, R=p-$(CH_2)_3CH_3$
3i, R=p-OCH_3
3j, R=m-OCH_3
3k, R=m,p-$(OCH_3)_2$
3l, R=m,m',p-$(OCH_3)_3$
3m, R=p-OC_2H_5
3n, R=m,p-(OCH_2O)

Since it is well known that the trimethoxyphenyl skeleton is the characteristic structural requirement to maximize activity in a large series of inhibitors of tubulin polymerization, such as colchicine, CA-4 and podophyllotoxin,[14] all newly prepared compounds **3a-n**, retain the 3',4',5'-trimethoxybenzoyl group at the C-1 position of the 1,2,4-triazole ring. The newly synthesized derivatives were evaluated for their antiproliferative activity in a panel of human cancer cell lines, for their antitubulin activity (including cell cycle and

apoptotic effects) and their antivascular activity in HUVEC cells. Finally, the antitumor activity of **3c**, the most potent member of the group in the *in vitro* studies, was evaluated *in vivo* in a syngeneic hepatocellular carcinoma in Balb/c mice in comparison with CA-4P.

2.1.3.3 BIOLOGICAL RESULTS

In vitro antiproliferative activities.

Table 1 summarizes the antiproliferative effects of 1-(3',4',5'-trimethoxybenzoyl)-3-anilino-5-amino 1,2,4-triazoles **3a-n** against a panel of seven human cancer cell line, using CA-4 (**1**) as the reference compound.

Table 1. *In vitro* cell growth inhibitory effects of compounds **3a-n** and CA-4 (**1**)

Compd	IC_{50} [a](nM)						
	Jurkat	CCRF-CEM	SEM	HeLa	HT-29	A549	MCF-7
3a	1200±270	1000±90	1200±190	>10,000	6200±1200	>10,000	500±240
3b	1900±400	2200±400	2400±210	410±70	2000±700	3800±160	370±30
3c	0.81±0.03	0.21±0.04	0.51±0.10	3.2±1.3	0.82±0.10	0.51±0.22	1.0±0.61
3d	42±16	330±60	30±10	440±50	460±80	870±30	15±3.2
3e	2.0±0.11	0.81±0.10	0.40±0.11	2.0±0.82	3.0±0.91	1.0±0.82	4.0±0.21
3f	1.0±0.09	3.0±0.09	0.81±0.21	6.0±1.0	0.21±0.08	0.92±0.51	5.0±1.0
3g	520±40	1800±90	500±10	130±28	800±100	550±70	510±70
3h	>10,000	>10,000	>10,000	>10,000	>10,000	>10,000	5200±110
3i	51±10	1000±200	44±16	120±30	480±15	2400±100	260±80
3j	7.2±2.0	120±30	1.0±0.4	30±1.2	700±32	54±4.3	11±4.2
3k	>10,000	9000±330	>10,000	>10,000	>10,000	>10,000	>10,000
3l	>10,000	>10,000	>10,000	>10,000	>10,000	>10,000	>10,000
3m	2500±220	2000±100	1900±170	2100±800	3700±400	6200±540	34±18
3n	24±7.2	40±3.3	30±6	930±54	60±10	150±50	19±5.2
CA-4	5±0.6	12±2.5	5±0.1	4±0.1	3100±100	180±50	370±100

[a] IC_{50}= compound concentration required to inhibit tumor cell proliferation by 50%. Data are expressed as the mean ± SE from the dose-response curves of at least three independent experiments carried out in triplicate.

The 1-(3',4',5'-trimethoxybenzoyl)-3-amino-5-anilino 1,2,4-triazole isomers **7a-c**, **7g-h** and **7k-l** were also evaluated for their activities, but, since they were all inactive (IC_{50}>10 μM), the data are not shown in Table 1. Three of the synthesized compounds, corresponding to the *p*-Me, *m*,*p*-di-Me and *p*-Et phenyl analogues **3c**, **3e** and **3f**, respectively, were significantly more active than the rest of derivatives, with IC_{50} values of 0.21-3.2, 0.4-4.0, and 0.21-6.0 nM, respectively, in the seven cell lines, as compared with 4-3100 nM for CA-4. With average IC_{50} values of 1.0, 1.9 and 2.4 nM for **3c**, **3e** and **3f**, respectively, **3c** appears to be the most active compound in the series (for CA-4, the average value was 525 nM or, excluding the HT-29 cell line from the average, 96 nM). Thus, these three compounds are substantially more active than CA-4, and they are also more potent than their previously described isosteres **2a** and **2b**.[11] In addition to these highly potent three derivatives, the *m*-OMe and *m*,*p*-methylenedioxy phenyl derivatives **3j** and **3n**, respectively, were more active than CA-4 against HT-29, A549 and MCF-7 cells. In short, the data shown in Table 1 indicate the importance of substituents and their relative position on the phenyl ring of the arylamino moiety at the C-3 position of the 1,2,4-triazole skeleton for activity and selectivity against different cancer cell lines.

The unsubstituted anilino derivative **3a** was weakly active (IC_{50}>0.5 μM), and the introduction of a weak electron-releasing fluorine atom at the *para*-position of the phenyl (compound **3b**) had the opposite effect, with slightly improved antiproliferative activity with respect to **3a** against HeLa, HT-29, A549 and MCF-7 cells, while the activity was reduced against Jurkat, CCRF-CEM and SEM cells.

We found that the small methyl group at the *para*-position of the phenyl ring, to furnish derivative **3c**, improved significantly antiproliferative activity relative to **3a**. Moving the methyl group from the *para*- to the *meta*-position, to furnish isomer derivative **3d**, reduced antiproliferative activity from one to three orders of magnitude, with double digit nanomolar activity against Jurkat, SEM and MCF-7 cells. Since the *para*-toluidino moiety of **3c** was favourable for potency, it is important to point out that the introduction of an additional methyl group at the *meta*-position, resulting in the *meta*, *para*-dimethyl

derivative **3e**, produced a 2- to 4-fold reduction in antiproliferative activity against five of the six cancer cell lines, while **3c** and **3e** were equipotent against SEM and HeLa cells.

The *para*-ethyl homologue **3f** was 2-15-fold less active than methyl counterpart **3c** against four of the seven cancer cell lines, with a minimal difference between the two compounds in the Jurkat and SEM cells, while **3f** was 4-fold more potent than **3c** against HT-29 cells. Replacing the *para*-ethyl group with branched (*i*-Pr) or larger (*n*-butyl) moieties (compounds **3g** and **3h**, respectively) was detrimental for activity in all cell lines, suggesting that an increase in steric bulk at this position caused a decrease in potency.

The number and position of methoxy substituents on the phenyl ring (compounds **3i-l**) had a major influence on antiproliferative activity. Replacement of the methyl moiety with a more electron-releasing methoxy group at the *para*-position of the phenyl ring (compound **3i**) decreased antiproliferative activity by 100-fold compared with **3c**, indicating that the methyl and methoxy group are not bioequivalent at the *para*-position of the phenyl ring. The contribution of methyl or methoxy groups on the phenyl ring to activity (**3c** *vs.* **3d** and **3i** *vs.* **3j**, respectively) was position dependent, with opposite effects. While for the methyl group, as previously observed, the *para*-derivative **3c** was considerably more potent than *meta*-isomer **3d**, an opposite effect was observed for the two methoxy isomers **3i** and **3j**, with the *meta*-isomer **3j** from 4- to 44-fold more potent than the *para*-isomer **3i** in six of the seven cancer cell lines, the exception being the HT-29 cells. Either two or three methoxy substituents (derivatives **3k** and **3l**, respectively) caused substantial loss in antiproliferative activity relative to **3i** and **3j**, suggesting that steric factors account for the loss of activity observed with these two compounds. With the exception of the MCF-7 cells, the *para*-ethoxy derivative **3m** was 2- to 50-fold less potent than its methoxy counterpart **3m**. The 3',4'-methylenedioxy derivative **3n**, with IC_{50} values in the double-digit nanomolar range in five of the seven cancer cell lines, showed an antiproliferative activity intermediate between those of *para*- and *meta*-methoxy analogues **3i** and **3j**, respectively.

Evaluation of cytotoxicity in human non-cancer cells.

To obtain a preliminary indication of the cytotoxic potential of these derivatives for normal human cells, two of the most active compounds (**3c** and **3f**) were assayed *in vitro* against peripheral blood lymphocytes (PBL) from healthy donors (Table 2).

Table 2. Cytotoxicity of **3c** and **3f** in human non-cancer cells

	IC_{50} (μM) [a]	
Cell line	**3c**	**3f**
$PBL_{resting}$ [b]	31.2±8.7	34.0±11.7
PBL_{PHA} [c]	8.5±2.6	8.8±2.7
HUVEC	11.9±3.8	n.d.

[a] Compound concentration required to reduce cell growth inhibition by 50%.
[b] PBL not stimulated with PHA.
[c] PBL stimulated with PHA.
Values are the mean ± SEM for three separate experiments. n.d. not determined

Both compounds were practically ineffective in quiescent lymphocytes, with an IC_{50} of about 30 μM. In the presence of the mitogenic stimulus phytohematoagglutinin (PHA), the IC_{50} decreased to about 8 μM for both compounds, a value that is thousands of times higher than those observed against the lymphoblastic cell lines Jurkat and CCRF-CEM. Furthermore, compound **3c** was also evaluated in human umbilical vein endothelial cells (HUVECs), and again the IC_{50} value was negligible compared with those found in the panel of cancer cell lines. Altogether these data suggest that these compounds may have cancer cell selective antiproliferative properties.

Effect of compound 3c on drug-resistant cell lines

Drug resistance has become a serious problem in cancer chemotherapy.[17,18] One of the common mechanisms of resistance so far identified both in preclinical and clinical studies

involves the overexpression of a cellular membrane protein called P-glycoprotein (P-gp) that mediates the efflux of various structurally unrelated drugs.[17,18] We evaluated sensitivity of compound **3c** in two multidrug-resistant cell lines, one derived from a colon carcinoma ($Lovo^{Doxo}$),[19] the other derived from a lymphoblastic leukaemia ($CEM^{Vbl-100}$).[20] Both these lines express high levels of the P-gp.[19,20] As shown in Table 3, compound **3c** was almost equally potent toward cells resistant to doxorubicin or vinblastine showing a resistance index (RI), which is the ratio between GI_{50} values of resistant cells and sensitive cells, of 1.2 and 5.7 respectively, while doxorubicin in $LoVo^{Doxo}$ and vinblastine in CEM^{Vbl100} showed a high RI of 118 and 193 respectively.

Table 3. In vitro cell growth inhibitory effects of compounds **3c** on drug resistant cell lines.

Compd	IC_{50} [a](nM)		
	LoVo	**$LoVo^{Doxo}$**	**Resistance ratio[b]**
3c	0.9±0.1	1.1± 0.5	1.2
Doxorubicin	95.6 ± 43.2	11296 ± 356	118
	CEM	**CEM^{Vbl100}**	**Resistance ratio[b]**
3c	0.21 ± 0.4	1.2± 0.5	5.7
Vinblastine	1.0 ± 0.3	193 ± 39	193

[a]IC_{50}=compound concentration required to inhibit tumor cell proliferation by 50%. Data are presented as the mean ± SE from the dose-response curves of two independent experiments performed in triplicate.
[b]The values express the ratio between IC_{50} determined in resistant and non-resistant cell lines.

Altogether these results suggest that this compounds might be useful in the treatment of drug refractory tumors.

Inhibition of tubulin polymerization and colchicine binding

A subset of the compounds (**3c-g**, **3i-j** and **3n**) was evaluated for their *in vitro* inhibition of tubulin polymerization in comparison with CA-4. The same compounds were also examined for inhibitory effects on the binding of [^{3}H]colchicine to tubulin (Table 4).

Table 4. Inhibition of tubulin polymerization and colchicine binding by compounds **1a**, **3c-g**, **3i-j** and **3n**.

Compound	Tubulin assembly[a] IC_{50}±SD (μM)	Colchicine binding [b] % ±SD
3c	0.75±0.1	92±2
3d	1.8±0.0	67±1
3e	1.2±0.0	83±1
3f	1.4±0.0	80±2
3g	13±0.7	n.d
3i	3.7±0.4	48±2
3j	2.5±0.0	70±0.9
3n	2.0±0.0	51±0.3
1a	1.2±0.1	98±0.5

[a] Inhibition of tubulin polymerization. Tubulin was at 10 μM.
[b] Inhibition of [^{3}H]colchicine binding. Tubulin, colchicine and tested compound were at 1, 5 and 5 μM, respectively.
n.d: not determined

In the assembly assay, with 10 μM tubulin, compound **3c** was highly potent, yielding an IC_{50} of 0.75 μM, almost twice as active as CA-4. Derivatives **3e** and **3f** had IC_{50} values of 1.2 and 1.4 μM, comparable to value obtained with CA-4. Compounds **3d**, **3i-j** and **3n** were less active as inhibitors of tubulin polymerization , with IC_{50} values of 1.8, 3.7, 2.5 and 2.0 μM, respectively, while **3g** was, relatively speaking, almost inactive. The order of inhibitory effects on tubulin assembly was **3c**>**3e**=CA-4>**3f**>**3d**>**3n**>**3j**>**3i**>>**3g**. This order of activity as inhibitors of tubulin assembly correlates well with their order of activity as antiproliferative agents against Jurkat, CCRF-CEM, SEM and HeLa cells.

In the competition assay, compound **3c** was again the most active derivative, inhibiting colchicine binding by 92%, versus 98% for CA-4. In the experiments summarized in Table 4, the concentration of tubulin was 1.0 μM, while that of both the inhibitors and [^{3}H]colchicine was 5.0 μM. Inhibition of colchicine binding by compounds **3e** and **3f** was lower, with 83% and 80% inhibition occurring with these agents. With the exception of compounds **3j** and **3n**, a good correlation was observed between antiproliferative activities, inhibition tubulin polymerization and inhibition of colchicine binding.

To further investigate if the new derivatives interfered with the microtubule network, we examined the effects of **3c** on HeLa cells by immunofluorescence microscopy. Following a 24 h treatment with **3c** at 50, 100 and 250 nM, the microtubule network was substantially modified in comparison with the untreated cells (Figure S1, Supporting Information). Altogether these results are consistent with the conclusion that the antiproliferative activity of these compounds derived from an interaction with the colchicine site of tubulin, and this ultimately results in interference with microtubule assembly.

Molecular Modeling. To rationalize the experimental data observed for **3a-n**, we performed a series of molecular docking simulations of these compounds in the colchicine site of tubulin. The proposed binding mode for **3c** is very similar to the one presented by the co-crystallized DAMA-colchicine (Figure 1, panel A). In particular, it is possible to observe how the trimethoxyphenyl ring is in proximity of Cys241, while the phenyl ring occupies a hydrophobic region deep in the binding site, establishing a series of interactions with Met259, Thr314 and Lys352. Indeed, this sub-pocket is relatively small and, while the methyl substituent on the phenyl ring of **3c** is able to fit in properly, larger groups, such as the isopropyl (**3g**) or the *n*-butyl (**3h**), cannot be accommodated into it. In these cases, the docking simulations are not able to generate a reasonable binding pose. The docking results are in accordance with the experimental data and they provide a possible structural justification of the SARs observed (Figure 1, panel B). Finally, it is interesting to note that the **3c** binding conformation generated in the docking simulation is very similar to the conformation of the structure obtained experimentally by X-ray crystallography (Figure 1, panel C).

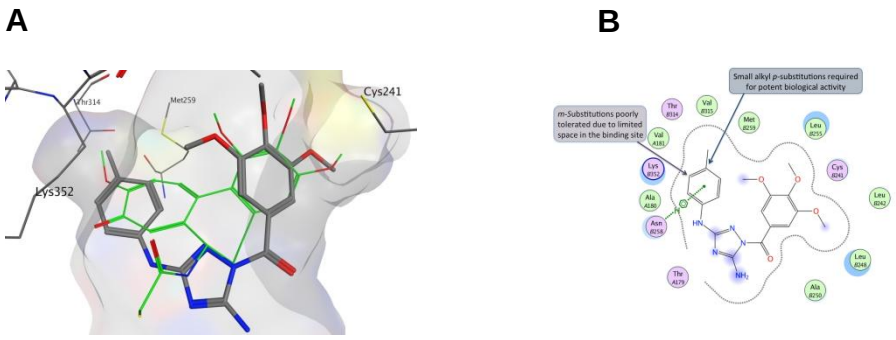

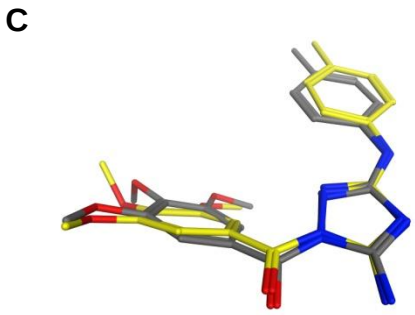

Figure 1. Panel A. Proposed binding for **3c** (in grey) in the colchicine site. Co-Crystallized DAMA-colchicine is shown in green. Panel B. Representation of the binding mode of **3c** in the colchicine binding site, with a summary of the SARs observed for the reported series of compounds. Panel C. Superposition of the conformation obtained from the docking simulations (in grey) and the crystal structure (in yellow) of **3c**.

Analysis of 3-arylamino 1,2,4-triazole derivatives for effects on the cell cycle.

The effects of a 24 h treatment with different concentrations of **3c** on cell cycle progression in HeLa and Jurkat cells were determined by flow cytometry (Figure 2, panels A, B).

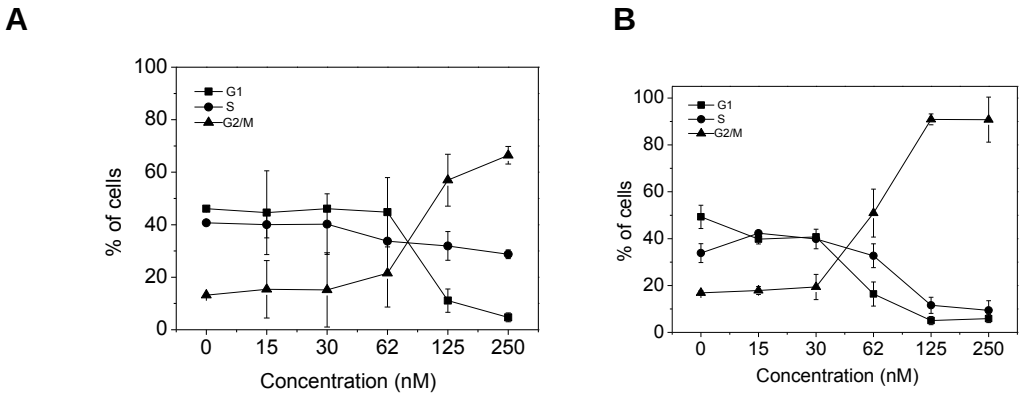

Figure 2. Percentage of cells in each phase of the cell cycle in HeLa (Panel A) and Jurkat cells (Panel B) treated with **3c** at the indicated concentrations for 24 h. Cells were fixed and labeled with PI and analyzed by flow cytometry as described in the experimental section. Data are represented as mean ± SEM of three independent experiments.

The compound caused a significant G2/M arrest in a concentration-dependent manner in the cell lines tested, with a rise in G2/M cells occurring at a concentration as low as 60 nM, while, at higher concentrations, more than 70% of the cells were arrested in G2/M. The cell cycle arrest in the G2/M phase was accompanied by a corresponding reduction in cells in the other phases of the cell cycle. In particular, the G1 phase decreased in both cell lines whereas S phase reduction was mainly evident in Jurkat cells. We next studied the association between **3c**-induced G2/M arrest and alterations in expression of proteins that regulate cell division. As shown in Figure 3 in HeLa cells, a 24 h treatment with **3c** at concentrations lower than 100 nM caused no significant variation in cyclin B expression, which, in association with cdc2 controls both entry into and exit from mitosis,[21,22] while at 100 and 250 nM we observed a clear increase in the cyclin B1 band.

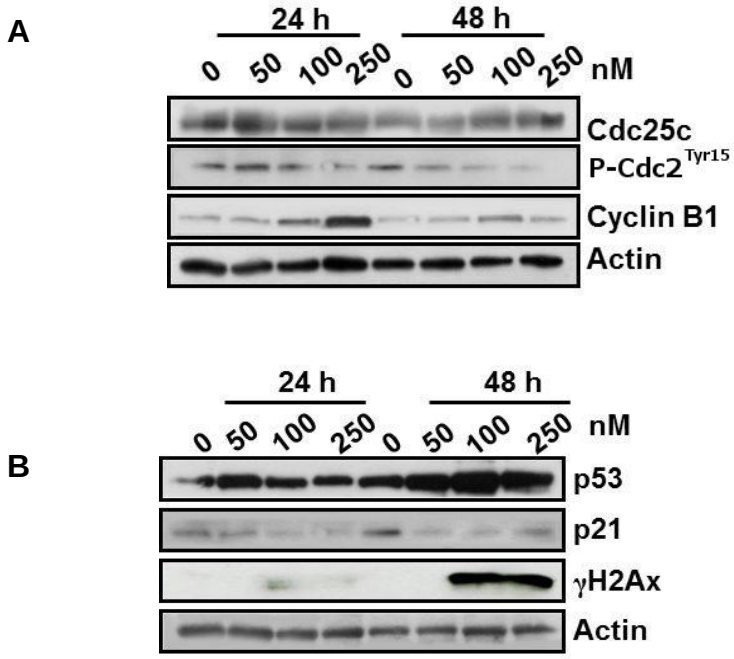

Figure 3. Effects of **3c** on G2/M regulatory proteins (Panel A) and on p53, p21 and γH2AX expression (panel B). HeLa cells were treated for 24 or 48 h with the indicated concentration of **3c**. The cells were harvested and lysed for the detection of cyclin B1, p-cdc2^{Tyr15} and cdc25C (panel A) or p53, p21 and γH2AX expression (panel B) by western blot analysis.

To confirm equal protein loading, each membrane was stripped and reprobed with anti-β-actin antibody. After a 48 h treatment, cyclin B1 expression decreased. More importantly,

p-cdc2^{Tyr15} expression decreased after either 24 or 48 h of treatment. However, no major changes in the expression of phosphatase cdc25c were observed. These results indicate that arrest at G2/M induced by **3c** is caused by an immediate block of cyclin B1 activity, followed by its accumulation, leading to a persistent and marked decrease of p-cdc2 ^{Tyr15} more detectable at the highest concentrations (100-250 nM) examined.

In addition to the analysis of proteins that control cell cycle checkpoints, we also examined the expression of the tumor suppressor p53 after treatment of Hela cells with **3c**. It is well known that prolonged mitotic arrest induces DNA damage and, consequently, p53 up-regulation.[23,24] As shown in Figure 3 (panel B), we detected in a concentration-dependent manner an increase in p53 expression that is particularly evident after 48 h of treatment. At the same time, we also observed a marked increase in the expression of phosphorylated histone γH2A.X, which is an early sensitive indicator of DNA damage.[25] Interestingly, the expression of the cyclin-dependent kinase inhibitor p21, which was previously demonstrated to have an anti-apoptotic role,[26] decreased both after 24 and 48 h of treatment.

Compound 3c induces apoptosis

To characterize the mode of cell death induced by **3c,** a biparametric cytofluorimetric analysis was performed using propidium iodide (PI), which stains DNA and enters only dead cells, and fluorescent immunolabeling of the protein annexin-V, which binds to phosphatidylserine (PS) in a highly selective manner.[27] Dual staining for annexin-V and with PI permits discrimination between live cells (annexin-V^-/PI^-), early apoptotic cells (annexin-V^+/PI^-), late apoptotic cells (annexin-V^+/PI^+) and necrotic cells (annexin-V^-/PI^+). As shown in Figure 4, both HeLa (panel A) and Jurkat cells (panel B) treated with the two compounds for 24 h showed an accumulation of annexin-V positive cells that further increased after 48 h in comparison with the untreated cells. Analogous results were also obtained for compound **3e** (see Figure S2, Supporting Information).

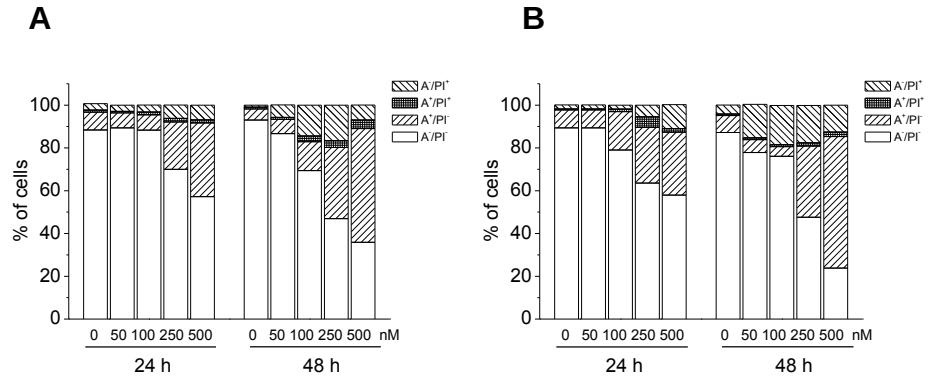

Figure 4. Flow cytometric analysis of apoptotic cells after treatment of HeLa cells (Panel A) or Jurkat cells (Panel B) with **3c** at the indicated concentrations after incubation for 24 or 48 h. The cells were harvested and labeled with annexin-V-FITC and PI and analyzed by flow cytometry. Data are represented as mean ± SEM of three independent experiments

Compound 3c induces caspase-dependent apoptosis

We then analyzed by western blot which proteins are involved on the triggered apoptotic pathway upon treatment. HeLa cells were treated with different concentrations of **3c** for 24 and 48 h (Figure 5).

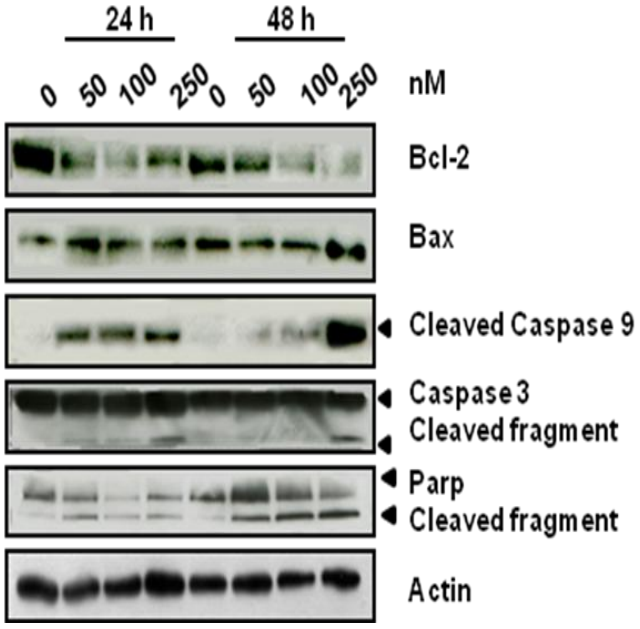

Figure 5. Western blot analysis of caspase-3, cleaved caspase-9, PARP Bcl-2 and Bax after treatment of HeLa cells with **3c** at the indicated concentrations and for the indicated times., To confirm equal protein loading, each membrane was stripped and reprobed with anti-β-actin antibody.

Interestingly, **3c** induced activation of the initiator caspase-9, in a time and concentration-dependent manner. We observed also an activation of the effector caspase-3 and cleavage of its substrate PARP (Figure 5). Furthermore, the anti-apoptotic protein Bcl-2 was

decreased by treatment with **3c** in a time dependent manner, while the expression of a pro-apoptotic protein, Bax was slightly increased only at 250 nM and at 48 h.

Derivative 3c has antivascular effects *in vitro*

Tumor growth requires an oxygen supply, so the tumor microenvironment stimulates the development of additional blood vessels.[28] Recent antitumor strategies are based on the use of chemotherapeutics with anti-angiogenic or antivascular drugs, in order to increase the efficacy of the treatment.[29] Many tubulin binding agents show antivascular effects against tumor endothelium,[30] including CA-4, and for that reason we evaluated **3c** for effects on endothelial cells *in vitro*. We used human umbilical vein endothelial cells (HUVECs) as a model for angiogenesis/vasculogenesis processes *in vitro*. Endothelial cell migration to the tumor site is one of the described mechanisms of angiogenesis.[31] Inhibiting this mechanism could be a strategy to arrest the development of tumor vasculature. We evaluated cell motility by scratching a HUVEC monolayer and monitoring the ability of cells to reclose the wound. As shown in Figure 6, (panel A), **3c** is very efficient in arresting cell motility. The effect is statistically significant after a 24 h incubation, at all the tested concentrations (5, 10, 25 nM), while, after 6 h, **3c** significantly inhibited cell motility at 10 and 25 nM, with a dose-response relationship observed (Figure 6, panel B).

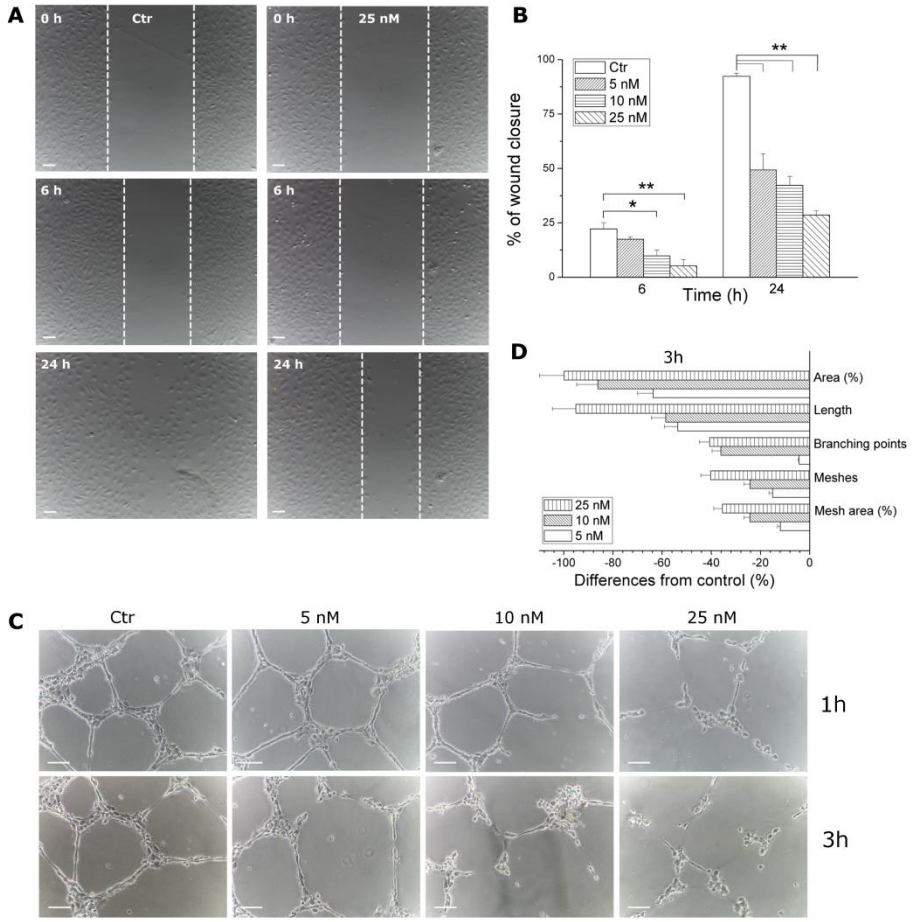

Figure 6. Compound **3c** has antivascular activity *in vitro*. Panel A. Confluent HUVECs in a monolayer were wounded, and cells treated with different concentrations of **3c** and at different times were photographed, 7x magnification; bar=100 μm. The dotted lines define the areas lacking cells. Panel B. The graph shows the quantitative effect of **3c**. Migration was quantified by measuring the gap closure at the indicated times as shown in panel A. Data are represented as mean ± S.E.M. of three independent experiments. *p<0.05, **p<0.01 vs control. Panel C. Inhibition of endothelial cell capillary-like tubule formation by **3c**. Tubule formation on Matrigel was carried out as described in the Experimental section. Representative pictures (10X magnification; bar=100 μm) of preformed capillary-like tubules treated with increasing concentration of **3c** for 1 or 3 h. Panel D. Quantitative analysis of the effects of **3c** on the dimensional and topological parameters of the preformed capillary-like tubule networks, after a 3 h treatment. Data were represented as mean ± S.E.M. of three independent experiments. *p<0.05, **p<0.01 *vs.* control.

To support the antivascular activity of **3c** we evaluated the ability of the compound to disrupt the "tubule-like" structures, formed by HUVECs seeded on Matrigel. Matrigel is an

extracellular matrix, rich in pro-angiogenic factors that stimulate single endothelial cells to assume an extended shape. The overall effect results in a reticulum similar to a capillary network.

As shown in Figure 6, panel C, after a 1 h incubation, 25 nM **3c** visibly disrupted the network of HUVECs, as compared with the control. After 3 h, all the tested concentrations were effective in altering the tubule-like structures. An image analysis[32] was performed to obtain a quantitative measurement of the total length of the tubules, the area and the number of meshes, the percent of area covered by HUVECs, and the number of branching points (Figure 6, panel D) after a 3 h treatment.

The results indicate that the effects on endothelial cells induced by **3c** are similar to those observed after CA-4 treatment, in the same experimental conditions, carried out by our group.[33]

Evaluation of antitumor activity of compound 3c *in vivo*

To evaluate the *in vivo* antitumor activity of **3c**, a syngeneic hepatocellular carcinoma model in mice was used.[34] Tumors were established by subcutaneous injection of BNL 1ME A.7R.1 cells into the backs of Balb/c mice. In preliminary experiments *in vitro*, we determined that both compound **3c** and CA-4, used as a reference compound, showed similar, potent cytotoxic activity (**3c** IC_{50} = 3.4±1.1 nM; CA-4 IC_{50} = 1.1±0.5 nM) against BNL 1ME A.7R.1 cells. Once the allografts reached a measurable size (about 100 mm^3), twenty mice were randomly assigned to one of four groups. In two of the groups, compound **3c** was injected intraperitoneally at doses of 5 and 10 mg/kg, respectively. In a third group, CA-4P was injected at 5 mg/kg, while the fourth group was used as a control. As depicted in Figure 7 (panel A), compound **3c** caused a significant reduction in tumor growth, as compared with administration of vehicle, at 10 but not 5 mg/kg. The effect of 5 mg/kg of CA-4P was not as great as that of 10 mg/kg of **3c**, but the CA-4P effect was still significant relative to the control. During the treatment period, only a small decrease in body weight occurred in the **3c**-treated animals (Figure 7, Panel B).

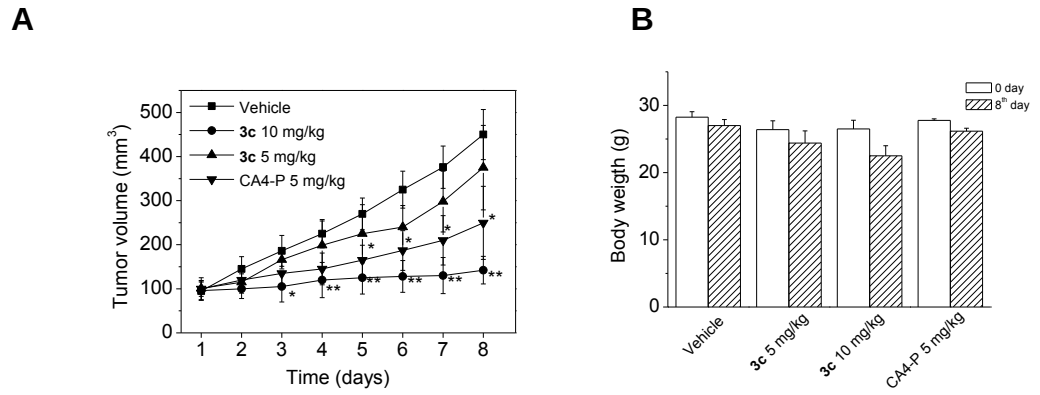

Figure 7. Inhibition of mouse allograft tumor growth *in vivo* by compound **3c**. (A). Male mice were injected subcutaneously in their dorsal region with 10^7 BNL 1MEA.7R.1 cells, a syngenic hepatocellular carcinoma cell line. Tumor-bearing mice were administered the vehicle, as control, or the indicated doses of **3c** or CA-4P as reference compound at the concentration of 5 mg/kg. Daily injections were given intraperitoneally starting on day 1. The figure shows the average measured tumor volumes (A) and body weights of the mice (B) recorded at the beginning and at the end of the treatments. Data are presented as mean ± SEM of tumor volume and body weight at each time point for 5 animals per group. *p<0.05, **p<0.01 *vs.* control.

2.1.3.4 CONCLUSIONS

The bioisosteric equivalence between thiazole and 1,2,4-triazole prompted us to synthesize a series of 1-(3',4',5'-trimethoxybenzoyl)-3-arylamino-5-amino 1,2,4-triazole derivatives with general formula **3**, in which the 1,2,4-triazole ring replaced the thiazole system of previously published analogues with general structure **2**. The substitution pattern on the phenyl of the arylamino moiety had variable effects.

Compound **3c**, bearing a *p*-toluidino moiety at the C-3 position of 1,2,4-triazole ring, its *p*-ethyl homologue **3f** and the *m,p*-dimethyl analogue **3e** exhibited the greatest antiproliferative activity among the tested compounds, with IC_{50} values of 0.21-3.2, 0.21-6.0 and 0.4-4.0 nM, respectively. These results were superior or comparable with those of the reference compound CA-4 against all cancer cell lines. The *para*-position tolerates small substituents, such as methyl (**3c**) or ethyl (**3f**) groups, while the inactivity of *i*-Pr or *n*-Bu derivatives **3g** and **3h**, respectively, indicates that bulky substituents were detrimental for activity. Placing the methyl group in the *meta*-position (**3d**) led to a dramatic drop in potency as compared with the *para*-isomer **3c**, even though we observed excellent activity

with the *meta*, *para*-dimethyl derivative **3e**. Compound **3c** was the most potent inhibitor of tubulin polymerization and of colchicine binding (IC_{50}=0.75 μM for assembly, 92% inhibition of the binding of 5 μM colchicine), and the antiproliferative activity of **3c**, in terms of $IC_{50's}$, ranged from 0.21 to 3.2 nM in the seven cell tumor lines examined, values lower than that of previously published isosteric analogues.[11] In addition, in preliminary experiment **3c** had low toxicity in non tumoral cells and is active also in drug-resistant cell lines. Although **3c** was almost twice as active as CA-4 as an inhibitor of tubulin polymerization, these two compounds showed similar activity as inhibitors of colchicine binding. Moreover, in a detailed series of biological assays, we clearly demonstrated that **3c** induced caspase-dependent apoptosis and late DNA damage and p53 induction. Compound **3c**, in addition to its ability to inhibit tubulin polymerization, efficiently targeted endothelial cells, acting as a VDA. More importantly, *in vivo* experiments showed that this compound was able to significantly reduce the growth of a syngenic tumor model in mice, indicating that it is a very promising anticancer compound that warrants further evaluation for its potential clinical use.

2.1.3.5 EXPERIMENTAL SECTION

Cell growth conditions and antiproliferative assay. Human T-leukaemia (CCRF-CEM and Jurkat) and human B-leukaemia (SEM) cells were grown in RPMI-1640 medium (Gibco, Milano, Italy). Breast adenocarcinoma (MCF7), human cervix carcinoma (HeLa), and human colon adenocarcinoma (HT-29) cells were grown in DMEM medium (Gibco, Milano, Italy), all supplemented with 115 units/mL penicillin G (Gibco, Milano, Italy), 115 μg/mL streptomycin (Invitrogen, Milano, Italy), and 10% fetal bovine serum (Invitrogen, Milano, Italy). $CEM^{Vbl\text{-}100}$ cells are a multidrug-resistant line selected against vinblastine.[20] $LoVo^{Doxo}$ cells are a doxorubicin resistant subclone of LoVo cells[21] and were grown in complete Ham's F12 medium supplemented with doxorubicin (0.1 μg/mL). $LoVo^{Doxo}$ and $CEM^{Vbl\text{-}100}$ were a kind gift of Dr. G. Arancia (Istituto Superiore di Sanità, Rome, Italy). Stock solutions (10 mM) of the different compounds were obtained by dissolving them in DMSO. Individual wells of a 96-well tissue culture microtiter plate were inoculated with 100 μL of complete medium containing 8×10^3 cells. The plates were incubated at 37 °C in a humidified 5% CO_2 incubator for 18 h prior to the experiments. After medium

removal, 100 μL of fresh medium containing the test compound at different concentrations was added to each well in triplicate and incubated at 37 °C for 72 h. The percentage of DMSO in the medium never exceeded 0.25%. This was also the maximum DMSO concentration in all cell-based assays described below. Cell viability was assayed by the (3-(4, 5-dimethylthiazol-2-yl)-2,5-diphenyltetrazolium bromide test as previously described.[37] The IC_{50} was defined as the compound concentration required to inhibit cell proliferation by 50%, in comparison with cells treated with the maximum amount of DMSO (0.25%) and considered as 100% viability.

Peripheral blood lymphocytes (PBL) from healthy donors were obtained by separation on Lymphoprep (Fresenius KABI Norge AS) gradient. After extensive washing, cells were resuspended (1.0×10^6 cells/mL) in RPMI-1640 with 10% fetal bovine serum and incubated overnight. For cytotoxicity evaluations in proliferating PBL cultures, non-adherent cells were resuspended at 5×10^5 cells/mL in growth medium, containing 2.5 μg/mL PHA (Irvine Scientific). Different concentrations of the test compounds were added, and viability was determined 72 h later by the MTT test. For cytotoxicity evaluations in resting PBL cultures, non-adherent cells were resuspended (5×10^5 cells/mL) and treated for 72 h with the test compounds, as described above.

Effects on tubulin polymerization and on colchicine binding to tubulin.

To evaluate the effect of the compounds on tubulin assembly *in vitro*,[38a] varying concentrations of compounds were preincubated with 10 μM bovine brain tubulin in 0.8 M monosodium glutamate (pH adjusted to 6.6 with HCl in a 2.0 M stock solution) at 30 ˚C and then cooled to 0 ˚C. After addition of 0.4 mM GTP, the mixtures were transferred to 0 °C cuvettes in a recording spectrophotometer and warmed to 30 °C. Tubulin assembly was followed turbidimetrically at 350 nm. The IC_{50} was defined as the compound concentration that inhibited the extent of assembly by 50% after a 20 min incubation. The capacity of the test compounds to inhibit colchicine binding to tubulin was measured as described,[38b] except that the reaction mixtures contained 1 μM tubulin, 5 μM [^{3}H]colchicine and 5 μM test compound.

Molecular modeling. All molecular modeling studies were performed on a MacPro dual 2.66GHz Xeon running Ubuntu 12.04. The tubulin structure was downloaded from the

PDB data bank (http://www.rcsb.org/ - PDB code: 1SA0).[39] Hydrogen atoms were added to the protein, using the Protonate 3D routine of the Molecular Operating Environment (MOE).[40] Ligand structures were built with MOE and minimized using the MMFF94x forcefield until a RMSD gradient of 0.05 kcal mol^{-1} $Å^{-1}$ was reached. The docking simulations were performed using PLANTS.[41]

Flow Cytometric Analysis of Cell Cycle Distribution.

5×10^5 HeLa or Jurkat cells were treated with different concentrations of the test compounds for 24 h. After the incubation period, the cells were collected, centrifuged, and fixed with ice-cold ethanol (70%). The cells were then treated with lysis buffer containing RNase A and 0.1% Triton X-100 and then stained with PI. Samples were analyzed on a Cytomic FC500 flow cytometer (Beckman Coulter). DNA histograms were analyzed using MultiCycle for Windows (Phoenix Flow Systems).

Apoptosis Assay.

Cell death was determined by flow cytometry of cells double stained with annexin V/FITC and PI. The Coulter Cytomics FC500 (Beckman Coulter) was used to measure the surface exposure of PS on apoptotic cells according to the manufacturer's instructions (Annexin-V Fluos, Roche Diagnostics).

Western Blot Analysis. HeLa cells were incubated in the presence of **3c** and after different times, were collected, centrifuged, and washed two times with ice cold phosphate buffered saline (PBS). The pellet was then resuspended in lysis buffer. After the cells were lysed on ice for 30 min, lysates were centrifuged at 15000 x g at 4 °C for 10 min. The protein concentration in the supernatant was determined using the BCA protein assay reagents (Pierce, Italy). Equal amounts of protein (10 μg) were resolved using sodium dodecyl sulfate-polyacrylamide gel electrophoresis (SDS-PAGE) (7.5−15% acrylamide gels) and transferred to PVDF Hybond-P membrane (GE Healthcare). Membranes were blocked with a bovine serum albumin (BSA) solution (BSA 5% in Tween PBS 1X), the membranes being gently rotated overnight at 4 °C. Membranes were then incubated with primary antibodies against Bcl-2, Bax, PARP, cleaved caspase-9, cdc25c (Cell Signaling), caspase-3 (Alexis), H2AX (Cell Signaling), p53 (Cell Signaling), cyclin B (Cell

Signaling), p-cdc2^{Tyr15} (Cell Signaling), p21 (Cell Signaling), or β-actin (Sigma-Aldrich) for 2 h at room temperature. Membranes were next incubated with peroxidase labeled secondary antibodies for 60 min. All membranes were visualized using ECL Select (GE Healthcare) and exposed to Hyperfilm MP (GE Healthcare). To ensure equal protein loading, each membrane was stripped and reprobed with anti-β-actin antibody.

Antivascular activity.

HUVECs were prepared from human umbilical cord veins, as previously described.[33] The adherent cells were maintained in M200 medium supplemented with LSGS (Low Serum Growth Supplement), containing FBS, hydrocortisone, hEGF, bFGF, heparin, gentamycin/amphotericin (Life Technologies, Monza, Italy). Once confluent, the cells were detached by trypsin–EDTA solution and used in experiments from the first to sixth passages.

The motility assay for HUVECs was based on "scratch" wounding of a confluent monolayer.[42] Briefly, HUVECs ($1x10^5$) were seeded onto 0.1% collagen type I (BD Biosciences, Italy)-coated six well plates in complete medium until a confluent monolayer was formed. The cells were wounded using a pipette tip, and wells were washed with PBS to remove the undetached cells. Then, the cells were treated with the test compounds, and at different times from the scratch, the cells were photographed under a light microscope. At all indicated time points, the wound width was measured in four areas and compared with the initial width.

Matrigel matrix (Basement Membrane Matrix, BD Biosciences, Italy) was kept at 4 °C for 3 h, when 230 µL of Matrigel solution was added to each well of a 24-well plate. After gelling at 37°C for 30 min, gels were overlaid with 500 µL of medium containing 6×10^4 HUVECs. The cells were incubated over Matrigel for 6 h to allow capillary tubes to form. Different concentrations of test compound were added in the cultures and incubated for different times, and the disappearance of existing vasculature was monitored and photographed (five fields for each well: the four quadrants and the center) at a 10x magnification. Phase contrast images were recorded using a digital camera and saved as TIFF files. Image analysis was carried out using the ImageJ image analysis software, and the following dimensional parameters (percent area covered by HUVECs and total length

of HUVECs network per field) and topological parameters (number of meshes and branching points per fields) were estimated.[32] Values were expressed as percent change from control cultures grown with complete medium.

Antitumor activity *in vivo.*

The *in vivo* cytotoxic activity of compound **3c** was investigated using a syngeneic murine hepatocellular carcinoma cell line (BNL 1ME A.7R.1) in Balb/c mice.[34] Male mice, 8 weeks old, were purchased from Harlan (S. Pietro al Natisone Udine, Italy), and tumors were induced by a subcutaneous injection in their dorsal region of 10^7 cells in 200 µL of sterile PBS. Animals were randomly divided into four groups, and, starting on the second day, the first group was daily dosed intraperitoneally (i.p.) with 7 µL/kg of free vehicle (0.9% NaCl containing 5% polyethylene glycol 400 and 0.5% Tween 80). Groups two and three were treated with compound **3c** at the doses of 5 and 10 mg/kg body weight, respectively. The fourth group received the reference compound CA-4P at the dose of 5 mg/kg body weight. Both compound **3c** and CA-4P were dissolved in free vehicle. Tumor sizes were measured daily for 7 days using a pair of calipers. In particular, the tumor volume (*V*) was calculated by the rotational ellipsoid formula: $V = A \times B2/2$, where *A* is the longer diameter (axial) and *B* is the shorter diameter (rotational). All experimental procedures followed guidelines recommended by the Institutional Animal Care and Use Committee of Padova University.

Statistical Analysis. Unless indicated otherwise, the results are presented as the mean ± SEM. The differences between different treatments were analyzed using the two-sided Student's t test. P values lower than 0.05 were considered significant.

Supporting information available. Detailed characterization of synthesized compounds **7a-c**, **7g-h** and **7k-l**. Immunofluorescence analysis of tubulin network and apoptosis assay on HeLa cells. This material is available free of charge via the Internet at http://pubs.acs.org.

2.1.3.6 REFERENCES

1. a) Amos, L. A. What tubulin drugs tell us about microtubule structure and dynamics. *Semin. Cell Dev. Biol.* **2011**, *22*, 916-926; b) Amos, L. A. Microtubule structure and its stabilisation. *Org. Biomol. Chem.* **2004**, *2*, 2153-2160.

2. Dumontet, C.; Jordan, M. A. Microtubule-binding agents: a dynamic field of cancer therapeutics. *Nat. Rev. Drug. Discov.* **2010**, *9*, 790-803.

3. Risinger, A. L.; Giles, F. J.; Mooberry, S. L. Microtubule dynamics as a target in oncology. *Cancer Treat. Rev.* **2008**, *35*, 255-261.

4. Chen, S.-M.; Meng, L.-H.; Ding, J. New microtubule-inhibiting anticancer agents. *Expert Opin. Invest. Drugs* **2010**, *3*, 329-343.

5. Pettit, G.R.; Singh, S.B.; Hamel, E.; Lin, C.M.; Alberts, D.S.; Garcia-Kendall, D. Isolation and structure of the strong cell growth and tubulin inhibitor combretastatin A-4. *Experientia* **1989**, *45*, 209-211.

6. Lin, C.M.; Ho, H.H.; Pettit, G.R.; Hamel, E. Antimitotic natural products combretastatin A-4 and combretastatin A-2: studies on the mechanism of their inhibition of the binding of colchicine to tubulin. *Biochemistry* **1989**, *28*, 6984-6991.

7. Pettit, G.R.; Temple, C. Jr.; Narayanan, V.L.; Varma, R.; Boyd, M.R.; Rener, G.A.; Bansal, N. Antineoplastic agents 322. Synthesis of combretastatin A-4 prodrugs. *Anti-Cancer Drug Des.* **1995**, *10*, 299-309.

8. a) Zweifel, M.; Jayson, G. C.; Reed, N. S.; Osborne, R.; Hassan, B.; Ledermann, J.; Shreeves, G.; Poupard, L.; Lu, S. P.; Balkissoon, J.; Chaplin, D. J.; Rustin, G. J. S. Phase II trial of combretastatin A4 phosphate, carboplatin, and paclitaxel in patients with platinum resistant ovarian cancer. *Ann. Oncol.* **2011**, *22*, 2036-2041; b) Rustin, G. J.; Shreeves, G.; Nathan, P. D.; Gaya, A.; Ganesan, T. S.; Wang, D.; Boxall, J.; Poupard, L.; Chaplin, D. J.; Stratford, M. R. L.; Balkissoon, J.; Zweifel, M. A Phase Ib trial of CA-4P (combretastatin A-4 phosphate), carboplatin, and paclitaxel in patients with advanced cancer. *Br. J. Cancer*, **2010**, *102*, 1355-1360.

9. Siemann, D. W.; Chaplin, D. J.; Walike, P. A. A review and update of the current status of the vasculature-disabling agent combretastatin-A4 phosphate (CA4P). *Expert Opin. Investig. Drugs* **2009**, *18*, 189-197.

10. Romagnoli, R.; Baraldi, P. G.; Carrion, M. D.; Cruz-Lopez, O.; Lopez-Cara, C.; Basso, G.; Viola, G.; Khedr, M.; Balzarini, J.; Mahboobi, S.; Sellmer, A.; Brancale, A.; Hamel, E. 2-Arylamino-4-amino-5-aroylthiazoles. "One-pot" synthesis and biological evaluation of a new class of inhibitors of tubulin polymerization. *J. Med. Chem.* **2009**, *52*, 5551-5555.

11. a) Moreira Lima, L.; Barreiro, E. J. Bioisosterism: a useful strategy for molecular modification and drug design. *Curr. Med. Chem.* **2005**, *12*, 23-49, b) Shan, Y.; Zhang, J.; Liu, Z.; Wang, M.; Dong, Y. Developments of combretastatin A-4 derivatives as anticancer agents. *Curr. Med. Chem.* **2011**, *18*, 523-538.

12. Lange, J. H. M.; van Stuivenberg, H. H.; Coolen, H. K. A. C.; Adolfs, T. J. P.; McCreary, A. C.; Keizer, H. G.;. Wals, H. C.; Veerman, W.; Borst, A. J. M. ; de Looff, W.; Verveer, P. C.; Kruse, C. G. Bioisosteric replacements of the pyrazole moiety of rimonabant: Synthesis, biological properties, and molecular modeling investigations of thiazoles, triazoles, and imidazoles as potent and selective CB1 cannabinoid receptor antagonists. *J. Med. Chem.* **2005**, *48*, 1823-1838.

13. For anticancer molecules based on the 1,2,4-triazole ring see: a) Zhang, Q.; Peng, Y.; Wang, X. I.; Keeman, S. M.; Aurora. S.; Welsh, W. J. Highly potent triazole-based tubulin polymerization inhibitors. *J. Med. Chem.* **2007**, *50*, 749-754, b) Romagnoli, R.; Baraldi, P. G.; Cruz-Lopez, O.; Lopez-Cara, C.; Carrion, M. D.; Brancale, A.; Hamel, E.; Chen, L.; Bortolozzi, R.; Basso, G.; Viola, G. Synthesis and antitumor activity of 1,5-disubstituted 1,2,4-triazoles as cis-restricted combretastatin analogs, *J. Med. Chem.* **2010**, *53*, 4248-4258; c) Ouyang, X.; Chen, X.; Piatnitski, E. L.; Kiselyov, A. S.; He, H.-Y.; Mao, Y.; Pattaropong, V.; Yu, Y.; Kim, K. H.; Kincaid, J.; Smith II, L.; Wong, W. C.; Lee, S. P.; Milligan, D. L.; Malikzay, A.; Fleming, J.; Gerlak, J.; Deevi, D.; Doody, J. F.; Chiang, H.-H.; Patel, S. N.; Wang, Y.; Rolser, R. L.; Kussie, P.; Labelle, M.; Tuma, M. C. Synthesis and structure-activity relationships of 1,2,4-triazoles as a novel class of potent tubulin polymerization inhibitors. *Bioorg. Med. Chem. Lett.* **2005**, *15*, 5154-5158; d) Ohsumi, K.; Hatanaka, T.; Fujita, K.; Nakagawa, R.; Fukuda, Y.; Nihai, Y.; Suga, Y.; Morinaga, Y.; Akiyama, Y.; Tsuji, T. Synthesis and antitumor activity of cis-restricted combretastatins 5-membered heterocyclic analogues. *Bioorg. Med. Chem. Lett.* **1988**, *8*, 3153-3158; e) Shi, Y.-J., Song, X.-J.; Li, X.; Ye, T.-H.; Xiong, Y.; Yu, L.-T. Synthesis and biological evaluation of 1,2,4-triazole and 1,3,4-thiadiazole derivatives as potential cytotoxic agents. *Chem. Pharm. Bull.* **2013**, *61*, 1099-1104; f) Singha, T., Sing, J.; Naskar, A.; Ghosh, T.; Mondal, A.; Kundu, M.; Harwansh, R. K.; Maity, T. K. Synthesis and evaluation of antiproliferative activity of 1,2,4-triazole derivatives against EAC bearing mice model. *Ind. J. Pharm. Edu. Res.* **2012**, *46*, 346-351; g) Li, X., li, X.-Q.; Liu, H.-M.; Zhou, X.-Z.; Shao, Z.-H. Synthesis and evaluation of antitumor activities of novel chiral 1,2,4-triazole Schiff bases bearing γ-butenolide moiety. *Org. Med. Chem. Lett.* **2012**, *2*, 26-31.

14. a) Gaukroger, K.; Hadfield, J. A.; Lawrence, N. J.; Nlan, S.; McGown, A. T. Structural requirements for the interaction of combretastatins with tubulin: how important is the trimethoxy unit? *Org. Biomol. Chem.* **2003**, *1*, 3033-3037; b) Cushman, M.; Nagarathnam, D.; Gopal, D.; He, H.-M.; Lin, C. M.; Hamel, E. Synthesis and evaluation of analogues of (Z)-1-(4-methoxyphenyl)-2-(3,4,5-trimethoxyphenyl)ethene as potential cytotoxic and antimitotic agents. *J. Med. Chem.* **1992**, *35*, 2293-2306.

15. Thomae, D.; Perspicace, E.; Hesse, S.; Kirsch, G.; Seck, P. Synthesis of substituted [1,3]thiazolo[4,5-*d*][1,2.3]triazines. *Tetrahedron*, **2008**, *64*, 9306-9314;

16. Webb, R. L.; Eggleston, D. S.; Labaw, C. S.; Lewis, J. J.; Wert, K. Diphenyl cyancarbonimidate and dichlorodiphenoxymethane as synthons for the construction of heterocyclic systems of medicinal interest. *J. Heterocycl. Chem.* **1987**, *24*, 275-278.

17 Szakács, G.; Paterson, J.K.; Ludwig, J.A.; Booth-Genthe, C.; Gottesman, M.M. Targeting multidrug resistance in cancer *Nat. Rev. Drug Discov*. **2006**, 5, 219-234.

18 Baguley B.C. Multidrug resistance mechanism in cancer *Mol. Biotechnol.* **2010**, *46*, 308-316.

19 Toffoli, G.; Viel, A.; Tumiotto, I.; Biscontin, G.; Rossi, G.; Boiocchi, M. Pleiotropic-resistant phenotype is a multifactorial phenomenon in human colon carcinoma cell lines. *Br. J. Cancer* **1991**, *63*, 51–56.

20 Dupuis, M.; Flego, M.; Molinari, A.; Cianfriglia, M. Saquinavir induces stable and functional expression of the multidrug transporter P-glycoprotein in human CD4 T-lymphoblastoid CEM rev cells. *HIV Medicine* **2003,** *4*, 338–345.

21. Clarke, P. R.; Allan, L. A. Cell-cycle control in the face of damage- a matter of life or death. *Trends Cell Biol.* **2009**, *19*, 89-98.

22. Mollinedo, F.; Gajate, C. Microtubules, microtubule-interfering agents and apoptosis. *Apoptosis* **2003**, *8*, 413-450.

23. Ganem, N. J.; Pellman, D. Linking abnormal mitosis to the acquisition of DNA damage. *J Cell Biol.* **2012**, *199*, 871-881

24. Orth, J. D.; Loewer, A.; Lahav, G.; Mitchison, T. J. Prolonged mitotic arrest triggers partial activation of apoptosis, resulting in DNA damage and p53 induction. *Mol Biol Cell*. **2012,** *23*, 567-576.

25. O. Fernandez-Capetillo, A. Lee, M. Nussenzweig, A. Nussenzweig. H2AX: the histone guardian of the genome. *DNA Repair* **2004**, *3*, 959-967.

26. Weiss, R. H. p21Waf1/Cip1 as a therapeutic target in breast and other cancers *Cancer Cell* **2003,** *4*, 425-429.

27. Vermes, I.; Haanen, C.; Steffens-Nakken, H.; Reutelingsperger, C. A novel assay for apoptosis. Flow cytometric detection of phosphatidylserine expression on early apoptotic cells using fluorescein labelled annexin V. *J. Immunol. Methods* **1995**, *184*, 39-51.

28. Baeriswyl, V.; Christofori, G. The angiogenic switch in carcinogenesis. *Semin. Cancer Biol.* **2009**, *19*, 329-337.

29. Siemann, D.; Bibby, M.; Dark, G. Differentiation and definition of vascular-targeted therapies. *Clin. Cancer Res.* **2005**, *2*, 416-420.

30. Kanthou, C.; Tozer, G. M. The tumor vascular targeting agent combretastatin A-4-phosphate induces reorganization of the actin cytoskeleton and early membrane blebbing in human endothelial cells. *Blood* **2002**, *99*, 2060-2069.

31. Bergers, G.; Benjamin L, E. Tumorigenesis and the angiogenic switch. *Nat. Rev. Cancer*. **2003**, *3*, 401-410.

32. Guidolin, D.; Vacca, A.; Nussdorfer, G. G.; Ribatti, D. A new image analysis method based on topological and fractal parameters to evaluate the angiostatic activity of docetaxel by using the Matrigel assay in vitro. *Microvasc. Res.* **2004**, *67*, 117-124.

33. Porcù, E.; Viola, G.; Bortolozzi, R.; Mitola, S.; Ronca, R.; Presta, M.; Persano, L.; Romagnoli, R.; Baraldi, P. G.; Basso, G. TR-644 a novel potent tubulin binding agent induces impairment of endothelial cells function and inhibits angiogenesis *Angiogenesis* **2013**, *16*, 647-662.

34 Gasparotto, V.; Castagliuolo, I.; Chiarelotto, G.; Pezzi, V.; Montanaro, D.; Brun, P.; Palù, G.; Viola, G., Ferlin, M. G. Synthesis and biological activity of 7-phenyl-6,9-dihydro-3H-pyrrolo[3,2-*f*]quinolin-9-ones: a new class of antimitotic agents devoid of aromatase activity. *J. Med. Chem*. **2006** ;*49*, 1910-1915.

35. Altomare, A.; Burla, M. C.; Camalli, M.; Cascarano, G.; Giacovazzo, C.; Guagliardi, A.; Moliterni, A. G:, Polidori, G:; Spagna, R. *SIR*97: a new tool for crystal structure determination and refinement. *J. Appl. Crystallogr*. **1999**, *32*, 115-121.

36. Sheldrick, G. M. SHELXL-97, *Program for Refinement of Crystal Structures*. University of Göttingen, Germany, 1997.

37. Romagnoli, R.; Baraldi, P. G.; Kimatrai Salvador, M.; Brancale, A.; Fu, X-H.; Li, J.; Zhang, S.-Z.; Hamel, E.; Bortolozzi, R.; Basso, G.; Viola, G. Synthesis and evaluation of 1,5-disubstituted tetrazoles as rigid analogues of combretastatin A-4 with potent antiproliferative and antitumor activity. *J. Med. Chem.* **2012**, *55*, 475-488.

38 a) Hamel, E. Evaluation of antimitotic agents by quantitative comparisons of their effects on the polymerization of purified tubulin. *Cell Biochem. Biophys.* **2003**, *38*, 1-21; b) Verdier-Pinard, P.; Lai J.-Y.; Yoo, H.-D.; Yu, J.; Marquez, B.; Nagle D.G.; Nambu, M.; White, J.D.; Falck, J.R.; Gerwick, W.H.; Day, B.W.; Hamel, E. Structure-activity analysis of the interaction of curacin A, the potent colchicine site antimitotic agent, with tubulin and effects of analogs on the growth of MCF-7 breast cancer cells. *Mol. Pharmacol.* **1998**, *53*, 62-67.

39. Ravelli, R. B. G.; Gigant, B.; Curmi, P. A.; Jourdain, I.; Lachkar, S.; Sobel, A.; Knossow, M. Insight into tubulin regulation from a complex with colchicine and a stathmin-like domain. *Nature* **2004**, *428*, 198-202.

40. Molecular Operating Environment (MOE 2008.10). Chemical Computing Group, Inc. Montreal, Quebec, Canada. http://www.chemcomp.com.

41. Korb, O.; Stützle, T.; Exner, T. E. PLANTS: Application of ant colony optimization to structure-based drug design. In Dorigo, M.; Gambardella, L. M.; Birattari, M.; Martinoli, A.; Poli, R.; Stützle, T. (Eds.). *Ant Colony Optimization and Swarm Intelligence*, 5th International Workshop, ANTS 2006, Springer: Berlin, **2006**; LNCS 4150, pp 247-258.

42. Liang, C.C.; Park, A.Y; Guan, J.L. In vitro scratch assay: a convenient and inexpensive method for analysis of cell migration in vitro. *Nat Protoc*. **2007,** *2***,** 329-333

2.2 OXIDATIVE STRESS-INDUCING AGENTS

2.2.1 GENERAL INTRODUCTION

In eukaryotic cells Reactive Oxygen Species (ROS) are constantly generated and eliminated in the biological system[22]. Growing evidences suggest that compared to normal cells, cancer cells exhibit increased intrinsic ROS stress, due in part to oncogenic stimulation, increased metabolic activity and mitochondrial malfunction. Therefore cancer cells survival depends on the alternative enzymatic detoxification reactions which are activated to overcome to the imbalanced redox status. As such, to develop drugs that target this cancer-specific biochemical alteration might be a feasible approach to achieve antitumor therapy[23].

2.2.1.1 REACTIVE OXIGEN SPECIES (ROS)

Reactive oxygen species (ROS), such as superoxide anion (O2−), hydrogen peroxide (H_2O_2), and hydroxyl radical (HO•), hydroxyl ion, and nitric oxide, consist of radical and non-radical oxygen species formed by the partial reduction of oxygen[24].

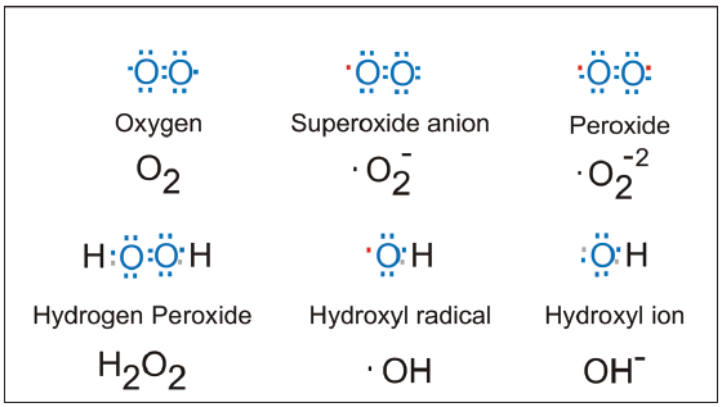

Figure 1: Reactive oxygen species (ROS)

ROS are constantly produced by both enzymatic and non-enzymatic reactions. Enzyme-catalysed reactions that generate ROS include those involving NADPH oxidase, xanthine oxidase, uncoupled endothelial nitric oxide synthase (eNOS), arachidonic acid and metabolic enzymes such as the cytochrome P450 enzymes, lipoxygenase and cyclooxygenase. The mitochondrial respiratory chain is a non-enzymatic source of ROS. Since the maintenance of ROS intracellular homeostasis is fundamental for the

mitochondrial, metabolic and cellular function, the intracellular ROS normally exist in balance with biochemical antioxidants in all aerobic cells. Moreover oxidative stress occurs when this critical balance is disrupted because of excess ROS or antioxidant depletion.

2.2.1.2 ANTIOXIDANT ENZYMES

In normal and cancer cells the ROS intracellular homeostasis is maintained through ROS-scavenging systems such as superoxide dismutases (SOD1, SOD2 and SOD3), catalase, and the two non-enzymatic small molecule antioxidants, thioredoxin (TRX) and glutathione (GSH)[25,26].

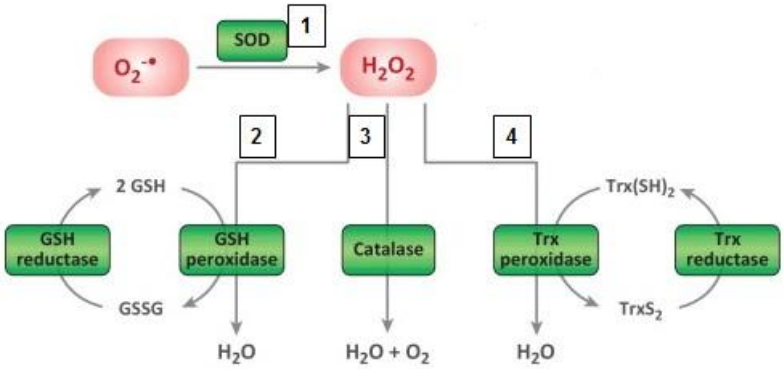

Figure 2: ROS-scavenging systems SOD (1), GSH (2), Catalase (3), Thioredoxin (4). (Adapted from Ref[27])

Superoxide dismutase (SOD) catalyzes the conversion of two superoxide anions into a molecule of hydrogen peroxide (H_2O_2) and oxygen (O2) (Eq. 1) whereas in the peroxisomes of eukaryotic cells, the enzyme catalase converts H_2O_2 to water and oxygen, and thus completes the detoxification initiated by SOD (Eq. 2)[28,26].

Eq. 1. $2\ O_2^{-} + 2H^{+} \rightarrow H_2O_2 + O_2$

Eq. 2. $2\ H_2O_2 \rightarrow 2\ H_2O + O_2$

Thioredoxin system (Trx), which is composed of NADPH, thioredoxin reductase (TrxR), and thioredoxin provides the electrons to thiol-dependent peroxidases (peroxiredoxins) to remove reactive oxygen and nitrogen species with a fast reaction rate.

Glutathione system is the most important intracellular defense against the deleterious effects of reactive oxygen species. This tripeptide (glutamyl-cysteinyl-glycine) plays as a sulfhydryl (-SH) antioxidant[29]. Reduced GSH is the biological active form that is oxidized to glutathione disulfide (GSSG) during oxidative stress. The glutathione GSH oxidation to GSSG is catalyzed by the antioxidant enzyme GSH peroxidase, whereas the recycling of GSSG to GSH is accomplished mainly by the enzyme glutathione reductase. Therefore the ratio of the oxidized form of glutathione (GSSG) and the reduced form (GSH) is a dynamic indicator of the oxidative stress of an organism[30].

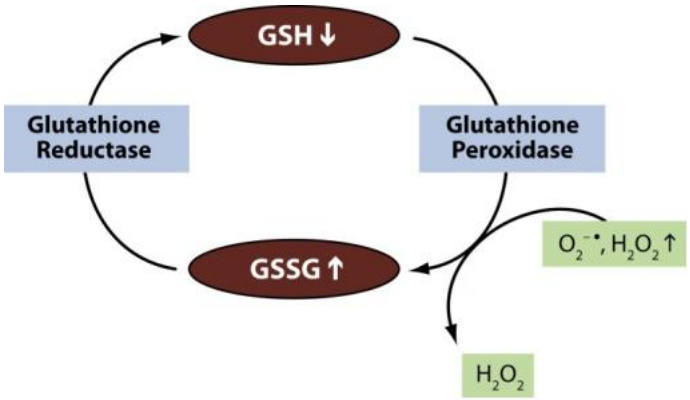

Figure 3: The glutathione antioxidant system

Furthermore, Vitamin C or ascorbic acid is a water soluble molecule capable of reducing ROS, while vitamin E (α-tocopherol) is a lipid soluble molecule that has been suggested as playing a similar role in membranes.

2.2.1.3 ROS HOMEOSTASIS IN CANCER CELLS

Mounting evidences suggest that, compared with their normal counterparts, many types of cancer cell have increased levels of ROS[1]. The high ROS levels in cancer cells are a consequence of altered metabolism, increased aerobic glycolysis (the so called Warburg effect), activation of oncogenes and mitochondrial dysfunction[1,31,32]. As such, while normal cells can tolerate a certain level of exogenous ROS stress owing to their 'reserve' antioxidant capacity, cancer cells are more vulnerable to further oxidative stress. In fact, an

additional increase of ROS stress in cancer cells could cause elevation of ROS above the threshold level of toxicity, leading to cancer cell death.

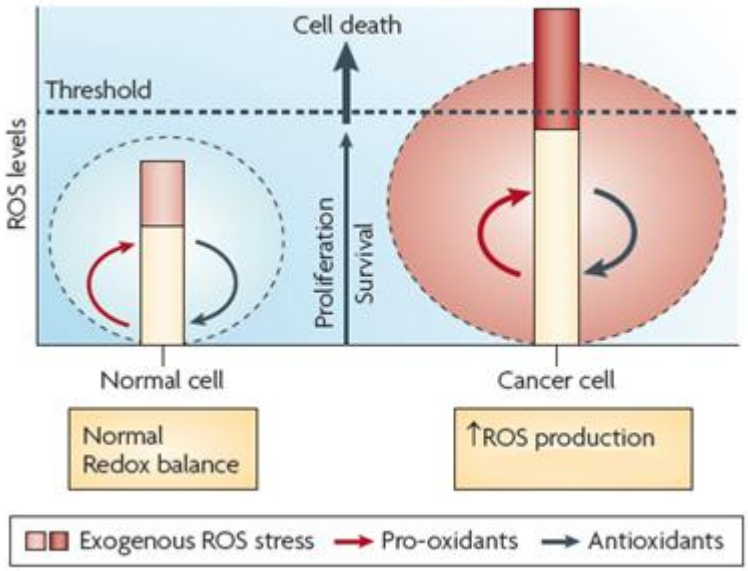

Figure 4: Different ROS homeostasis in normal and cancer cells. (Adapted from Ref[1])

For this reason, compared to the normal counterpart, cancer cells would be more dependent on the enzymatic antioxidant systems and more vulnerable to further oxidative stress induced by exogenous ROS-generating agents or compounds that inhibit the antioxidant system. Therefore, to manipulate ROS levels treating cells with ROS-generating agents or compounds that inhibit the antioxidant systems might be a way to selectively kill cancer cells without causing significant toxicity to normal cells[1].

2.2.1.4 OXIDATIVE STRESS-INDUCING AGENTS

The induction of oxidative stress can lead to the preferential killing of cancer cells. Several compounds have been described to exert their potent antitumoral activity by either activating a ROS-dependent apoptotic pathway (isoobtusilactone) or blocking the intracellular antioxidant systems such as Glutathione, SOD (elesclomol, piperlongumine, camalexin)[6,33]. GSH metabolism appears to be actively involved in protecting cancer cells from apoptosis and in mechanisms of multidrug and radiation resistance. In particular, increased levels of GSH within tumour cells have been associated with resistance to

platinum-containing anticancer compounds, anthracyclines and alkylating agents[23]. Thus, a therapeutic approach that modulates GSH levels in cancer cells could affect the efficacy of other anticancer therapies. Several approaches for blocking GSH synthesis in cancer cells have been attempted. Piperlongumine perturbs GSH/GSSG antioxidant activity then increasing intracellular ROS in tumour cells. Moreover piperlongumine failed to raise ROS levels in non-cancerous cells probably resulted from their lower levels of these antioxidants, exerting then a selective antitumor activity[34]. Similarly the L-Buthionine sulphoximine (BSO) treatment provokes glutathione (GSH) intracellular depletion, followed by an increase in ROS[35].

Because of the strong efficiency and selectivity of these 'oxidative stress inducing' compounds, to find molecules that associated with normal chemotherapeutic agents or by themselves exert a strong antitumoral citotoxity is the most important aim of several pharmaceutical enterprises[23].

2.2.2 AIM OF THE PROJECT

To increase the intracellular ROS levels could be an important strategy to selectively kill cancer cells. Cancer cells are characterized by higher levels of reactive oxidative species (ROS) compared to the normal counterpart. As such cancer cells are more vulnerable to damage by further ROS insults induced by exogenous agents. In this study we evaluated the antiproliferative effect of a series of new compounds which covalently combine two pharmacophores: the arylcinnamide skeleton and the α-bromoacryloyl moiety. The biological effects of various substituents on the *N*-phenyl ring of the benzamide portion were also described.

We evaluated the effects of α-bromoacryloylamido arylcinnamides **4a-r** on antiproliferative activity and tubulin polymerization *in vitro*. Furthermore we evaluated sensitivity of two of the most active compounds **4p** and **4r** in two multidrug-resistant cell lines, $Lovo^{Doxo}$ and $CEM^{Vbl\text{-}100}$) both expressing high levels of the P-gp. Since a high antitumoral activity was observed, we further monitored their effect on ROS intracellular homeostasis using two fluorescent probes 2',7'-dichlorodihydrofluorescein diacetate (H_2DCFDA) and hydroethidine (HE). Moreover we analysed if the phenylcynnamides could affect the intracellular GSH content.

2.2.3 RESULTS

Design, Synthesis and Biological Evaluation of Arylcinnamide Hybrid Derivatives as Novel Anticancer Agents

Romeo Romagnoli*[a], Pier Giovanni Baraldi*[a], Maria Kimatrai Salvador[a], Mariem Khayah[a], Delia Preti[a], Mojgan Aghazadeh Tabrizi[a], Ernest Hamel[b], Francesca Consolaro[c], Giuseppe Basso[c], Giampietro Viola*[c]

EUR J MED CHEM. 2014 Jun 23;81:394-407. doi: 10.1016/j.ejmech

2.2.3.1 ABSTRACT

The combination of two pharmacophores into a single molecule represents one of the methods that can be adopted for the synthesis of new anticancer molecules. A series of novel antiproliferative agents designed by pharmacophore hybridization approach, combining the arylcinnamide skeleton and a α-bromoacryloyl moiety, was synthesized and evaluated for its antiproliferative activity against a panel of seven human cancer cell lines.

The biological effects of various substituents on the *N*-phenyl ring of the benzamide portion were also described. In order to study the possible mechanism of action, we observed that **4p** slightly increased the Reactive Oxygen Species (ROS) production in HeLa cells, but more importantly a remarkable decrease of intracellular GSH content was detected in treated cells compared to controls. These results were confirmed by the observation that only thiol-containing antioxidants were able to significantly protect from induced cell death.

Keywords. Apoptosis, phenylcinnamides, Michael acceptor, *in vitro* antiproliferative activity, GSH depletion, oxidative stress.

2.2.3.2 INTRODUCTION

Molecular hybridization which covalently combines into a single molecule two different bioactive molecules with complementary pharmacophoric functions or with different mechanism of action is an effective tool to design highly active novel anticancer agents [1-9]. Antitumor activity of cinnamic acid derivatives was explored by many research group [10-17]. Several laboratories reported that the low molecular weight compounds, phenylcinnamide showed anticancer activity against various human cancer cell lines and in cell lines which are resistant to conventional antimitotics, expressing P-gp efflux pumps. Phenylcinnamide derivatives with general structure **1** (Chart 1), are a class of compounds initially identified by Hergenrother et al. as potential anticancer agents [18, 19], with a moderate cytotoxic activity (IC_{50} ranging from 1 to 10 μM). These compounds interact with microtubules by interfering with the dynamic of tubulin polymerization. By the screening of 100-membered library of amides, compound **1a** was identified as one of the most active derivatives, resulting moderately active against U-937 (lymphoma) and HeLa (cervical) cancer cells, with IC_{50} value of 3.0 and 11.3 μM, respectively. This derivative arrested the cell cycle growth at the G2/M phase and induced apoptotic cell death in HeLa cancer cell line. Since the 3,4,5-trimehoxyphenyl substitution was demonstrated to be the essential structural requirement for optimal biological activity in numerous tubulin inhibitors, the antiproliferative activity of **1a** was associated to the inhibition of tubulin polymerization, although it weakly binds to the colchicine site of tubulin. Increasing the bulk of the meta-substitution on the phenyl ring of the styryl portion, from methoxy to benzyloxy, to furnish derivative **1b**, allow to increase the antiprolferative activity relative to **1a**, with IC_{50} values of 1.8 and 2.1 μM, against U-937 and HeLa cells, respectively. Raffa et al. described a series of cinnamoyl anthranilates with general structure **2**, which inhibited the proliferation of human leukaemia K562 cells with IC_{50} values ranging from 0.57 to 5 μM [20]. COMPARE analysis, effects on tubulin polymerization and on cell cycle distribution indicated that these compounds act as antitubulin agents.

The compound α-bromoacrylic acid is an alkylating moiety with low chemical reactivity and devoid of cytotoxic effects (IC_{50}>120 μM on the murine leukaemia L1210 cells) [21]. The α-bromoacryloyl moiety is present in a series of potent anticancer distamycin-like minor groove binders, including PNU-166196 (brostallicin, **3**), which was evaluated as a

first-line single agent chemotherapy in patients with advanced or metastatic soft tissue sarcoma [22, 23]. It has been hypothesized that the reactivity of the α-bromoacryoyl moiety results from a first-step Michael-type nucleophilic attack, followed by a further reaction of the former vinylic bromo substituent alpha to the carbonyl, leading successively either to a second nucleophilic substitution or to a beta elimination [24].

Phenylcinnamids are characterized by the presence of a α,β-unsaturated carbonyl moiety, which can be considered as an Michael acceptor, an active pharmacophore often employed in the design of anticancer drugs [10,25]. Because of their ability to interact with cellular nucleophiles, Michael acceptors are often employed as a powerful tool in the design of anticancer agents [26, 27]. Combining two bioactive pharmacophores, corresponding to the phenylcinnamide skeleton and α -bromoacryoyl moiety, within a unique structure might exhibited synergic effects in anticancer activities. In a continuing study of hybrid compounds containing the α-bromoacryloyl moiety as potential anticancer drugs, we synthesized a novel series of hybrid compounds with general structure **4**, in which this moiety was linked to the arylcinnamide scaffold.

In particular, we have synthesized two different series of compounds, characterized by the α-bromoacryloyl moiety located at the *meta*- or *para*-position on the phenyl of the benzylidene fragment, corresponding to compounds **4a-p** and **4q-r**, respectively. The structure-activity relationship (SAR) was investigated by the insertion of different substitutions [both electron-releasing (CH_3, alkoxy, OCF_3, SCF_3, morpholin-4-yl) and electron-withdrawing (F and Cl) groups] at different positions on the phenyl ring of the benzamide portion.

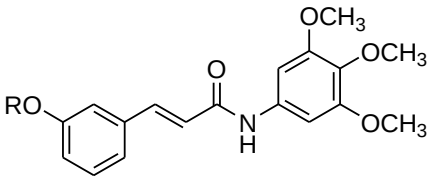

1a, R=CH_3
1b, R=$CH_2C_6H_5$

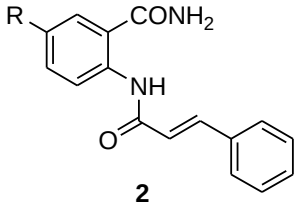

2

R=Cl, Br, I or CH_3.

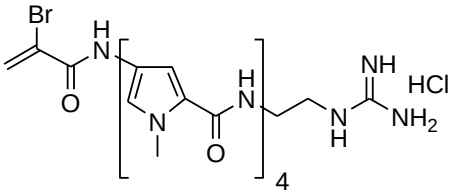

PNU-166196 or Brostallicin (**3**)

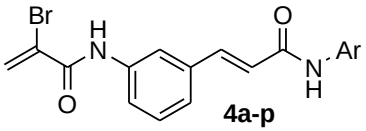

4a-p

4a, Ar=C_6H_5
4b, Ar=napht-1-yl
4c, Ar=4-F-C_6H_5
4d, Ar=3-F-C_6H_5
4e, Ar=3,4-F_2-C_6H_4
4f, Ar=4-Cl-C_6H_5
4g, Ar=4-CH_3-C_6H_5
4h, Ar=4-CH_3-$C_6H_4CH_2$
4i, Ar=4-OCH_3-C_6H_5
4j, Ar=4-OC_2H_5-C_6H_5
4k, Ar=4-OCF_3-C_6H_5
4l, Ar=4-SCF_3-C_6H_5
4m, Ar=3,4-$(OCH_3)_2$-C_6H_4
4n, Ar=3,5-$(OCH_3)_2$-C_6H_4
4o, Ar=3,4,5-$(OCH_3)_3$-C_6H_3
4p, Ar=4-(morpholin-4'-yl)-C_6H_5

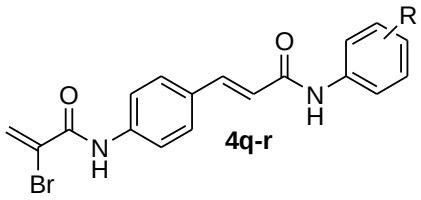

4q-r

4q, R=4-OCH_3
4r, R=3,4,5-$(OCH_3)_3$

Chart 1. Structure of phenylcinnamides **1a**, **1b** and **2**, brostallicin (**3**) and □-bromoacryloylamido arylcinnamides **4a-r**.

2.2.3.3 BIOLOGICAL RESULTS AND DISCUSSION

In vitro antiproliferative activities.

In Table 1, we report the antiproliferative effects of α-bromoacryloylamido arylcinnamides **4a-r** against the growth of human cervix carcinoma (HeLa), colorectal carcinoma (HT-29 and LoVo), lymphoblastic leukaemia (CEM, Jurkat and SEM) and breast carcinoma (MCF-7) cells, using the phenylcinnamides **1a** and **1b** as positive controls.

Table 1. In vitro cell growth inhibitory effects of compounds **1a-b**, **4a-r** and **7o**

Compound	IC_{50} [a](μM)						
	HeLa	HT-29	LoVo	CEM	Jurkat	SEM	MCF-7
4a	7.3±2.1	16.6±5.9	3.9±0.18	0.19±0.09	5.0±0.7	1.1±0.26	27.3±3.9
4b	1.4±0.1	6.5±0.6	1.16±0.11	1.8±0.44	0.68±0.22	0.83±0.25	2.8±0.5
4c	16.8±4.8	36.6±2.6	4.8±0.8	16.6±4.5	6.2±1.8	8.4±3.7	13.6±3.8
4d	1.2±0.4	4.6±0.4	1.0±0.2	26.0±4.1	1.0±0.3	0.62±0.31	3.3±0.5
4e	1.9±0.1	8.7±3.9	0.54±0.07	0.013±0.006	0.55±0.19	0.09±0.03	2.69±0.2
4f	2.8±0.3	7.9±1.0	5.9±1.0	0.46±0.02	2.6±0.16	1.19±0.45	11.0±1.3
4g	1.5±0.12	1.2±0.3	1.5±0.3	0.27±0.05	0.24±0.04	0.19±0.04	2.5±0.5
4h	1.7±0.4	2.7±0.3	1.9±0.3	0.55±0.13	0.74±0.17	1.3±0.2	2.2±0.8
4i	0.79±0.25	2.3±0.2	0.55±0.08	0.026±0.01	0.47±0.15	0.07±0.03	2.5±0.3
4j	2.0±0.13	3.4±0.3	0.85±0.03	0.098±0.033	0.93±0.12	0.18±0.04	5.5±1.0
4k	29.0±3.4	61.2±11.1	30.3±0.9	13.0±4.0	30.3±4.5	19.3±2.3	43.3±1.8
4l	19.0±3.2	39.8±2.8	29.3±2.2	15.3±2.5	30.1±2.1	12.7±2.6	30.1±1.4
4m	0.56±0.18	1.9±0.4	0.15±0.02	0.021±0.005	0.19±0.05	0.003±0.0004	2.8±0.4
4n	2.2±0.18	3.6±0.2	1.21±0.32	0.011±0.004	0.98±0.33	0.04±0.017	3.0±0.4
4o	0.88±0.19	2.3±0.5	0.14±0.04	0.059±0.025	0.29±0.03	0.018±0.003	1.8±0.3
4p	0.43±0.1	1.6±0.4	0.51±0.11	0.61±0.08	0.04±0.01	0.057±0.013	2.6±0.2
4q	1.6±0.3	3.1±0.3	0.06±0.01	0.022±0.005	1.4±0.47	0.08±0.03	3.0±0.2
4r	0.49±0.17	3.7±0.9	2.1±0.9	0.025±0.013	0.41±0.05	0.11±0.09	3.0±0.6
7o	53.1±4.6	63.1±6.5	45.2±5.6	40.9±13.6	43.3±4.8	2.81±2.8	55.4±11.1
1a	16.5±2.6	44.1±0.9	43.0±3.0	23.4±4.1	12.5±0.9	18.2±1.9	27.0±4.5
1b	2.2±0.39	3.6±0.2	21.7±5.0	17.3±6.0	3.5±0.5	8.5±2.3	2.4±0.8

[a]IC_{50}= compound concentration required to inhibit tumor cell proliferation by 50%. Data are expressed as the mean ± SE from the dose-response curves of at least three independent experiments*).*

Compound **1b**, with IC_{50}'s ranging from 2.2 to 21.7 μM, was 1.5- to 12-fold more potent than its methoxy counterpart **1a**. With only two exceptions (**4k** and **4l**), all the molecules that were generated by the hybridization of the α-bromoacryloyl moiety with the arylcinnamide system were more active than **1a**. For the benzyloxy derivative **1b**, its activity was lower than that of derivatives **4b**, **4e-j**, **4m-r** against the LoVo, CEM, Jurkat and SEM cells. Among the hybrid compounds, six of them (**4e**, **4i**, **4m-o** and **4q**) exhibited potent activity, with double-digit nanomolar IC_{50} values against both the CEM and SEM cell lines. The validity of the hybridization approach was confirmed comparing the potency of compound **4o** with that of the amino phenylcinnamide derivative **7o**. This latter compound was 30-700 fold less active than the corresponding α-bromoacryloylamido derivative **4o**, demonstrating that the presence of a α -bromoacryloyl moiety significantly enhanced antiproliferative activity.

With the exception of the CEM cells, compound **4b** bearing the more lipophilic 1-naphthyl moiety exerted a more pronounced antiproliferative activity toward cell lines tested in comparison with the unsustituted phenyl derivative **4a**.

The antiproliferative activities of the hybrid molecules were influenced by the substituents on the phenyl ring of the aniline/benzylamino moiety. A comparison of the *para*-position substitution on the phenyl ring demonstrated that ERGs such as methyl (**4g** and **4h**), methoxy (**4i**) or ethoxy (**4j**) and morpholin-4-yl (**4p**) increased antiproliferative activity compared with the unsubstituted benzene derivative **4a**, whereas trifluoromethoxy (OCF_3, **4k**) or trifluoromethylsulfanyl (SCF_3, **4l**) substituents produced a dramatic loss of potency.

Introduction of a weak electron-withdrawing group, a *para*-fluorine atom (**4c**), decreased the activity relative to **4a** on six cancer cell lines, the exception being the MCF-7 cells. Moving the fluorine from the *para*- (**4c**) to the *meta*-position (**4d**) enhanced antiproliferative activity 4-15 fold in six of the seven cell lines, the exception being the CEM cells. Antiproliferative activity increased 2-30 fold by increasing halogen size from fluorine to chlorine (**4f**). Relative to the activity of derivative **4c**, insertion of an additional fluorine atom at the *meta*-position to yield **4e** increased antiproliferative activity (4-1300 fold) against all cancer cell lines. By comparing the effect of substituents with opposite electronic properties at the *para*-position of phenyl ring, a 2-10 fold increase in potency

was observed by replacing the electron withdrawing chlorine atom (**4f**) with an electron-donating methyl group (**4g**). The cell growth inhibitory activities of *N*-4'-tolyl and *N*-4'-methylbenzyl derivatives **4g** and **4h**, respectively, were very similar against the HeLa, LoVo and MCF-7 cells, while **4h** had significantly reduced activity (from 2-7 fold) as compared with **4g** against the remaining cell lines. The antiproliferative activity of hybrid compounds can be further characterized in terms of the substitution pattern and the number of methoxy groups on the phenyl ring. The results show that mono-, di- or trimethoxy substitution on the 3', 4', and/or 5'-positions of the phenyl ring (compounds **4i**, **4m-o** and **4q-r**) were well tolerated and increased activity, usually substantially, as compared with the unsubstituted benzamide derivative **4a**. A single methoxy substituent on the *para*-position of the phenyl ring (compound **4i**) led to a 7-15 fold increase in antiproliferative activity relative to **4a**. Comparing **4i** with **4m**, an additional methoxy group at the *meta*-position had little effect on activity against HeLa, HT-29, CEM and MCF-7, but there were 2-, 3- and 20-fold increases in activity against the Jurkat, Lovo and SEM cells, respectively. The 3',4'-dimethoxy derivative **4m** was generally (6 out of 7 cell lines) more active than the isomeric 3',5'-dimethoxy analogue **4n.** Finally, adding a third methoxy group to produce the 3', 4', 5'-trimethoxyphenyl derivative **4o** caused a reduction in activity against five of the seven cancer cell lines.

Turning specifically to the *para*-substituted phenyl derivatives, replacing 4'-methoxy (**4i**) with the 4'-ethoxy homologue (compound **4j**) produced a 2-4 fold reduction in activity. This loss of activity became much more pronounced if the methoxy group was replaced with a bulkier trifluromethoxy (**4k**) or trifluoromethoxysulfanyl (**4l**) moiety. This activity loss cannot be explained simply as being caused by a steric effect of the substitution at the *para*-position of the phenyl ring because insertion of an electron poor heterocycle such as morpholin-4-yl (compound **4p**) enhanced antiproliferative activity 8-100 fold relative to **4a** with six of the seven cancer cell lines (the exception was the CEM cells). Changing the location of α -bromoacryloylamido moiety from the *meta*- in **4i** to the *para*-position in **4q** had little effect on activity, except in the LoVo cells. Similarly, there was little difference in activity between the two isomeric trimethoxyphenyl derivatives **4o** and **4r**, except in two cell lines (LoVo and SEM cells).

Evaluation of cytotoxicity in human peripheral mononuclear cells (PBMC).

To obtain more insights into the cytotoxic potential of these new compounds for normal human cells, two of the most active compounds (**4p** and **4r**) were assayed *in vitro* against human peripheral mononuclear cells (PBMC) obtained from healthy donors. As showed in Table 2, compounds **4r** and **4p** showed, in resting PBMC, a lesser degree of toxicity having an IC_{50} of about 3-5-4.0 μM that is roughly 10-100 fold lower respect to the lymphoblastic cell lines Jurkat and CEM. On the contrary they proved cytotoxic only for PHA-stimulated PBMC, suggesting that these compounds acts only in proliferating cells.

Table 2. Cytotoxicity of **4p** and **4r** for human peripheral blood mononuclear cells (PBMC)

Cell line	IC_{50} (μM) [a]	
	4p	**4r**
$PBMC_{resting}$ [b]	4.0±1.9	3.5±1.8
$PBMC_{PHA}$ [c]	0.50±0.27	0.24±0.12

[a] Compound concentration required to reduce cell growth inhibition by 50%.
[b] PBMC not stimulated with PHA.
[c] PBMC stimulated with PHA.
Values are the mean ± SEM for three separate experiments.

Effects of phenylcynnamides on drug-resistant cell lines

Drug resistance is an important therapeutic problem caused by the appearance of tumor cells endowed with differing mechanisms that confer resistance against a variety of anticancer drugs.[29, 30] Among the most common mechanisms of resistance are those related to the over-expression of a cellular membrane protein called P-gp that mediates the efflux of various structurally unrelated drugs.[29, 30] In this context, we evaluated sensitivity of two of the most active compounds **4p** and **4r** in two multidrug-resistant cell lines, one derived from a colon carcinoma ($Lovo^{Doxo}$) [31], the other derived from a T-cell leukaemia ($CEM^{Vbl\text{-}100}$) [32], both expressing high levels of P-gp. As shown in Table 3, compounds **4p** and **4r** were equally potent toward parental cells and cells resistant to

vinblastine or doxorubicin, suggesting that these compounds might be useful in the treatment of drug refractory tumors.

Table 3. In vitro cell growth inhibitory effects of compounds **4p** and **4r** on drug resistant cell lines.

Compd	IC_{50} [a] (μM)		
	LoVo	**LoVo^{Doxo}**	**Resistance ratio** [b]
4p	0.51±0.11	1.05± 0.44	2.0
4r	2.1 ± 0.9	1.37 ± 0.24	0.6
Doxorubicin	0.096 ± 0.043	11.3 ± 0.35	118
	CEM	**CEM ^{Vbl100}**	**Resistance ratio** [b]
4p	0.61 ± 0.08	0.41 ± 0.09	0.7
4r	0.025 ± 0.013	0.015 ± 0.005	0.6
Vinblastine	0.002 ± 0.0005	0.021 ± 0.008	105

[a] IC_{50}=compound concentration required to inhibit tumor cell proliferation by 50%. Data are presented as the mean ± SE from the dose-response curves of at least three independent experiments.

[b] The values express the ratio between IC_{50} determined in resistant and non-resistant cell lines.

In vitro inhibition of tubulin polymerization.

Previous studies have shown that compound **1a** most likely derived its antiproliferative activity from an interaction at the colchicine site of tubulin, causing inhibition of tubulin polymerization [19]. To investigate whether the antiproliferative activities of the most active hybrid compounds (**4e**, **4i**, **4m**, **4o**-**p**, **4r**) were related to an interaction with the microtubule system, these molecules were evaluated for their *in vitro* inhibition of the polymerization of purified tubulin [33]. All tested compounds did not inhibit tubulin assembly at concentrations as high as 20 μM, indicating that they were inactive as inhibitors of tubulin polymerization. To further evaluate if the new derivatives interfered with the microtubule network, we examined the effects of **4r** and **4p** on HeLa cells by immunofluorescence microscopy. Shown in Figure 1 (Panel A) is the normal microtubule network of untreated cells. Following 24 h of treatment with **4p** or **4r** at 2.5 or 5.0 μM (Figure 1, panels B-D), the microtubule network was not substantially modified in comparison with the untreated cells. Altogether these results were consistent with the

conclusion that the antiproliferative activity of these hybrid compounds was not derived from a direct interaction with tubulin and that it is unlikely that they act as microtubule binding agents.

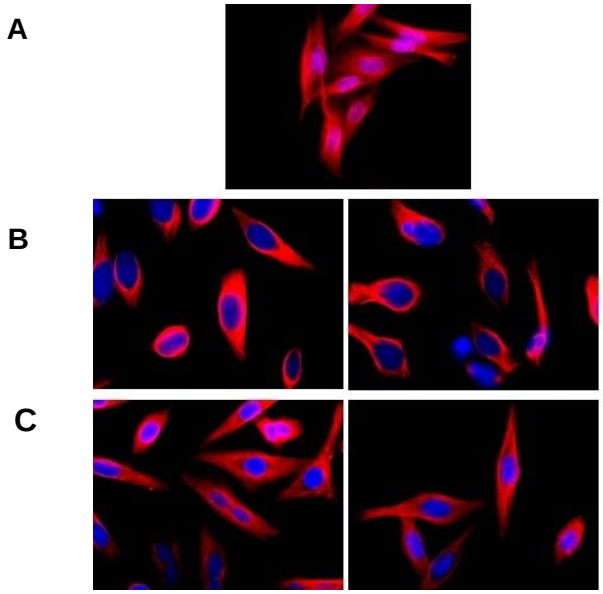

Figure 1. Effects of compounds **4p** (panels B and C) and **4r** (panels D and E) on microtubule networks in Hela cells. Panel A, untreated cells. Cells were incubated with 2.5 µM (panels B and D) or 5.0 µM (panels C and E) of the compounds for 24 h and then stained with anti-β-tubulin primary antibody and secondary Alexa-conjugated antibody and then observed by confocal microscopy (magnification 20x). Cells were also counterstained with DAPI to visualize the nuclei.

Analysis of cell cycle effects.

The effects of a 24 h treatment with different concentrations of **4r** and **4p** on cell cycle progression in HeLa cells were determined by flow cytometry (Figure 2, Panels A and B). The compounds caused a significant G2/M arrest in a concentration-dependent manner in the cell line tested, with a rise in G2/M cells occurring at a concentration as low as 2 µM. Importantly, the increase in G2/M phase cells was accompanied by a remarkable reduction in S phase cells for both compounds.

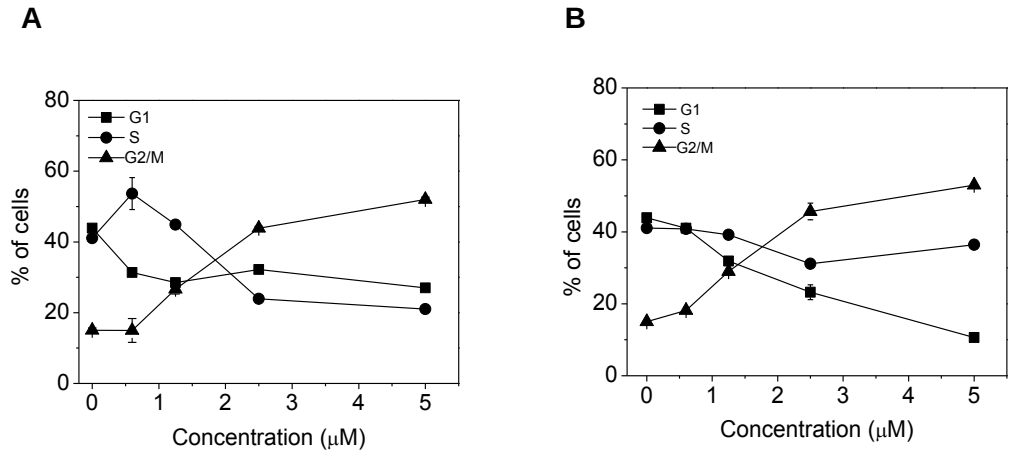

Figure 2. Percentage of cells in each phase of the cell cycle in HeLa cells treated with the **4r** (Panel A) and **4p** (Panel B) at the indicated concentrations for 24 h. Cells were fixed and labeled with PI and analyzed by flow cytometry as described in the experimental section.

Phenylcynnamides induce apoptosis in Hela cells

To characterize the mode of cell death induced by **4r** and **4p**, a biparametric cytofluorimetric analysis was performed using PI, which stains DNA and enters only dead cells, and fluorescent immunolabeling of the protein annexin-V, which binds to phosphatidylserine in a highly selective manner [34]. Dual staining for annexin-V and with PI permits discrimination between live cells (annexin-V^-/PI^-), early apoptotic cells (annexin-V^+/PI^-), late apoptotic cells (annexin-V^+/PI^+) and necrotic cells (annexin-V^-/PI^+). As shown in Figure 3 (Panels A and B), Hela cells treated with the two compounds for 24 h showed an accumulation of annexin-V positive cells that further increased after 48 h in comparison with the untreated cells.

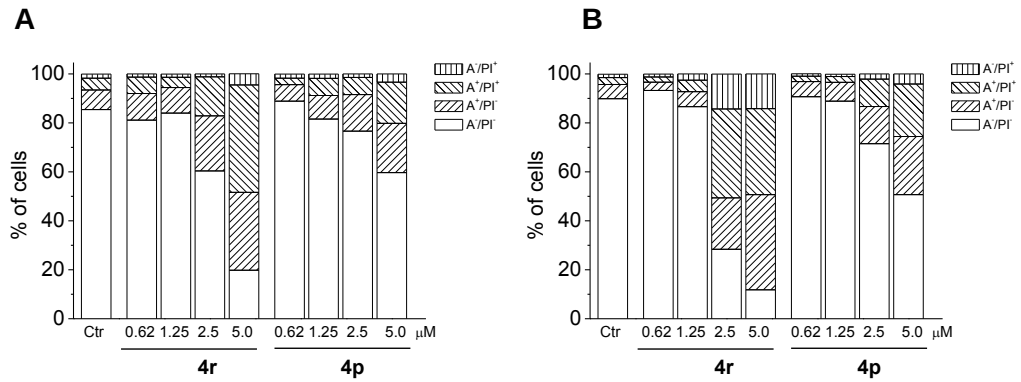

Figure 3. Flow cytometric analysis of apoptotic cells after treatment of HeLa cells with **4r** (Panel A) or **4p** (Panel B) at the indicated concentrations after incubation for 24 or 48 h. The cells were harvested and labeled with annexin-V-FITC and PI and analyzed by flow cytometry. Data are represented as means of three independent experiments. For the sake of clarity, error bars were omitted.

Phenylcynnamides induce caspase-dependent cell death

To evaluate if the apoptotic cell death induced by **4p** and **4r** is caspase-dependent, Hela cells were treated with the two compounds in the absence or presence of the pan-caspase inhibitor z-VAD.fmk. As shown in Figure 4 (panel A), the inhibition of caspases significantly increased cell viability suggesting a caspase-dependent process of cell death. To determine which caspases were involved in phenylcinnammide-induced cell death, the expression of caspases was evaluated by immunoblot analysis. We observed an activation, in a time- and concentration-dependent manner, of the effector caspase-3 and cleavage of its substrate PARP (Figure 4, panel B). Interestingly, the two compounds did not induce activation of caspase-9, the major initiator caspase of the mitochondrial apoptotic pathway (Figure 4, panel B). Indeed a clear activation of caspase-8 was observed for both compounds, suggesting that the induced apoptosis followed the extrinsic pathway.

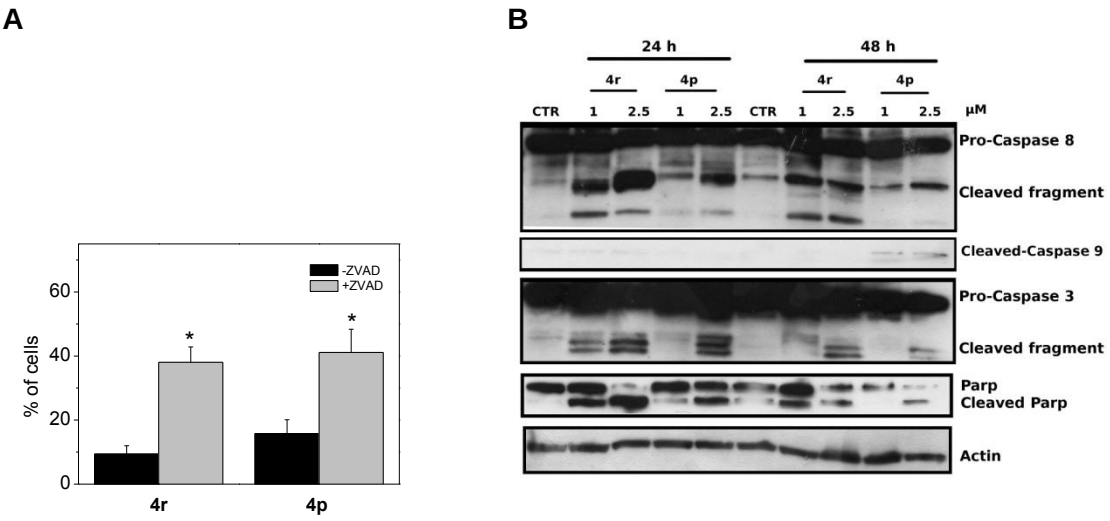

Figure 4. (A). Percentage of cell viability after a 48 h incubation of HeLa cells with **4r** or **4p** (2.5 μM) in the presence or in the absence of z-VAD.fmk (100 μM). Means ± SEM of three independent experiments. **P<0.01 *vs*. **4p** or **4r** treated cells. (B). Western blot analysis of caspase-3, cleaved caspase-9, caspase-8 and PARP after treatment of HeLa cells with **4r** or **4p** at the indicated concentrations and for the indicated times. To confirm equal protein loading, each membrane was stripped and reprobed with anti-β-actin antibody

Phenylcynnamides induce downregulation of Bcl-2 family proteins and DNA damage

To further study the mechanism of apoptosis induction by phenylcinnamides, we evaluated the expression of proteins of the Bcl-2 family. As shown in Figure 5, the anti-apoptotic protein Bcl-2 was decreased by treatment with **4r** in a time dependent manner. Also **4p** produced similar effects, but they were more evident after 48 h of treatment. The expression of another anti-apoptotic protein, Mcl-1, was decreased by both compounds at 2.5 μM, especially at 48 h. In contrast, two pro-apoptotic proteins of the Bcl-2 family, Bak and Bax, remained practically unchanged after treatment. Of particular interest was the nearly complete disappearance of Bid expression after treatment with either compounds an effect that is clearly evident after only a 24 h treatment at the lowest concentration used. Bid is a pro-apoptotic member of the Bcl-2 family, and many studies have demonstrated that, following apoptotic stimuli, activation of caspase-8 induces cleavage of Bid [35, 36].

We also investigated whether **4r** and **4p** induced DNA damage by examining the expression of phosphorylated histone H2AX at Ser139 (γH2A.X). γH2A.X phosphorylation occurs shortly after DNA double strand break (DSB) induction, thus

identifying γH2A.X as an early sensitive indicator of DSBs, whether induced by ionizing radiation, oxidative stress or chemical agents [37]. As shown in Figure 5 (panel B), after a 24 h treatment **4r** induced γH2A.X expression, while **4p** induced this effect only after 48 h. These findings show that both compounds induce DNA damage. Bid is also involved in promoting apoptosis following DNA damage and contributes to induction of a cell cycle arrest [38]. Thus, our findings that phenylcinnamides induce DNA damage along with strong activation of Bid could explain the arrest of the cell cycle observed after treatment of cells with these compounds.

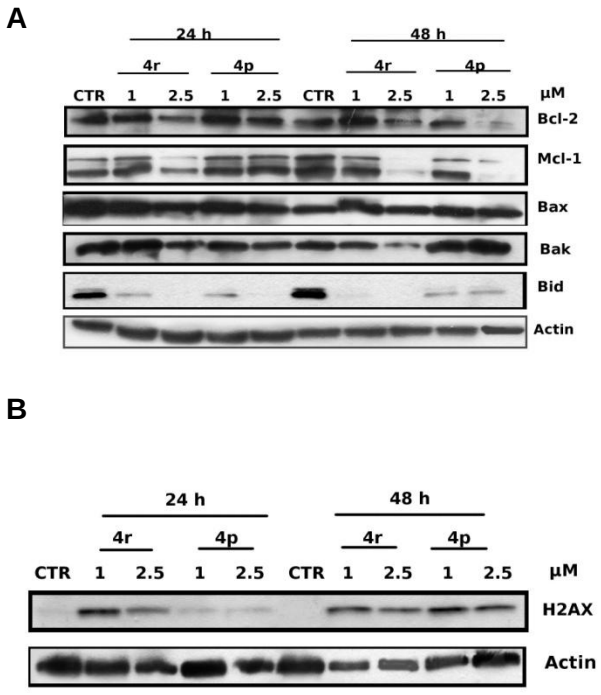

Figure 5. Western blot analysis of Bcl-2, Bax, Bak, Mcl-1and Bid (Panel A), and γH2A.X (panel B) after treatment of Hela cells with **4p** and **4r** at the indicated concentrations and for the indicated times. To confirm equal protein loading, each membrane was stripped and reprobed with anti-β-actin antibody.

Phenyl cynnamides induce ROS production

To better understand the mechanism of action of **4r**, we analyzed ROS production. HeLa cells were treated for different times and with different concentrations of **4r**, and the level of intracellular ROS were monitored using two fluorescent probes, 2',7'-dichlorodihydrofluorescein diacetate (H_2DCFDA) and hydroethidine (HE) [39]. As shown in Figure 6 (panel A), flow cytometric analysis showed an early but modest increase (1-6 h) in the H_2DCFDA-positive cells, and this occurred in a concentration-dependent manner.

Using HE, which mainly detects superoxide anion [40], we did not detect any increase in fluorescence emission (data not shown), suggesting that superoxide anion does not play a major role. In addition, a time-course study was performed, in which the mitochondrial potential was monitored by flow cytometry with the fluorescent probe 5,5',6,6'-tetrachlo-1,1',3,3'-tetraethylbenzimidazol-carbocyanine (JC-1) (Figure 6, panel B). We found significant mitochondrial depolarization beginning after a 12 h treatment with **4r**. Since the mitochondrial membrane depolarization has been associated with mitochondrial production of ROS [41,42], these findings suggest that ROS, detected by H_2DCFDA prior to the onset of apoptosis, were not produced as a consequence of mitochondrial damage.

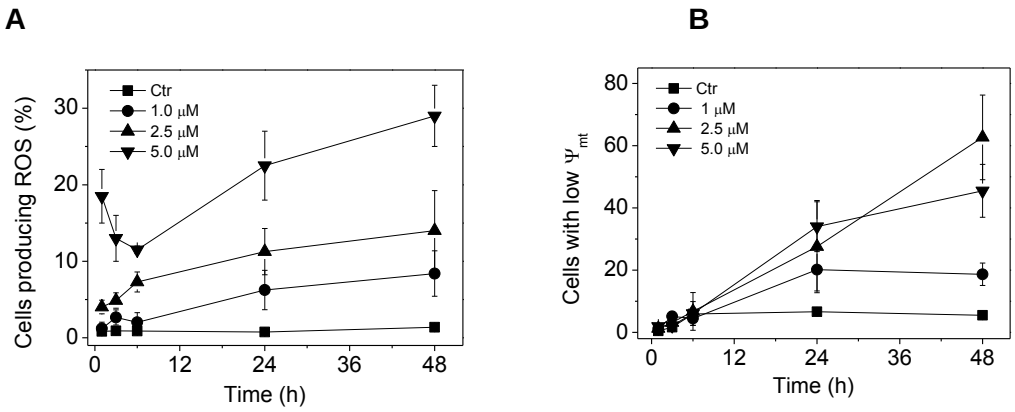

Figure 6. Production of ROS (Panel A) and assessment of mitochondrial membrane potential ($\Delta\psi_{mt}$) (Panel B) following treatment of HeLa cells with compound **4r** at the indicated concentrations. A. Cells were stained with H_2DCFDA at the indicated times and analyzed by flow cytometry to measure production of ROS. B. The change in $\Delta\psi_{mt}$ was measured by flow cytometry using JC-1 at the indicated times.

More importantly, to prove that ROS are involved in the mechanism of cell death of compounds **4p** and **4r** we analyzed cell viability in the presence of different antioxidants, including tocopherol acetate (TOC), 2,6-di-tert-butylhydroxyanisole (BHA), *N*-acetylcysteine (NAC), reduced glutathione (GSH) and dithiothreitol (DTT). Surprisingly, as shown in Figure 7 (panels A and B), only the thiol-containing scavengers (NAC, GSH and DTT) significantly increased cell viability. This suggests that ROS do not play a major role in the antiproliferative effects observed with **4p** and **4r**.

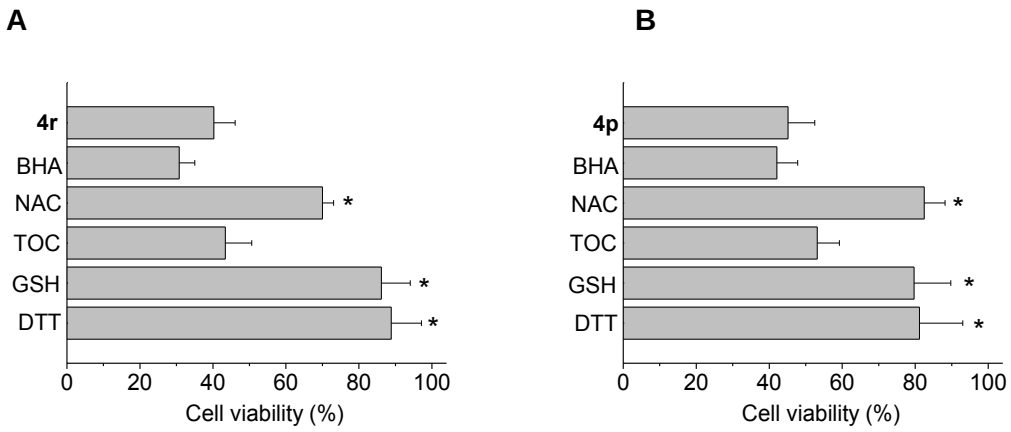

Figure 7. Effect of ROS scavengers on cell death induced by compounds **4r** and **4p.** HeLa cells were treated with the two compounds at 2.5 µM for 48 h in the presence of BHA (10 µM) TOC (100 µM) NAC (100 µM), GSH (1 mM) or DTT (1 mM). Cell viability was measured by the MTT assay. Data are represented as means ± S.E.M. for four independent experiments. *p<0.01 vs compound alone.

Phenyl cynnamides induce GSH depletion

Since only thiol containing scavengers protect from cellular death induced by phenylcinnamides, we determined whether these compounds caused a decrease in intracellular GSH content. Therefore, we analyzed HeLa cells for changes in their GSH levels using the fluorescent probe 5-chloromethylfluorescein diacetate (CMFDA) and flow cytometry. CMFDA is a membrane permeable dye used for determining intracellular levels of GSH [43]. As shown in Figure 8 (Panels A and B), 24 h incubations with either **4p** or **4r**, concentration-dependent manners, substantially reduced CMFDA fluorescence, indicating GSH depletion. Moreover, the effect was significantly counteracted by addition of NAC to the culture medium GSH is the most abundant thiol in mammalian cells and is involved in many cellular processes, including antioxidant defense, drug detoxification, cell signaling, and cell proliferation [43, 45]. Intracellular GSH loss is an early feature in the progression of cell death in response to different apoptotic stimuli and, because of its action as a primary intracellular antioxidant in the cells, a reduction in intracellular GSH content is generally believed to reflect generation of ROS [46]. Nevertheless, our findings suggest that phenylcinnamides induce apoptosis in HeLa cells by directly interacting with GSH or other intracellular thiols independently of ROS generation. In this context, we speculate that a possible mechanism of action of phenylcinnamides results from the

reactivity of the α-bromoacryoyl moiety and its forming an irreversible adduct with GSH through a Michael-type nucleophilic attack. This would readily lead to depletion of intracellular thiols [47].

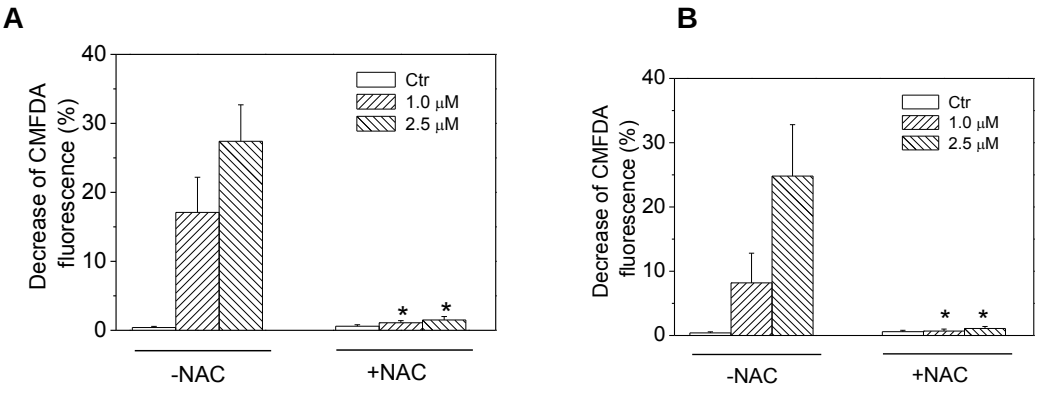

Figure 8. Compounds **4p** (panel A) and **4r** (panel B) induced GSH depletion in HeLa cells. Cells were treated with the indicated concentration of **4p** or **4r** and 100 μM NAC, as indicated. After 24 h incubations, the cells were stained with the fluorescent probe CMFDA and analyzed by flow cytometry. Data represent means ± S.E.M. of three independent experiments. *$p<0.01$ vs compound alone.

2.2.3.4 CONCLUSIONS

The observation that the α,β-unsaturated carbonyl system of phenylcinnamide and the α-bromoacryloyl group are capable of undergoing Michael addition and thus can act as trapping agents of cellular nucleophiles led us to prepare and evaluate a series of α-bromoacryloylamido arylcinnamide derivatives with general structure **4**. These compounds incorporate the two moieties within their structures. We found that most of the new hybrid compounds displayed high antiproliferative activity towards a panel of seven cancer cell lines, with one-digit micromolar to double-digit nanomolar IC_{50} values. The new derivatives had antiproliferative activity that was significantly greater than that of the two parent compounds **1a** and **1b** against six of the seven cancer cell lines. The least active compounds were derivatives with fluorine (**4c**), trifluoromethoxy (**4k**) and trifluoromethylsulfanyl (**4l**) at the *para*-position of the phenyl ring. A positive effect was observed by the replacement of phenyl with 1-naphthyl (compounds **4a** and **4b**,

respectively), with **4b** having IC_{50} values of 0.68-6.5 μM as compared with 0.19-27.3 μM for **4a**. Comparing the activity of hybrid compound **4o** with that of the corresponding amino phenylcinnamide **7o**, the latter showed weak or no antiproliferative activity (IC_{50}=2.81-63.1 μM) against the panel of cancer cell lines, and the insertion of the μ-bromoacryloyl moiety was an important molecular change, leading to a significant increase in potency (IC_{50}=0.018-2.3 μM for **4o**).

Preliminary mechanism of action studies demonstrated that the most potent hybrid compounds did not inhibit tubulin polymerization, but their activity seems to be related to depletion of intracellular GSH. Studies are underway to determine the precise molecular mechanism that leads to the decrease in intracellular GSH levels. Whether this occur through a direct chemical reaction or through interfering with the enzymatic synthesis of GSH remains to be determined. Understanding the precise mechanism may result in development of new cancer therapeutic strategies and possibly new drugs using phenylcinnamides as a lead chemotype.

2.2.3.5 MATERIAL AND METHODS

Human T-cell leukaemia (Jurkat and CEM) and acute B-cell lymphoblastic leukaemia (SEM) cells were grown in RPMI-1640 medium, (Gibco Milano Italy). Human cervix carcinoma (HeLa), breast adenocarcinoma (MCF-7) and colon adenocarcinoma (HT-29 and LoVo) cells were grown in DMEM medium (Gibco, Milano, Italy). Both media were supplemented with 115 units/mL of penicillin G (Gibco, Milano, Italy), 115 μg/mL streptomycin (Invitrogen, Milano, Italy) and 10% fetal bovine serum (Invitrogen, Milano, Italy). $CEM^{Vbl\text{-}100}$ cells are a multidrug-resistant line selected against vinblastine [32] and were grown in complete RPMI 1640 medium supplemented with vinblastine 100 ng/ml. $LoVo^{Doxo}$ cells are a doxorubicin resistant subclone of LoVo cells [33] and were grown in complete Ham's F12 medium supplemented with doxorubicin (0.1 μg/mL). Individual wells of a 96-well tissue culture microtiter plate were inoculated with 100 μL of complete medium containing 8 x 10^3 cells. The plates were incubated at 37 °C in a humidified 5% CO_2 incubator for 18 h prior to the experiments. Stock solutions (10 mM) of the different compounds were obtained by dissolving them in DMSO. After medium removal, 100 μL

of the drug solution, dissolved in complete medium at different concentrations, was added to each well and incubated at 37 °C for 72 h. The percentage of DMSO in the medium never exceeded 0.25%. This was also the maximum DMSO concentration in all cell-based assays described below. Cell viability was measured by the (3-(4,5-dimethylthiazol-2-yl)-2,5-diphenyl tetrazolium bromide (MTT) assay as previously described [48]. The IC_{50} was defined as the compound concentration required to inhibit cell proliferation by 50%. Some experiments were performed in the presence of different scavengers, such as BHA, GSH, TOC, DTT or NAC, all purchased from Sigma-Aldrich (Milano, Italy).

Cell growth inhibitory activity in peripheral blodd mononuclear cells (PBMC)

PBMC from healthy donors were obtained by separation on Lymphoprep (Fresenius KABI Norge AS) gradient. After extensive washing, cells were resuspended (1.0×10^6 cells/mL) in RPMI-1640 with 10% fetal bovine serum and incubated overnight. For cytotoxicity evaluations in proliferating PBL cultures, non-adherent cells were resuspended at 5×10^5 cells/mL in growth medium, containing 2.5 μg/mL PHA (Irvine Scientific). Different concentrations of the test compounds were added, and viability was determined 72 h later by the MTT test. For cytotoxicity evaluations in resting PBMC cultures, non-adherent cells were resuspended (5×10^5 cells/mL) and treated for 72 h with the test compounds, as described above.

Effects on tubulin polymerization and on colchicine binding to tubulin.

Bovine brain tubulin was purified as described previously [33]. To evaluate the effect of the compounds on tubulin assembly *in vitro* [49], varying concentrations were preincubated with 10 μM tubulin in glutamate buffer at 30 ˚C and then cooled to 0 ˚C. After addition of GTP, the mixtures were transferred to 0 °C cuvettes in a recording spectrophotometer and warmed to 30 °C, and the assembly of tubulin was observed turbidimetrically.

Immunofluorescence analysis.

Cells were fixed in cold 4% formaldehyde for 15 min, rinsed and stored prior to analysis. Primary antibody staining was performed for β-tubulin (mouse, monoclonal 1:1000, Sigma-Aldrich, Milano, Italy). After incubation, cells were washed and incubated with an Alexa conjugated secondary antibody (1:2000, Life Technologies, Monza, Italy). Cells were counterstained with 4',6-diamidin-2-phenylindole (DAPI) (1:10000, Sigma-Aldrich, Milano, Italy). Images were obtained on a video-confocal microscope (Vico, Eclipse Ti80, Nikon), equipped with a digital camera.

Annexin-V assay.

Surface exposure of phosphatidylserine on apoptotic cells was measured by flow cytometry with a Coulter Cytomics FC500 (Beckman Coulter) by adding Annexin-V-FITC to cells according to the manufacturer's instructions (Annexin-V Fluos, Roche Diagnostic). Simultaneously the cells were stained with PI. Excitation was set at 488 nm, and the emission filters were set at 525 nm and 585 nm for FITC and DAPI, respectively.

Flow cytometric analysis of cell cycle distribution.

For flow cytometric analysis of DNA content, 2.5 x 10^5 Hela cells in exponential growth were treated with different concentrations of the test compounds for 24 and 48 h. After an incubation period, the cells were collected, centrifuged and fixed with ice-cold ethanol (70%). The cells were then treated with lysis buffer containing RNAse A and 0.1% Triton X-100, and then stained with PI. Samples were analyzed on a Cytomic FC500 flow cytometer (Beckman Coulter). DNA histograms were analyzed using MultiCycle for Windows (Phoenix Flow Systems).

Assessment of mitochondrial changes and ROS production.

The mitochondrial membrane potential was measured with the lipophilic cation JC-1 (Molecular Probes, Eugene, OR, USA), while the production of ROS was followed by flow cytometry using the fluorescent dyes HE (Molecular Probes) and H_2DCFDA (Molecular Probes), as previously described[50].

Detection of the intracellular GSH content.

Cellular GSH levels were analyzed using CMFDA (Molecular Probes) [42]. Cells were treated with the test compound for different times. Cells were harvested, centrifuged and incubated in the presence of a solution of 5 µM CMFDA at 37 °C for 30 min. Cytoplasmic esterases convert non-fluorescent CMFDA to fluorescent 6-chloromethylfluorescein, which can then react with GSH. Fluorescence intensity was determined by flow cytometry.

Western blot analysis.

Aliquots of HeLa cell cultures, both control and containing the desired compounds at the indicated concentrations, were removed at time points as indicated. The cells were collected by centrifugation and washed twice with phosphate-buffered saline chilled to 0 °C. The cells were then suspended in a lysis buffer at 0 °C for 30 min. The resulting suspensions were clarified by centrifugation (15000 x g, 4 °C, 10 min) and the protein concentrations of the supernatants determined with the BCA protein kit (Pierce, Italy). Protein aliquots of 20 µg were subjected to sodium-dodecyl sulphate-polyacrylamide gel electrophoresis using 7.5-15% gradient polyacrylamide gels. Proteins were then electroblotted to PVDF Hybond-p memberanes from GE Healthcare, Milano, Italy. The membranes were then treated with ECL Blocking Agent from GE Healthcare, using a rotary shaker at 4 °C, as instructed by the manufacturer. Membranes were next incubated for 2 h at room temperature with a variety of primary antibodies from Cell Signaling, Alexis, Upstate, and Sigma-Aldrich, as indicated in the individual experiments. Finally, membranes were incubated with peroxidase-labeled secondary antibodies for 60 min. All membranes were visualized using ECL Select (GE Healthcare) and exposed to Hyperfilm MP (GE Healthcare). To ensure equal protein loading, each membrane was stripped and reprobed with an anti-β-actin antibody.

Statistical analysis.

Statistical significance of differences between means of control and treated samples were calculated using Student's *t*-test. *P* values < of 0.05 were considered significant.

2.2.3.6 REFERENCES

[1] C.V. Junior, A. Danuello, V.d.S. Bolzani, E.J. Barreiro, C.A.M. Fraga, Curr. Med. Chem. 14 (2007) 1829-1852.

[2] L.K. Gediya, V.C. Njar, Expert Opin. Drug Discov. 4 (2009) 1099-1111.

[3] Y.-C. Duan, Y.-C. Zheng, X.-C. Li, M.-M. Wang, X.-W. Ye, Y.-Y. Guan, G.-Z. Liu, J.-X. Zheng, H.-M. Liu. Eur. J. Med. Chem. 64 (2013) 99-110.

[4] M. Decker. Curr. Med. Chem. 18 (2011) 1464-1475.

[5] S. B. Tsogoeva. Mini-Rev. Med. Chem. 10 (2010) 773-793.

[6] B. Meunier. Acc. Chem. Res. 41 (2008) 69-77.

[7] F. W. Muregi, P. G. Kirira, A. Ishih. Curr. Med. Chem. 18 (2011) 113-143.

[8] Y. C. Mayur, G. J. Peters, V. V. Prasad, C. Lemo, N. K. Sathish. Curr. Cancer Drug Targets 9 (2009) 298-306.

[9] V. R. Solomon, C. Hu, H. Lee. Bioorg. Med. Chem. 18 (2010) 1563-1572.

[10] H. B. Zou, S. Y. Dong, C. X. Zhou, L. H. Hu, Y. H. Wu, H. B. Li, J. X. Gong, L. L. Sun, X. M. Wu, H. Bai, B. T. Fan, X. J. Hao, J. Stöckigt, Y. Zhao. Bioorg. Med. Chem. 14 (2006) 2060-2071.

[11] Y. Qian, H.-J. Zhang, H. Zhang, C. Xu, J. Zhao, H.-L. Zhu. Bioorg. Med. Chem. 18 (2010) 4991-4996.

[12] S. Dallavalle, R. Cincinelli, R. Nannei, L. Merlini, G. Morini, S. Penco, C. Pisano, L. Vesci, M. Barbarino, V. Zuco, M. D. Cesare, F. Zunino, Eur. J. Med. Chem. 44 (2009), 1900-1912.

[13] H. Zou, H. Wu, X. Zhang, Y. Zhao, J. Stöckigt, Y. Lou, Y. Yu. Bioorg. Med. Chem. 18 (2010) 6351-6359.

[14] Y. Luo, K.-M. Qiu, X. Lu, K. Liu, J. Fu, H.-L. Zhu. Bioorg. Med. Chem. 19 (2011) 4730-4738.

[15] N. Meydan, T. Grunberger, H. Dadi, M. Shahar, E. Arpaia, Z. Lapidot, J. S. Leeder, M. Freedman, A. Cohen, A. Gazit, A. Levitzki, C. M. Roifman. Nature 379 (1996) 645-648.

[16] D.-S. Shin, J. Kim, D. C. Han, K. H. Son, C. W. Lee, H.-M. Kim, S. H. Hong, B.-M. Kwon. Bioorg. Med. Chem. Lett. 17 (2007) 5423-5427.

[17] N.-H. Nam, Y.-J. You, Y. Kim, D.-H. Hong, H.-M. Kim, B. Z. Han. Bioorg. Med. Chem. Lett. 11 (2001) 1173-1176.

[18] R. S. Dothager, K. S. Putt, B. J. Allen, B. J. Leslie, V. Nesterenko, P. J. Hergenrother. J. Am. Chem. Soc. 127 (2005) 8686-8696.

[19] B.J. Leslie, C.R. Holaday, T. Nguyen, P.J. Hergenrother, J. Med. Chem. 53 (2010) 3964-3972.

[20] D. Raffa, B. Maggio, F. Plescia, S. Cascioferro, S. Plescia, M. V. Raimondi, G. Daidone, M. Tolomeo, S. Grimaudo, A. Di Cristina, R. M. Pipitone, R. Bai, E. Hamel. Eur. J. Med. Chem. 46 (2011) 2786-2796.

[21] S. Marchini, M. Broggini, C. Sessa, M. D'Incalci. Expert Opin. Invest. Drugs 10 (2001) 1703-1714.

[22] D. Lorusso, S. Mainenti, A. Pietragalla, G. Ferrandina, G. Foco, V. Masciullo, G. Scambia. Expert Opin. Invest. Drugs 18 (2009**)** 1939-1946.

[23] M. Leahy, I. Ray-Coquard, J. Verwei, A. Le Cesne, F. Duffaud, P. C. Hogendoorn, C. Fowst, C. De Balincourt, E. D. Di Paola, M. Van Glabbeke, I. Judson, J. Y. Blay. Eur. J. Cancer 43 (2007) 308-315.

[24] R. Romagnoli, P. G. Baraldi, O. Cruz-Lopez, C. Lopez-Cara, D. Preti. Mini-Rev. Med. Chem. 9 (2009) 81-94.

[25] B. Ahn, S. Sok. Curr. Pharm. Des. 2 (1996), 247-262.

[26] U. Das, R. K. Sharma, J. R. Dimmock. Curr. Med. Chem. 16 (2009) 2001-2020.

[27] H. N. Pati, U. Das, M. Kawase, H. Sakagami, J. Balzarini, E. De Clercq, J. R. Dimmock. Bioorg. Med. Chem. 16 (2008) 5747-5753.

[28] S. Vishnoi, V. Agrawl, V. K. Kasana. J. Agric. Food. Chem. 57 (2009), 3261-3265.

[29] G. Szakács, J. K. Paterson, J. A Ludwig, C. Booth-Genthe, M. M. Gottesman. Nat. Rev. Drug

[30] B. C. Baguley. Mol. Biotechnol. 46 (2010), 308-316.

[31] S Toffoli, G. Viel, A. Tuimoto, I. Bisconti, G. Rossi, G. Baoiocchi. Br. J. Cancer 63 (1991), 51-56.

[32] M. Dupuis, M. Flego, A. Molinari, M. Cianfruglia. HIV Medicine 4 (2003), 338-345.

[33] E. Hamel, C. M. Lin. Biochemistry 23 (1984) 4173-4184.

[34] I. Vermes, C. Haanen, H. Steffens-Nakken, C. Reutelingsperger, J. Immunol. Methods 184 (1995**)**, 39-51.

[35] H. Li, H. Zhou, C. Xu, J. Yua. Cell 94, (1998), 491-501.

[36] C. Kantari, H. Walczak. Biochim. Biophys. Acta 1813 (2011) 558-563.

[37] O. Fernandez-Capetillo, A. Lee, M. Nussenzweig, A. Nussenzweig. DNA Repair 3 (2004**)**, 959-967.

[38] a) I. Kamer, R. Sarig, Y. Zaltsman, H. Niv, G. Oberkovitz, L. Regev. G. Haimovich , Y. Lerenthal, R. C. Marcellus, A. Gross. Cell 122 (2005), 593-603. b) S. S. Zinkel, K. E. Hurov, C. Ong, F. M. Abtahi, A. Gross, S. J. Korsmeyer. Cell 122 (2005) 579-591.

[39] G. Rothe, G. Valet. J. Leukocyte Biol. 47 (1990) 440-448.

[40] A. Cossarizza. R. Ferraresi, L. Troiano, E. Roat, L. Gibellini, L. Bertoncelli, M. Nasi, M. Pinti. Nature protocols 4 (2009)**,** 1790-1797.

[41] J. Cai, D. P. Jones. J. Biol. Chem. 273 (1998), 11401-11404.

[42] H. Nohl, L. Gille, K. Staniek. Biochem. Pharmacol. 69 (2005), 719-723.

[43] D. W Hedley, S. Chow. Cytometry 15 (1994)**,** 349-358.

[44] M. L. Circu, Aw, T. Y. Free Radic. Res. 42 (2008), 689-706.

[45] S. C. Lu. Mol. Aspects Med. 30 (2009), 42-59.

[46] B. Zucker, J. Hanusch, G. Bauer. Cell Death Differ. 4 (1997), 388-395.

[47] I. Beria, P. G. Baraldi, P. Cozzi, M. Caldarelli, C. Geroni, S. Marchini, N. Mongelli, R. Romagnoli. J. Med. Chem. 47 (2004), 2611-2623.

[48] R. Romagnoli, P. G. Baraldi, A. Brancale, A. Ricci, E. Hamel, R. Bortolozzi, G. Basso, G. Viola. J. Med. Chem. 54 (2011), 5144-5153.

[49] E. Hamel. Cell Biochem. Biophys. 38 (2003) 1-21.

[50] G. Viola, R. Bortolozzi, M. G. Ferlin, P. Brun, I. Castagliuolo, S. Moro, E. Hamel, G. Basso G. Biochem. Pharm. 83 (2012), 16-26.

2.3 CONCLUSIONS

Two classes of antitumoral agents were synthesized with the aim to selectively target cancer cells at low concentration efficacy. More specifically each series of compounds targeted the unique biochemical alterations which distinguish cancer cells from normal cells: unscheduled proliferation and higher levels of intracellular ROS.

Compounds with general formula **3** included the 1-(3',4',5'-trimethoxtbenzoyl)-3-arylamino-5-amino-1,2,4-triazole molecular skeleton and acted as tubulin polimerization inhibitors, colchicine site binders. Compound **3c**, bearing a *p*-toluidino moiety at the C-3 position of 1,2,4-triazole ring, its *p*-ethyl homologue **3f** and the *m,p*-dimethyl analogue **3e** exhibited the greatest antiproliferative activity among the tested compounds. These results were superior or comparable with those of the reference compound CA-4 against all cancer cell lines. Compound **3c** was the most potent inhibitor of tubulin polymerization and of colchicine binding (IC_{50}=0.75 μM for assembly, 92% inhibition of the binding of 5 μM colchicine), and the antiproliferative activity of **3c**, in terms of $IC_{50's}$, ranged from 0.21 to 3.2 nM in the seven cell tumor lines examined. In addition, **3c** showed low toxicity in non tumoral cells (peripheral blood lymphocytes from healthy donors) and was active also in drug-resistant cell lines ($LoVo^{Doxo}$, CEM^{Vbl100}). Although **3c** was almost twice as active as CA-4 as an inhibitor of tubulin polymerization, these two compounds showed similar activity as inhibitors of colchicine binding. Furthermore immunostaining analysis performed in Hela cells showed that the antiproliferative activity of **3c** compound resulted from its capability to interfere with microtubule assembly. In addition the compound **3c** caused a significant G2/M arrest in a concentration-dependent and it induced caspase-dependent apoptosis and late DNA damage and p53 induction. Interestingly compound **3c**, efficiently targeted endothelial cells, acting as a VDA. In fact after a 1 h incubation, **3c** visibly disrupted the network of HUVECs, as compared with the control. Furthermore results also indicated that the effects on endothelial cells induced by **3c** were similar to those observed after CA-4 treatment carried out by our group. More importantly, *in vivo* experiments showed that this compound was able to significantly reduce the growth of a syngenic tumor model in mice, indicating that it is a very promising anticancer compound that warrants further evaluation for its potential clinical use.

Cancer cells are also characterized by altered metabolic activity which provokes increased levels of intracellular oxidative stress. A series of α-bromoacryloylamido arylcinnamide

derivatives with general structure **4** were evaluated**.** More specifically they incorporated α,β-unsaturated carbonyl system and the α-bromoacryloyl groups which are capable of undergoing Michael addition and thus can act as trapping agents of cellular nucleophiles. The new derivatives had antiproliferative activity that was significantly greater than that of the two parent compounds **1a** and **1b** against six of the seven cancer cell lines. A positive effect was observed by the replacement of phenyl with 1-naphthyl (compounds **4a** and **4b**, respectively), with **4b** having IC_{50} values of 0.68-6.5 μM as compared with 0.19-27.3 μM for **4a**.

The compounds **4r** and **4p** caused a significant G2/M arrest in a concentration-dependent manner in Hela cells. Furthermore flow cytometric analysis showed an early but modest increase (1-6 h) in the H_2DCFDA-positive cells following treatment suggesting an immediated increase on intracellular ROS. However mitochondrial depolarization measured by flow cytometry with the fluorescent dye JC-1, appeared only after a 12 h treatment with **4r** suggesting that ROS detected by H_2DCFDA prior to the onset of apoptosis, were not produced as a consequence of mitochondrial damage. Studying the mechanism of action we demonstrated that their activity seems to be related to depletion of intracellular GSH. In fact following treatment with either **4p** or **4r** the CMFDA fluorescence levels were substantially reduced. Moreover, the effect was significantly counteracted by addition of NAC (one of the most important thiol containing scavenger) to the culture medium. However studies are underway to determine whether this occur through a direct chemical reaction or through interfering with the enzymatic synthesis of GSH. Understanding the precise mechanism may result in development of new cancer therapeutic strategies and possibly new drugs using phenylcinnamides as a lead chemotype.

2.4 REFERENCES

1. Trachootham D, Alexandre J, Huang P. Targeting cancer cells by ROS-mediated mechanisms: a radical therapeutic approach? *Nat. Rev. Drug Discov.* 2009;8:579-591.

2. Hoelder S, Clarke PA, Workman P. Discovery of small molecule cancer drugs: Successes, challenges and opportunities. *Mol. Oncol.* 2012;6:155-176.

3. Pérez de Castro I, de Cárcer G, Malumbres M. A census of mitotic cancer genes: New insights into tumor cell biology and cancer therapy. *Carcinogenesis* 2007;28:899-912.

4. Stanton RA, Gernert KM, Nettles JH, Aneja R. Drugs that target dynamic microtubules: A new molecular perspective. *Med. Res. Rev.* 2011;31:443-481.

5. Tozer GM, Kanthou C, Parkins CS, Hill SA. The biology of the combretastatins as tumour vascular targeting agents. *Int. J. Exp. Pathol.* 2002;83:21-38.

6. Adams DJ, Dai M, Pellegrino G, et al. Synthesis, cellular evaluation, and mechanism of action of piperlongumine analogs. *Proc. Natl. Acad. Sci.* 2012;109:15115-15120.

7. Jackson JR, Patrick DR, Dar MM, Huang PS. Targeted anti-mitotic therapies: can we improve on tubulin agents? *Nat. Rev. Cancer* 2007;7:107-117.

8. Dumontet C, Jordan MA. Microtubule-binding agents: a dynamic field of cancer therapeutics. *Nat. Rev. Drug Discov.* 2010;9:790-803.

9. Parker AL, Kavallaris M, McCarroll J a. Microtubules and their role in cellular stress in cancer. *Front. Oncol.* 2014;4:153.

10. Conde C, Cáceres A. Microtubule assembly, organization and dynamics in axons and dendrites. *Nat. Rev. Neurosci.* 2009;10:319-332.

11. Walczak CE, Cai S, Khodjakov A. Mechanisms of chromosome behaviour during mitosis. *Nat. Rev. Mol. Cell Biol.* 2010;11:91-102.

12. Tao W, South VJ, Zhang Y, et al. Induction of apoptosis by an inhibitor of the mitotic kinesin KSP requires both activation of the spindle assembly checkpoint and mitotic slippage. *Cancer Cell* 2005;8:49-59.

13. Elmore S. Apoptosis: a review of programmed cell death. *Toxicol. Pathol.* 2007;35:495-516.

14. Kavallaris M. Microtubules and resistance to tubulin-binding agents. *Nat. Rev. Cancer* 2010;10:194-204.

15. Hassan M, Watari H, Abualmaaty A, Ohba Y, Sakuragi N. Apoptosis and molecular targeting therapy in cancer. *Biomed Res. Int.* 2014;2014.

16. Haldar S, Basu A, Croce CM. Bcl2 is the guardian of microtubule integrity. *Cancer Res.* 1997;57:229-233.

17. Mason RP, Zhao D, Liu L, Trawick ML, Pinney KG. A perspective on vascular disrupting agents that interact with tubulin: preclinical tumor imaging and biological assessment. *Integr. Biol. (Camb).* 2011;3:375-387.

18. A. Spear M, LoRusso P, Mita A, Mita M. Vascular Disrupting Agents (VDA) in Oncology: Advancing Towards New Therapeutic Paradigms in the Clinic. *Curr. Drug Targets* 2011;12:2009-2015.

19. Marrelli M, Conforti F, Statti GA, et al. Biological potential and structure-activity relationships of most recently developed vascular disrupting agents: an overview of new derivatives of natural combretastatin a-4. *Curr. Med. Chem.* 2011;18:3035-3081.

20. Patterson DM, Rustin GJS, Serradell N, Rosa E, Bolós J. Combretastatin A-4 phosphate: Vascular disrupting agent oncolytic treatment of age-related macular degeneration. *Drugs Future* 2007;32:1025-1032.

21. Dorr RT, Dvorakova K, Snead K, Alberts DS, Salmon SE, Pettit GR. Antitumor activity of combretastatin-A4 phosphate, a natural product tubulin inhibitor. *Invest. New Drugs* 1996;14:131-137.

22. Fulda S, Gorman AM, Hori O, Samali A. Cellular stress responses: Cell survival and cell death. *Int. J. Cell Biol.* 2010.

23. Gorrini C, Harris IS, Mak TW. Modulation of oxidative stress as an anticancer strategy. *Nat. Rev. Drug Discov.* 2013;12:931-47.

24. Gill SS, Tuteja N. Reactive oxygen species and antioxidant machinery in abiotic stress tolerance in crop plants. *Plant Physiol. Biochem.* 2010;48:909-30.

25. Circu ML, Aw TY. Reactive oxygen species, cellular redox systems, and apoptosis. *Free Radic. Biol. Med.* 2010;48:749-762.

26. Scientist P, Instruments B. An Introduction to Reactive Oxygen Species. *Obstet. Gynecol. Clin. North Am.* 1998;25:1-13.

27. Li H, Horke S, Förstermann U. Oxidative stress in vascular disease and its pharmacological prevention. *Trends Pharmacol. Sci.* 2013;34:313-319.

28. Held P. An Introduction to Reactive Oxygen Species Measurement of ROS in Cells. *BioTek Instruments* 2012:1-14.

29. Forman HJ, Zhang H, Rinna A. Glutathione: Overview of its protective roles, measurement, and biosynthesis. *Mol. Aspects Med.* 2009;30:1-12.

30. Zhang H, Forman HJ. Glutathione synthesis and its role in redox signaling. *Semin. Cell Dev. Biol.* 2012;23:722-728.

31. Cairns RA, Harris IS, Mak TW. Regulation of cancer cell metabolism. *Nat. Rev. Cancer* 2011;11:85-95.

32. Finkel T, Holbrook NJ. Oxidants, oxidative stress and the biology of ageing. *Nature* 2000;408:239-247.

33. Kuo P-L, Chen C-Y, Hsu Y-L. Isoobtusilactone A induces cell cycle arrest and apoptosis through reactive oxygen species/apoptosis signal-regulating kinase 1 signaling pathway in human breast cancer cells. *Cancer Res.* 2007;67:7406-7420.

34. Raj L, Ide T, Gurkar AU, et al. Selective killing of cancer cells by a small molecule targeting the stress response to ROS. *Nature* 2011;475:231-234.

35. Armstrong JS, Steinauer KK, Hornung B, et al. Role of glutathione depletion and reactive oxygen species generation in apoptotic signaling in a human B lymphoma cell line. *Cell Death Differ* 2002;9:252-263.